



## **AFFIDAVIT**

I declare that I have authored this thesis independently, that I have not used other than the declared sources/resources, and that I have explicitly indicated all material which has been quoted either literally or by content from the sources used. The text document uploaded to TUGRAZonline is identical to the present master's thesis dissertation.

---

Date

---

Signature

## ACKNOWLEDGEMENT

I would like to take this opportunity to express my gratitude to all the people who supported me with the writing of this thesis.

First of all, I would like to thank my supervisor Univ.-Prof. Dipl. Ing. Dr. techn. Werner Lienhart. His expertise and knowledge delivered productive input to this thesis. The knowledge gained in your interesting and excellent lectures provided the foundation for this thesis.

I would also like to thank the entire IGMS-Team for the support with the experiments and the writing. Especially I would like to thank Mr. Denkmaier and Mr. Lummerstorfer for the technical support with the practical work in the laboratory.

The Institute of Mechanics of the TU Graz under supervision of Univ.-Prof. Dr. techn. Kathrin Ellermann thankfully provided a shaker and various other items for the experiments free of charge. Dr. tech. Stefan Haas from this institute gave me crucial insights to modal analysis. Thank you.

I would also like to thank my colleagues for all the support and input to this thesis.

## ABSTRACT

Deformation monitoring of civil structures like bridges is one of the core competences of engineering geodesy. The tasks of the today's engineering geodesist have been extended to change detection of buildings and areas on the earth's surface which means that the surveying engineer is accompanying a civil engineering structure also through its operational phase. Modern total stations as well as a wide area of other sensors like accelerometers enable dynamic deformation monitoring. The term dynamic deformation monitoring refers to the time in which changes of the measurement object can occur. For bridges this can be in the second or millisecond range, sometimes even lower. A civil structure like a bridge is excited by loads resulting from traffic or weather phenomena like wind which result in high frequent vibrations. Within this master's thesis a bridge model was developed for the Institute of Engineering Geodesy and Measurement Systems of TU Graz. Basically, the bridge model can be seen as a clamped beam. It was instrumented with prisms for total station measurements as well as with accelerometers and a laser triangulation sensor. Before the implementation of the bridge model a Finite-Element Model of it was designed for numerical simulation of deformation processes. This bridge model enables the evaluation of static and dynamic monitoring systems. The model is equipped with an electrodynamic permanent magnet shaker which can induce vibrations to the bridge deck to simulate dynamic deformation.

## KURZFASSUNG

Die geodätische Überwachung von Ingenieurbauwerken wie Brücken ist eine der Kernkompetenzen der Ingenieurgeodäsie. Die Aufgaben des Ingenieurgeodäten haben sich um die Erfassung von Veränderungen von Bauwerken und der Erdoberfläche erweitert. Ein Ingenieurbauwerk wird auch durch die Betriebsphase begleitet. Moderne Totalstationen sowie viele weitere Sensoren wie Beschleunigungsaufnehmer ermöglichen dynamische Überwachungsmessungen. Der Begriff dynamische Überwachungsmessung bezieht sich auf die Zeit. Veränderungen am Messobjekt treten im Sekunden- oder Millisekunden-Bereich auf, teilweise auch darunter. Auf Brücken wirken Lasten, welche durch Verkehr oder Wetterphänomene wie Wind verursacht werden. Diese können zu hochfrequenten Schwingungen des Bauwerkes führen. In dieser Arbeit wurde ein Brückenmodell für das Institut für Ingenieurgeodäsie und Messsysteme der TU Graz entwickelt. Prinzipiell kann das Modell als ein eingespannter Balken betrachtet werden. Es wurde mit Prismen für die Messung mit Totalstationen, mit Beschleunigungsaufnehmern und mit einem Lasertriangulationssensor instrumentiert. Ein Finite-Elemente Modell für die numerische Simulation von Deformationsprozessen wurde vor dem Bau des Modells entwickelt. Mit diesem Brückenmodell können statische und dynamische Überwachungssysteme (Monitoringsysteme) evaluiert werden. Durch einen elektrodynamischen Permanentmagnet-Shaker können Vibrationen zur Simulation von dynamischen Deformationen erzeugt werden.

# TABLE OF CONTENT

Acknowledgement.....	I
Abstract .....	III
Kurzfassung .....	III
Abbreviations .....	VI
1 Introduction.....	1
2 Modern Geodetic Monitoring .....	2
2.1 Introduction.....	2
2.2 Characteristics of deformation processes.....	5
2.2.1 Cause of deformation processes .....	6
2.2.2 Systems theory .....	6
2.2.3 System identification by parametric and non-parametric models .....	8
2.2.4 Geometrical and temporal discretization.....	9
2.3 Analysis of deformation measurements .....	11
2.3.1 Conventional deformation analysis.....	11
2.3.2 Advanced deformation analysis .....	12
2.4 Sensors and instruments .....	14
2.4.1 Overview of state of the art sensors .....	14
2.4.2 Conclusion About Sensor Technology .....	19
2.5 Bridge monitoring system .....	20
3 Simulating Bridge Deformation .....	22
3.1 A bridge model for the IGMS.....	22
3.2 Fundamentals of the applied mechanics .....	24
3.2.1 Vibrations .....	24
3.2.2 Experimental methods of structural dynamics .....	25
3.3 Fundamentals of the finite element method .....	26
3.4 Development of the model .....	27
3.5 Vibration stimulation.....	32
3.5.1 Vibration stimulation systems for laboratory experiments .....	32
3.5.2 Vibration stimulation systems for real bridges .....	33
4 Development of a measurement system .....	34
4.1 Instrumentation and Sensors .....	34
4.2 Test of the measurement system.....	36
4.3 Data Processing and Analysis .....	38
4.3.1 Post-processing of accelerometer measurements.....	38

4.3.2	Post-processing of total station measurements .....	44
4.3.3	Post processing of laser triangulation data .....	45
4.3.4	Data Synchronisation.....	46
4.4	Conclusion .....	50
5	Application to the bridge model .....	51
5.1	The IGMS bridge model.....	51
5.1.1	Mechanical configuration of the model .....	51
5.1.2	Operating limits of the bridge model .....	54
5.1.3	Instrumentation of the model.....	54
5.2	Experiments with the bridge model.....	55
5.2.1	Static Experimentes.....	55
5.2.2	Dynamic Experimentes.....	57
6	Conclusion and Outlook .....	66
	Source directory .....	67
	List of figures .....	71
	List of tables .....	73
	Appendix A Specifications for the Bridge Model.....	74
	Appendix B Shaker data sheet.....	76

# ABBREVIATIONS

**2D** two-dimensional

**3D** three-dimensional

**ATR** Automatic Target Recognition

**BIM** Building Information Modelling

**CCF** Cross-Correlation-Function

**CMOS** Complementary metal-oxide-semiconductor

**EDM** Electronic Distance Measurement

**FOS** Fiber Optical Sensor

**GBSAR** Ground Based Synthetic Aperture Radar

**IAM** Integrated Analysis Method

**IATS** Image Assisted Total Station

**IGMS** Institute of Engineering Geodesy and Measurement Systems

**LTS** Laser Triangulation Sensor

**MDOF** Multi Degree of Freedom

**MEMS** Microelectromechanical System

**PC** Personal Computer

**SDOF** Single Degree of Freedom

**SI** Système international d'unités (International System of Units)

**TLS** Terrestrial Laser Scanning

**TS** Total Station

**USB** Universal Serial Bus

# 1 INTRODUCTION

The content of this master's thesis is the development of a small-scale bridge model for the Institute of Engineering Geodesy and Measurement Systems (IGMS) of TU Graz. The task of monitoring civil structures has been and is more than ever one of the core competences of the engineering geodesists. The evolution of the sensor capabilities enables not only static observations but also dynamic deformation measurements. An advanced monitoring system for bridges includes a mix of different sensor types as well as deformation analysis. The small-scale bridge model enables the institute to simulate vibrations for the test and evaluation of static and dynamic monitoring systems. A Finite Element Model of the bridge model was developed with specialized software. The model was instrumented with accelerometers and prisms for total station measurements.

Chapter two describes the characteristics of deformation processes, explains briefly the classic as well as the advanced deformation analysis methods and covers some of the most common sensors suitable for monitoring tasks in relation with bridges. The attempt was made to outline the requirements for a bridge monitoring system as well as possible challenges.

Chapter three deals with the simulation of bridge deformations. The purpose of the bridge model for the IGMS and its requirements are defined. The basics of the applied mechanics and the Finite Element Method (FEM) are covered. Finally, the development process of the model including finding the best parameters regarding the model geometry and the possibilities of vibration stimulation are explained.

Chapter four focusses on the design of a measurement system and the testing of the used sensors. Some faulty working sensors were identified and problems with the data acquisition of one total station were solved. The data analysis of the different sensors and the data synchronization is illustrated in the last part of this chapter.

Chapter five deals with the realized bridge model, testing that was carried out with it and finally compares the results from the FEM-model with measured vibrations.

Finally, in chapter 6 a conclusion and an outlook are given.

# 2 MODERN GEODETIC MONITORING

## 2.1 INTRODUCTION

Every modern society has a need for transportation due to social and economic reasons. A major factor for globalization are the advances in the world-wide transportation system enabling humans to travel and cargo to be hauled all around the world. Especially ships and aircrafts are providing intercontinental transportation. Highways and railroads are vital elements of every nation's infrastructure system. The economy has an urgent demand for fully developed infrastructure systems which offer fast, efficient and safe transportation of humans and goods.

Derived from these requirements every country has a need for a modern infrastructure system consisting of railroads, highways, waterways, airports and ports. Part of every traffic infrastructure are bridges, structures build to span obstacles like valleys or rivers. For example, the Austrian Federal Railways (ÖBB) have over 9000 bridges in their 9700 km long railway network. But also where space is scarce like in urban areas bridges can offer a solution to expand into the third dimension.

The classic definition of geodesy by Friedrich Helmert from 1880 is the "measurement and mapping of the earth's surface". The task of a surveying engineer is to accompany a construction project from the planning phase by providing spatial data of the construction site through its execution by transferring coordinates from the plan to the nature till the final acceptance. The tasks of the today's engineering geodesist have been extended to change detection of buildings and areas on the earth's surface which means that the surveying engineer is accompanying a civil engineering structure also through its operational phase. The surveying engineer turns the measured data into information as a basis for decision making by his clients. Kuhlmann et al. (2014, p.11) gave the following definition of engineering geodesy: "Engineering geodesy is the discipline of reality capture, setting-out and monitoring of local and regional geometry-related phenomena paying particular attention to quality assessment, sensor systems and reference frames."

The terms monitoring and deformation measurement are not used consistently in the literature. Monitoring in general means the systematic detection of all kinds of changes of a measurement object. The subject of deformation measurements is the detection of geometrical changes of an object (Heunecke et al. 2013, p.1). That is the detection of movement and deformation of an object through measurements and their analysis. The term deformation includes the actual deformations of a measurement object and rigid body motion.

In the last years the optimization of the operation of an engineering structure got more and more in focus. On the one hand every infrastructure operator wants to extend the service life of an engineering structure and to optimize maintenance costs. Therefore, information about the present state of the structure is fundamental. So-called geodetic structural health monitoring (SHM) systems (Lienhart & Erhart, 2015) collect data from the building and provide essential information as a basis for decision making. Therefore, an operation beyond the planned service life is possible. Normally maintenance work is carried out on a fixed interval basis because no data of the actual state of the infrastructure is available. During maintenance work the infrastructure is not fully operational. To reduce these out-of-service times and to execute maintenance at a proper stadium a so-called maintenance-on-condition

could be carried out. In doing so the structural health status of the building needs to be captured. On the other hand, modern civil engineering structures like the Gotthard base tunnel or the Øresund bridge are bigger and more sophisticated than ever before. The growth of the world's population makes it sometimes necessary to build structures in challenging areas regarding the environment like in deserts or in earthquake zones. Monitoring has to be established to guarantee the safety of a civil engineering structure and to optimize its operation.

The objective of deformation measurements can be described very briefly as the following:

- Proof of stability and functional safety of an engineering structure.
- Detection of changes to the measurement object, especially changes which affect the safety of the engineering structure.
- Prediction of the behavior of the measurement object in the future based on the collected data.
- Collection of data of the so called structural health status.
- Documentation, especially of damages of the structure.

In general, the process of deformation measurements consists of the measurement itself, data processing and producing information via interpretation of the data. More detailed information about the design and implementation of monitoring systems for bridges is given in chapter 2.5.

It is important to notice that a monitoring system can only be one component of a complete safety system for an engineering structure. The most important component is the structure itself.

The today's surveying engineer is not using solely geodetic sensors like total stations, on the contrary he is using also a variety of non-geodetic sensors like accelerometers or fiber optic sensors. The combination and integration of different sensors presents a new challenge. The following chapter is focusing on deformation processes, monitoring and a selection of sensors which are described in detail.

From time to time the need of a monitoring program is doubted. The performance of modern monitoring systems and the surplus value from the information obtained from the captured data is not always recognized at first sight. It is common knowledge that the costs of a monitoring program make only a small proportion of the total costs of the construction of a structure. It is a matter of fact that most buildings do not need any kind of monitoring. Critical infrastructure and complex engineering structures do need a monitoring program to a certain extent. There are no general rules when a monitoring is needed and also not for the extent. So why do we need a monitoring system or respectively why do we measure? Golser (2018) answered as follows:

- Determination of static stability
- Dimensioning of support measures during the construction phase (e.g. jet grouting)

- Optimization of construction activities
- Interpretation of geological and geotechnical situation
- Control of the construction process
- Delivery assurance (accordance with the requirements)
- Design verification (validate assumptions and predictions)
- Quality assurance
- Legislative compliance and preservation of evidence (especially in case of an accident or incident)
- Risk management (to trigger pre-planned actions)

## 2.2 CHARACTERISTICS OF DEFORMATION PROCESSES

The collected data from a deformation measurement is put through analysis and interpretation. The result is information as a basis for decision making. In order to draw the right conclusions, it is irremissible to have knowledge about the physical characteristics of the measurement object and the forces affecting it. The first question is if there is deformation or not. If deformation is detected, the second question is why there is deformation. Beside other sciences the mechanic is delivering the necessary knowledge. The mechanics is one of the oldest section of the physics. The task of the mechanics is the description and predetermination of body movements as well as the forces which are in conjunction with the movements (Gross et al., 2013, p.1).

Deformation measurement is used to detect changes of the measurement object. There are two main categories: movement respectively rigid body movement and distortion. Both have several sub-categories (figure 2-1) which are described below after Heunecke et al. (2013, p.92-93).

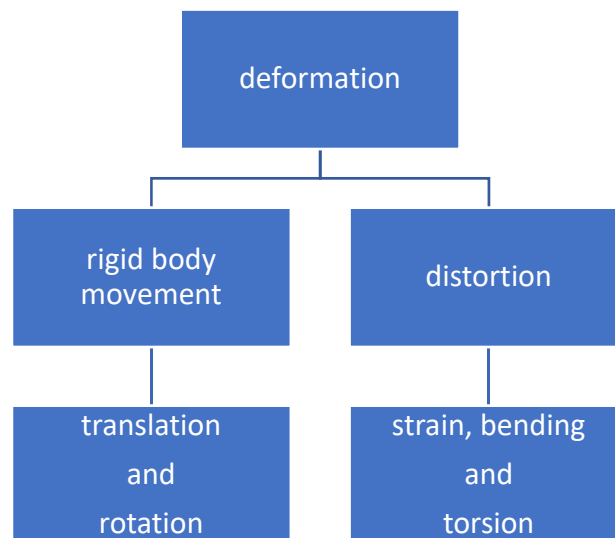


FIGURE 2-1 RIGID BODY MOVEMENT AND DEFORMATION (HEUNECKE ET AL., 2013, P.92-93)

- Rigid body movement: Movement is the translation and rotation of the whole measurement object in relation to its surrounding without any changes to its geometry.
- Translation: Translation designates movement of a point in a certain direction (e.g. settlement).
- Rotation: Rotation is the turn of a body around a rotation axis.
- Distortion: Deformation is the change of the inner geometry of an object.
- Strain: Strain and shear deformation is defined in direction of the axis and its angels of shear.
- Bending: Bending is deformation in relation to an axis of the object.
- Torsion: Torsion is distortion of the object around an axis.

## 2.2.1 CAUSE OF DEFORMATION PROCESSES

The possible causes of movement and deformation of a measurement object are myriad. It is impossible to determine all the possible causes in a structured list. It depends on the object itself, its purpose, its dimensions, its environment and a lot of other possible factors. Therefore, as mentioned above it is essential to have in depth knowledge of the physical characteristics of the measurement object and the forces affecting it.

In the following the most common causes of movement and deformation are listed:

- Weather phenomena like wind, temperature, rain, snow etc.
- Lateral earth and rock pressure
- Changes of the ground water level
- Load on the object by road traffic, trains, pedestrians etc.
- Water pressure (especially at a water dam)

Another classification is the differentiation between external and internal forces affecting the measurement object. Furthermore, a discrimination about the temporal development can be made. The acting forces have either static or dynamic characteristics.

## 2.2.2 SYSTEMS THEORY

Due to the infinitely complex world every description of it by physical and mathematical methods is imperfect. The scientific approach to overcome these problems is to describe only the most important and essential elements and processes them in models. It is obvious that every such model is just an approximation of the real world respectively only a small part of it.

The goal of systems theory is to describe the temporal behavior of systems with consistent mathematical methods. A bridge or every other measurement object can be seen as a dynamic system which consists of three major elements: input signal  $x$ , transfer through the object and output signal  $y$  (figure 2-2). For example, the change of the outside air temperature as an input signal causes a time-dependent reaction of the measurement object (transfer) and as a result a time-retarded deformation as an output signal of the system.

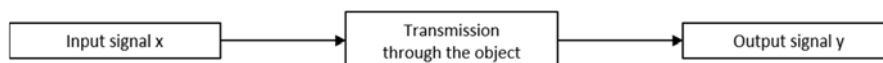


FIGURE 2-2 SYSTEM INPUT/OUTPUT RELATION AFTER LIENHART (2006)

Generally, systems can be classified in static and dynamic systems. In this thesis, only the dynamic systems are examined in more detail. A static system captures a new state of equilibrium after effected by a load and can be seen as a special case of a dynamic system. Dynamic systems are classified in different orders based on their response to a test function (e.g. step function, ramp function).

### Zero order systems:

A zero order system gives an immediate response to a change of the input signal  $x$  (figure 2-3). It is not time-retarded.  $K$  denotes the transfer factor and  $y$  the system output.

$$K \cdot x(t) = y(t) \quad (2.1)$$

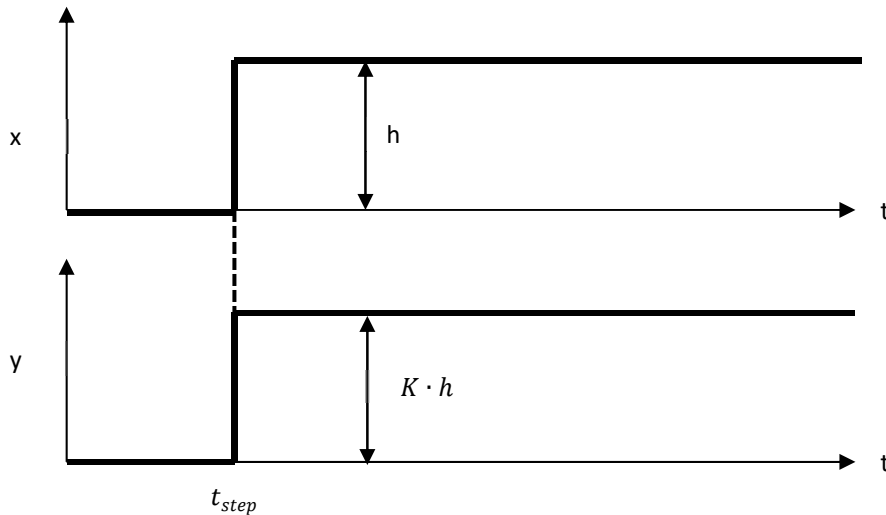


FIGURE 2-3 ZERO ORDER SYSTEM AFTER LIENHART (2006)

### First order systems:

First order systems have a delayed response to a change of the input signal figure (2-4). They are time-retarded.  $T$  denotes the time constant.

$$K \cdot x = y + T \frac{dy}{dt} \quad (2.2)$$

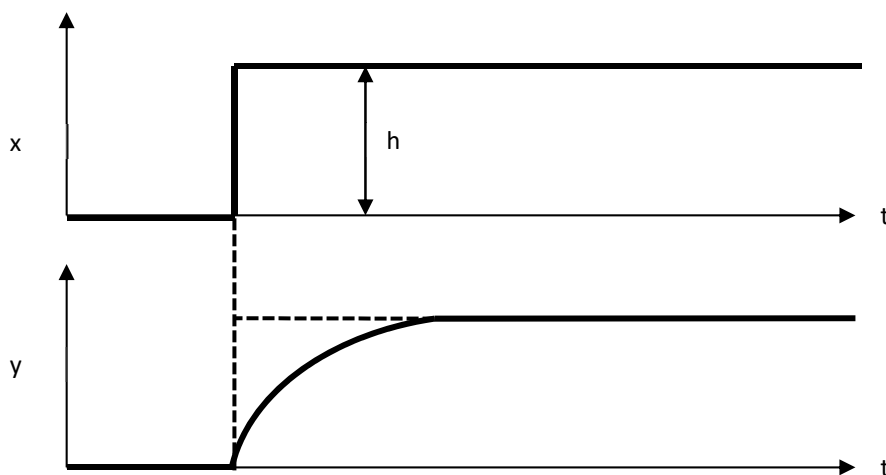


FIGURE 2-4 FIRST ORDER SYSTEM AFTER LIENHART (2006)

**Second order systems:**

Second order systems also include the second derivative of the output signal with respect to time (figure 2-5). They are time-retarded and damped ( $\beta$  denotes the damping).

$$K \cdot x = y + T \frac{dy}{dt} + \beta \frac{d^2y}{dt^2} \tag{2.3}$$

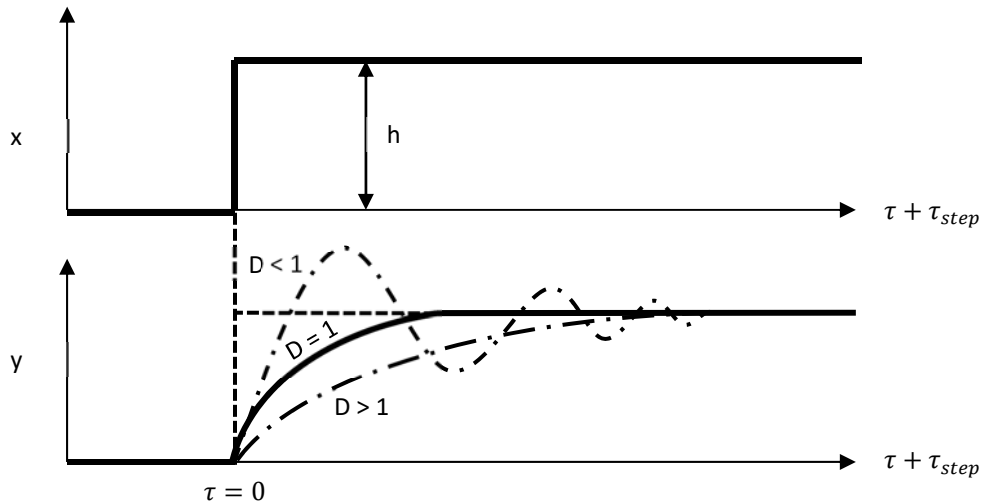


FIGURE 2-5 SECOND ORDER SYSTEM AFTER LIENHART (2006)

**2.2.3 SYSTEM IDENTIFICATION BY PARAMETRIC AND NON-PARAMETRIC MODELS**

System identification is needed for the set-up of an appropriate mathematical-physical representation of the transfer function (see figure 2-6).

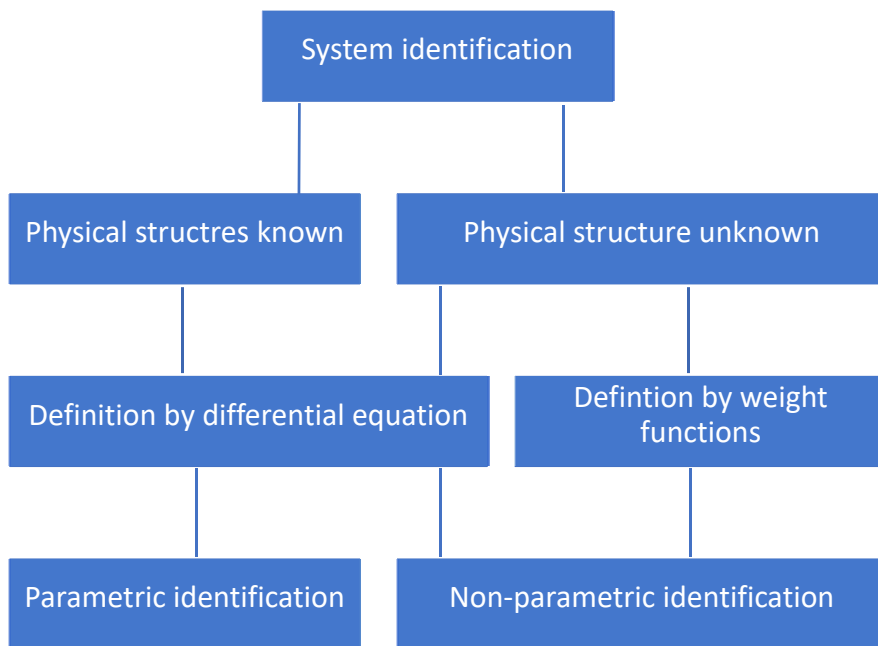


FIGURE 2-6 SYSTEM IDENTIFICATION (WELSCH & HEUNECKE, 2001, P.399)

A model is called a parametric model (or structural model) if the transfer function is known and can be described by differential equations (also called white box model). The fundamental equation of any dynamic model of a system is the differential equation of linear dynamic elasticity by Welsch & Heunecke (2001, p.399):

$$|K \quad D \quad M| \cdot \begin{vmatrix} y(t) \\ \dot{y}(t) \\ \ddot{y}(t) \end{vmatrix} = x(t) \quad (2.4)$$

With K...stiffness matrix  
D.....damping matrix  
M.....mass matrix  
y(t)...system output  
x(t)...system input

A parametric model of a deformation process represents the reality in the best way but is associated with a considerable effort to design the model.

If there is no appropriate information about the geometrical and the physical structure available the relationship between the input to output signal can be described by the determination of regression or correlation coefficients (behavior model). The input to output signal relationship is without any physical meaning. Therefore, the non-parametric models are also called black box models.

**Essential problems with dynamic systems (Nake, 1983):**

- Direct problem: The input signal and the transfer function are known. The output signal is unknown but it can be predicted.
- Inverse problem: The transfer function and the output signal are known. The input signal is unknown but the causative factors can be computed by reverse engineering.
- Identification problem: Input and output signal are known. The transfer function is unknown. The systems behavior can be described by the measurement of the input and output signals.

**2.2.4 GEOMETRICAL AND TEMPORAL DISCRETIZATION**

The measurement object and its behavior in space and time must be approximated by a determined number of survey points (geometrical discretization after Welsch & Heunecke (2001, p.390), table 2-1). In most cases the surrounding area of the measurement object must be discretized too. No general rules can be established. The quantity and the position of the survey points must be adequate for the deformation measurements but must also be economically justifiable. The measurement object is a continuum as defined by the mechanics. Every model is only an approximated and simplified copy of the reality.

TABLE 2-1 GEOMETRICAL DISCRETIZATION

	Measurement object	Modelling
Geometry domain	The object is a continuum	The object is prescinded by characteristic points
Time domain	The object is in permanent motion	Deformation measurements are conducted at certain time intervals

The temporal behavior of the measurement object must be predicted in order to design a measurement program (temporal discretization). Generally, two types of temporal deformations can be distinguished: static and dynamic deformations. Dynamic means that the measurement object is permanently in motion. The measurement rate of a sensor has to be taken under consideration. For the registration of dynamic movements, the sampling theorem of Shannon and Nyquist must be fulfilled:

$$f_s > 2f_m \tag{2.5}$$

A sufficient sampling rate respectively frequency ( $f_s$ ) is therefore more than twice as high as the frequency of the sampled signal ( $f_m$ ). The steps for deformation capture are shown in figure 2-7.

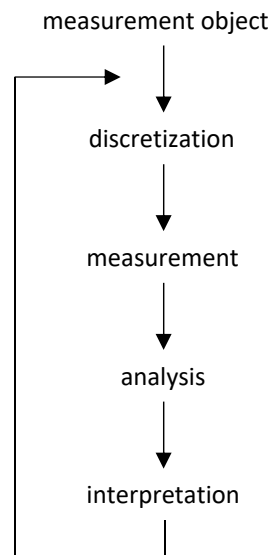


FIGURE 2-7 STEPS OF DEFORMATION CAPTURE AFTER HEUNECKE ET AL (2013, P.16)

## 2.3 ANALYSIS OF DEFORMATION MEASUREMENTS

The result of a deformation measurement is raw data which needs to be analyzed and interpreted. The product of this process is information about the movements and deformations of a measurement object.

In general, there are two types of deformation analysis models. The conventional models which roughly said consider only the change in geometry of an object in space and time characterized by a discrete number of points. The advanced models in addition analyze also the factors causing movement and deformation.

There are various approaches and models for deformation analysis. Some of the major challenges of every deformation analysis are the following:

- Significance: The effect of random errors must be lower than the expected deformations.
- Blunders: Not all blunders are eliminable. Therefore, information about the reliability is needed.
- Reference points: Stability of the reference points must be guaranteed.

### 2.3.1 CONVENTIONAL DEFORMATION ANALYSIS

#### **Congruence models**

The pivotal question is if a deformation is statistically detectable? This analysis is based on the hypothesis of identical point coordinates and therefore named congruence model (Niemeier, 2001, p.435).

The design of the observation net is double-staged in order to be able to detect relative as well as absolute changes of the object. The net consists of reference points which are assumed stable and of object points on the measurement object. The geometry respectively the coordinates of the reference points should be the same between the null epoch and the follow-on measurement epochs. The stability of this reference frame has to be ensured.

The assumption or so called null hypothesis is that the coordinates of the reference points as well of the object points have not changed between two epochs. The congruence of the coordinates at certain moments in time is statistically tested. Anyway, basic information about the object to be monitored is necessary for the design of an appropriate monitoring system.

#### **Kinematic models**

Kinematic models extend the purely geometrical contemplation by the factor of time. Deformations and object changes are described by parameters of space and additionally time. These parameters of time are for example speed, acceleration, oscillation and other time-dependent behavior of the measurement object. The relationship between deformations and its causative forces is not considered.

This system is called regression analysis. In order to capture the movement (hence the name kinematic model) of an object a continuous monitoring (sampling theorem) is necessary. In case of a short observation period extrapolation of the deformation and movement behavior is difficult.

**2.3.2 ADVANCED DEFORMATION ANALYSIS**

In comparison to the conventional systems advanced deformation analysis incorporates in addition to the measurement of object changes in space and time also the causative factors of the occurring deformation (figure 2-8). Forces, loads and other factors are causing deformation of the measurement object. The behavior of the object under the influence of these factors is dependent of its physical properties. The acting forces as input signal, the transmission through the object as transfer process and the response of the object as output signal form a causal chain which is called a dynamic process or a dynamic system (Welsch & Heunecke, 2001, p.397).

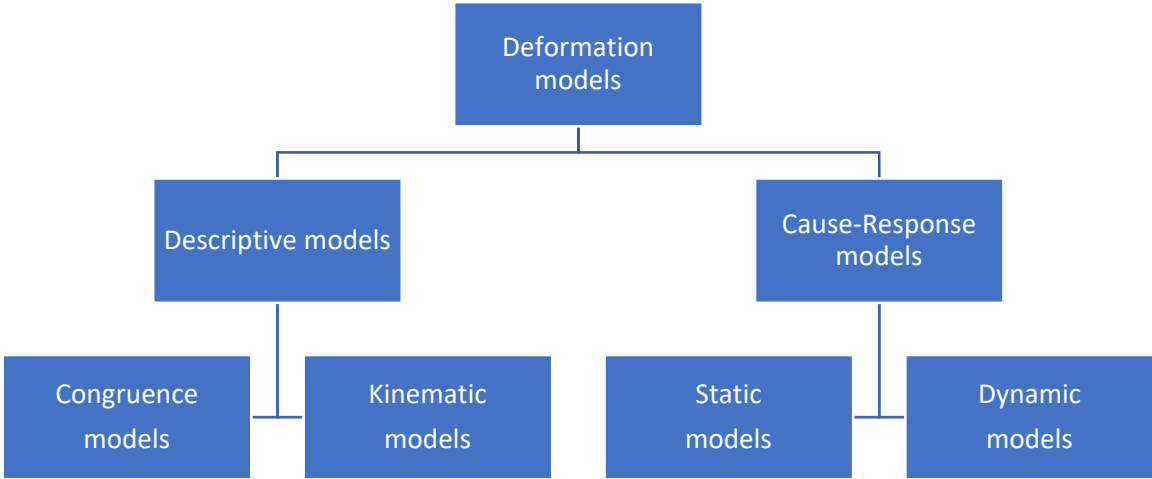


FIGURE 2-8 HIERARCHY OF DEFORMATION MODELS BY WELSCH AND HEUNECKE (1999)

The measurement object can be seen as a system (see chapter 2.2.2) on which forces and loads (for example temperature, rock pressure, traffic) are acting on. These input signals are transmitted (transfer function) through the system and cause deformation. This dynamic process can be modeled if the input signals and the transfer function are known (system identification). If additionally, the reaction of the system in the form of deformations is known by measurements the potential of advanced deformation analysis systems becomes clear. The comparison between the predicted to the observed deformation may reveal some deviation which is called innovation. It is possible to calibrate the model and identify the dynamic process by these steps: modelling the system, performing the measurement of input and output signals, evaluating functional and stochastic relationships and assessing the findings by verification and validation (Welsch & Heunecke, 2001, p.397). These advanced models are called cause-response models.

**Static model**

The static model establishes a connection between the input signals and the measured output signal of the measurement object. The measurement object is supposed to be not in motion before and after the exposure to the input signals. A time for retardation is not considered.

## Dynamic model

The dynamic model is the most complex model. All other deformation analysis models are approximations which either do not consider the time aspect or do not establish a causal chain between input and output signals. The dynamic system has a memory. Table 2-2 shows the classification of the four models after Welsch & Heunecke (2001, p.398).

TABLE 2-2 CLASSIFICATION OF DEFORMATION MODELS AFTER WELSCH

Deformation model	Congruence model	Kinematic model	Static model	Dynamic model
Time	no modeling	movement is function of time	no modeling	movement is function of time and loads
Acting forces	no modeling	no modeling	displacement is function of loads	
State of the object	at equilibrium	in permanent motion	in equilibrium under loads	in permanent motion

The integrated analysis method (IAM) processes all the available data (theoretical and empirical data) through one adjustment. The basic idea of this method is that the monitored structure is a physical system which reacts to the acting forces which result in deformation of the object. It consists of a measurement and a model part. In figure 2-9 the concept of this model is presented.

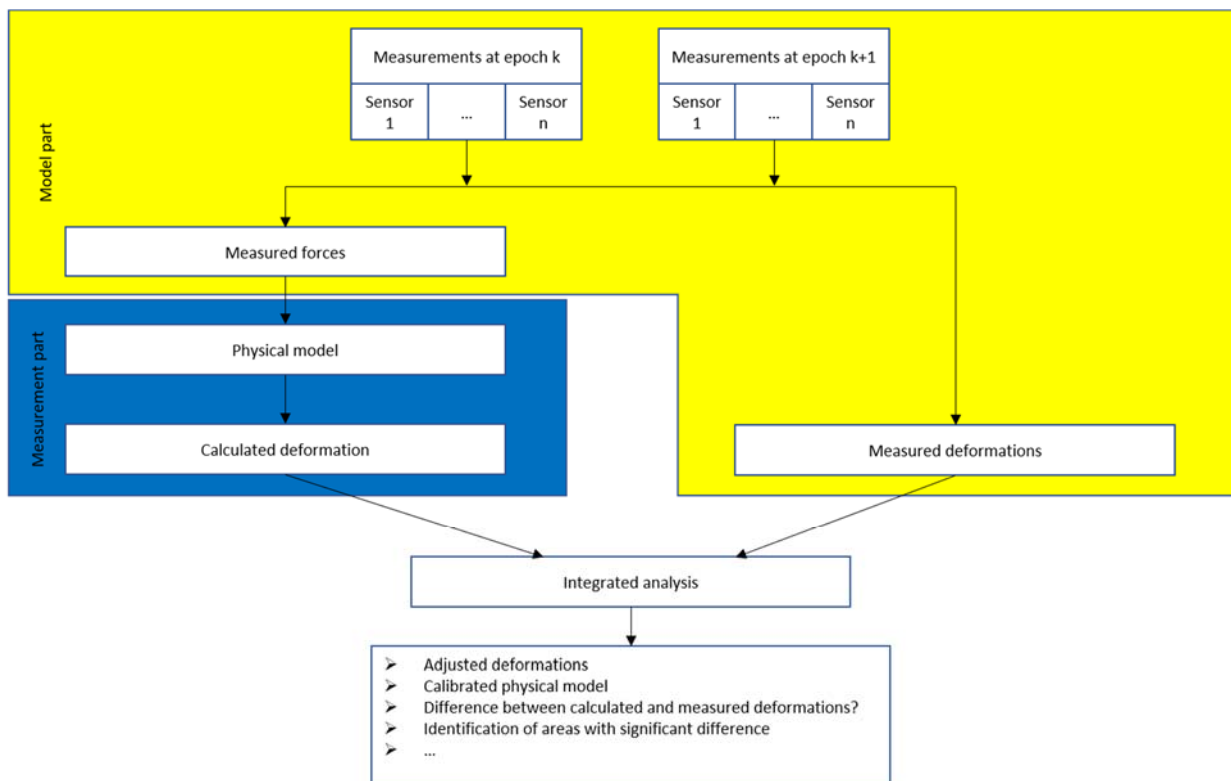


FIGURE 2-9 INTEGRATED ANALYSIS MODEL BY LIENHART (2006, P.7)

The physical model of the IAM can be realized as a Finite Element model (see chapter 3.3). Also, the introduction of Building Information Modelling (BIM) methods and procedures will affect geodetic monitoring in general and deformation analysis in particular but this thesis does not elaborate BIM methods.

## 2.4 SENSORS AND INSTRUMENTS

Geodetic sensors like total stations, levels, GNSS, laser scanners or cameras result in angles, distances, distance changes, height differences, pixel coordinates or positions. But surveying engineers are also using non-geodetic sensors. Especially in the tunneling and underground excavation non-geodetic sensors are used to a greater extent. Nowadays a lot of construction and monitoring projects require the use of these sensors. Through the integrated analysis method, the incorporation of different sensors in the adjustment is possible with the know-how of the surveying engineer. Also, the automation of measurement and analysis processes became important for the delivery of real time data.

Geodetic monitoring can only be a part of a so called structural health monitoring system (Lienhart & Erhart, 2015). For the monitoring of bridges there are a lot more sensors and techniques available and, in most cases, necessary (especially for corrosion monitoring of steel and concrete) to become a complete picture of the state of the construction. Reference is made here to the Ph.D. thesis “Bauwerksinspektion und –Überwachung” by Santa (2004).

Each sensor has both its advantages and disadvantages when used for deformation analysis. Beside of their delivered accuracy and resolution a lot of other factors designate the suitability of an individual sensor.

Some of the most common sensors are described in the following section but the list does not claim to be complete.

### 2.4.1 OVERVIEW OF STATE OF THE ART SENSORS

#### **Total station**

The total station evolved from the theodolite, an analogue instrument capable of measuring angles in the vertical and horizontal plane with high precision. In the second half of the 20<sup>th</sup> century digital theodolites were developed. Their main feature was the digital reading and storage of the data. The total station is a theodolite with a distance measuring unit. From the measurement of vertical (V) and horizontal (Hz) angles and the measurement of distances three dimensional coordinates are gathered. For state-of-the-art instruments the absolute accuracy for angles is about 0.3 mgon and 1 mm + 1.5 ppm for distances (Leica, 2015). A position accuracy of points is reached between 1 and 5 mm depending on the distance. With the minimization of electronic measurement equipment, more and more features were implemented. The modern total station is a multi-sensor platform in which dozens of sensors are integrated able to measure angles and distances with a high rate of up to 20 Hz. Thereby they are now also capable to track dynamic processes like oscillations of engineering structures of up to 10 Hz. They are also able to perform laser scanning with a measurement rate of up to 26.6 kHz like the Trimble SX10 (Trimble, 2017). A digital workflow was established and accelerated the whole process between measurement in the field and the end product. Due to automatization the so called “one-person” station is reality as well as remote controlled total stations (robotic total station) for monitoring applications. Further improvements are in the development pipeline. For example, cameras are added to the sensor package (image assisted total station), not only for documentation purpose. The images can be analyzed by photogrammetric methods (image-based measurements) and sooner or later the eyepiece will be replaced by cameras.

## **Levelling**

The level counts to the classic geodetic instruments. No other measurement technique is able to perform height measurements over long distances with higher accuracy than with levels. The levels were digitized during the last decades although the measurement principle with staff and frog is still the same. Nearly every monitoring system needs levels either for deformation measurements or to establish the reference network. State-of-the-art instruments are capable to measure height with an accuracy of up to 0.3 mm (standard deviation, 1 km double run). Due to the digitalization of the instruments a high degree of automatization was reached albeit the level measurement is still labor intensive. Classic procedures have to be exercised to reduce effects like critical distances, illumination of the staff, inaccurate focusing or line-up errors.

## **Hydrostatic levelling/pressure systems**

For the determination of height differences water level gauges can be used. There are two basic principles: measurement of the hydrostatic level or of the hydrostatic pressure. The method is based on the principle of communicating vessels. Hydrostatic leveling is a robust and accurate system (up to 5  $\mu\text{m}$ ) but with high installation effort and a small measurement range. Hydrostatic pressure systems measure the difference pressure. These systems can be used for dynamic measurements and offer a greater range in comparison to the hydrostatic level systems.

## **GNSS**

Modern Global Navigation Satellite System (GNSS) receivers can measure positions with precision in the mm range. With measurement rates of up to several hundred Hz they are also able to be used for a dynamic bridge monitoring as well as for static 3D deformation measurements of certain points. For high accuracy phase measurement is performed. Additionally, a reference station network has to be established. Examples for an automated bridge monitoring by GNSS sensors are the Tancarville bridge (span of 608 m) and Normandy bridge (span of 856 m) in France (Leica 2009, p.16-17). Access to the structure for installation of GNSS sensors (antenna and receiver) is needed. For the placement on the measurement object multipath and diffraction effects have to be considered.

## **Laser scanner**

Laser scanning offers the opportunity to capture an extensive bridge in short time without access to the structure. Terrestrial laser scanners (TLS) are capable of measuring up to 1 million points per second with a distance-dependent accuracy of up to 1.2 mm + 10 ppm and a position accuracy of up to 3 mm (Leica, 2016). The laser scanner rotates with a fixed angular speed and a predefined distance measurement rate. The raster respectively the point spacing is distance-dependent. The surface of the measurement object is sampled by a large number of points. The result in form of an unstructured point cloud and the fact that it is not possible to measure the exact same points again is a disadvantage. Because of that the scan data analysis for deformation measurements is time-consuming and complex. In each point cloud a surface has to be fitted which is demanding because of the not uniformly distributed points. Instead of a direct point to point comparison of different epochs, each epoch is represented by a meshed surface model.

## Ground based interferometric radar

Ground based synthetic aperture radar (GBSAR) systems are based on the principle of microwave interferometry (figure 2-10). Amplitude and phase of the reflected microwave are measured. Distance changes in the line of sight are measured contact-free with a high rate up to several hundred Hz which enables application for static as well for dynamic deformation measurements of structures. The distance-dependent accuracy is up to 0.1 mm (Metasensing, 2018). GBSAR can operate in darkness and is independent of weather phenomena. The deformation of different certain points with the same distance to the instrument cannot be separated. Only the relative movement in the line of sight (only one component of the 3D movement vector) is measured. These are the greatest disadvantages of this technique. Beside that the surface of the measurement object has to have certain characteristics (e.g. roughness) to guarantee reflection of the radar signal. Becker et al. (2012) investigated the experimental validation of a finite-element model based modal analysis of a bridge with a GBSAR system.



FIGURE 2-10 FASTGBSAR-R (METASENSING, 2018)

## Fiber optic sensors

Fiber optic sensors (FOS) can be either used to measure strain and temperature or as a relay for data transfer to remote located sensors. The principle is based on the travel of light through the fiber. The light never leaves the fiber and the signal is transformed inside it. If the fiber is influenced by mechanical stress or temperature changes the parameters of the light like the wavelength, the polarization, the transit time and the intensity change.

Basically, there exist two types of sensors: extrinsic and intrinsic sensors. Extrinsic means that the fiber is used to guide light to a sensor element. Intrinsic means that the fiber itself is the sensing element. There are single point sensors (Fabry Perot and SOFO based on the interferometric principle), quasi distributed sensor arrays (fiber bragg grating) and distributed sensing elements (using Raman, Brillouin or Rayleigh backscattering based on the optical time domain reflectometry).

The measurable direct strain ranges up to 6 % of the fiber length and the measurable temperature range is up to 800 °C. No power supply for the sensing element is needed, it is insensitive to

electromagnetic radiation, it is light weight and easy to embed in a structure. The disadvantages are that such systems are expensive and difficult to integrate in an existing engineering structure.

The advantages and capabilities offered by fiber optical sensors makes them predestined for long term deformation measurements on critical infrastructure.

### **Temperature sensors**

Temperature measurements are of interest because of the following three reasons: First temperature itself is a parameter of interest; second, temperature changes can cause deformation and movement; and third, other sensors are sensitive to temperature (Dunnicliff, 1993). Sensors with different measurement techniques are available.

There are various techniques to measure the temperature mechanically. Most of them are based on the thermal expansion of a liquid or a solid. The most common is the mercury thermometer. It is fragile and not suitable for remote read out. Bimetal thermometers use a bimetallic element with different coefficients of thermal expansion. These sensors are cheap and show no aging effects.

A thermistor (thermally sensitive resistor) is a resistor which is changing its resistance with temperature. The advantages are a high sensitivity and a fast adaption to temperature changes. The disadvantages are the non-linear connection between resistance and temperature and the necessity of a constant calibration.

A thermocouple produces a temperature dependent voltage which is based on the thermoelectric effect. They are well suited for the measurement of temperature differences.

Silicon bandgap temperature sensors are based on the principle that the forward voltage of a silicon diode is temperature dependent. They can be included in a silicon integrated circuit. The advantage is their small dimensions.

As mentioned before fiber optic sensors are also capable of measuring temperature.

### **Accelerometer**

One popular technique to measure acceleration is based on the piezoelectric effect. Piezoelectricity describes the change of voltage in a rigid body which is exposed to mechanical stress. See chapter 4.1 where accelerometers are described in more detail.

### **Tilt meters (clinometers)**

Tilt meters measure the tilt in regard to a reference plane. Tilt can be measured by various techniques like the optical principle, the thermodynamically principle, with electrolytes through the resistor change or with sensors based on a pendulum.

### **Extensometer**

Extensometers are instruments frequently used for measuring the axial deformation along a borehole. They are mostly used for monitoring of anchoring and support systems (e.g. slope protections, open cuts, underground constructions) to observe settlement and sliding.

The anchoring part is mounted in the borehole such that it will follow even very small movements in the rock or the ground. It is solidly attached to a measuring rod which transmits the movement to a pin in the measurement head which is mounted at the mouth of the borehole. In this way, the relative movement between the anchor and the mouth of the borehole can be established by sensing the distance between the anchor and the measurement head (figure 2-11). The possible accuracy is up to 0.1 mm.

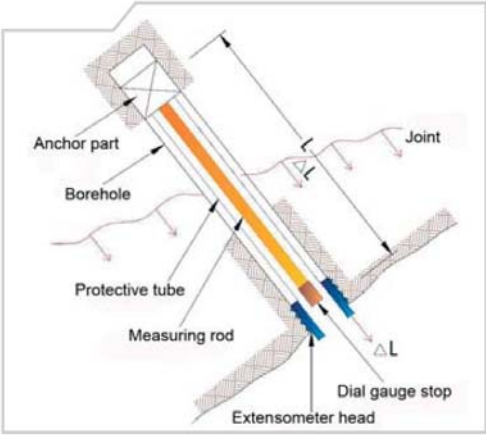


FIGURE 2-11 SCHEMATIC ASSEMBLY OF AN EXTENSOMETER (GEODATA ZT GMBH, 2008A)

**Strain gauge**

The most common principle used in strain gauges is the connection between the resistance of a conductor and its change in length respectively its geometry (figure 2-12). One realization of a strain gauge is based on the bridge circuit after Wheatstone, consisting of four resistors. The gauge is attached to the measurement object by a suitable adhesive. It's crucial that the adhesive is not influencing the measurement. A temperature compensation is viable by using one of the four resistors.

Strain gauges offer a high accuracy and resolution. They are suitable for static and dynamic application, can be used in a high temperature environment and are able to measure oscillations up to 50 Hz. On the other hand, they are prone to moisture, the strain measurement is often invasive to the measurement object and great deformations can destroy the strain gauge.



FIGURE 2-12 SHOTCRETE STRAINGAUGE (GEODATA ZT GMBH, 2008B)

## 2.4.2 CONCLUSION ABOUT SENSOR TECHNOLOGY

As mentioned before, only the most common sensors are covered in the previous subchapter. A classification can be done through various approaches. Normally more than one sensor type is used in a monitoring system. In table 2-3 the characteristics of some selected sensors are summarized.

TABLE 2-3 LIST OF SENSORS

Sensor	Resolution	Precision	Accuracy	Frequency	Measurement range
Tacheometer	1 mm	1 mg angel	1 mm/1'' <sup>1</sup>	20 Hz <sup>1</sup>	Dist. up to 3500 m
Accelerometer	12.5µg/Hz <sup>2</sup>	75 pm/g <sup>2</sup>	/	< 500 Hz <sup>2</sup>	plus minus 10 g <sup>2</sup>
Tiltmeter	0.0006° <sup>3</sup>	/	0.01° <sup>3</sup>	< 10 Hz <sup>3</sup>	plus minus 15° <sup>3</sup>
GNSS	2 mm <sup>4</sup>	1 mm <sup>4</sup>	0.03 mm <sup>4</sup>	< 20 Hz <sup>4</sup>	/
Leveling	0.01 mm <sup>5</sup>	0.4 mm <sup>5</sup>	< 1 mm <sup>5</sup>	< 0.3 Hz <sup>5</sup>	100 m <sup>5</sup>
FOS	10 nm <sup>6</sup>	2 µm <sup>6</sup>	0.1 µm <sup>6</sup>	1 kHz <sup>6</sup>	plus minus 5 mm <sup>6</sup>
TLS	0.4 mm <sup>7</sup>	/	3 mm <sup>7</sup>	1000 kHz <sup>7</sup>	100 m <sup>7</sup>
Strain gauge	1 mε <sup>8</sup>	/	2 µm/m <sup>8</sup>	/	8000 µm/m <sup>8</sup>
Inclinometer	0.005 mm <sup>9</sup>	0.002° <sup>9</sup>	2 mm <sup>9</sup>	/	225 m <sup>9</sup>
GBSAR	0.5 m <sup>10</sup>	/	0.01 mm <sup>10</sup>	4 kHz <sup>10</sup>	4 km <sup>10</sup>
Hydrostatic leveling	2 µm <sup>11</sup>	0.1 µm <sup>11</sup>	up to 3 µm <sup>11</sup>	30 Hz <sup>11</sup>	50 mm <sup>11</sup>

<sup>1</sup> Leica (2015a)

<sup>2</sup> HBM (2018)

<sup>3</sup> RST Instruments (2018a)

<sup>4</sup> Leica (2016b)

<sup>5</sup> Leica (2015b)

<sup>6</sup> Lienhart (2013)

<sup>7</sup> Leica (2016a)

<sup>8</sup> Geodata (2008c)

<sup>9</sup> RST Instruments (2018b)

<sup>10</sup> Metasensing (2018)

<sup>11</sup> Gassner (2009)

It can be asserted that the available sensors enable static as well as dynamic monitoring of bridges with accuracy up to the µm sphere. But it is still the task of the surveying engineer to choose the most suitable sensors. A single sensor respectively a sensor type can only be one part of a monitoring system. Which other factors must be taken into account is highlighted in the following subchapter.

## 2.5 BRIDGE MONITORING SYSTEM

Kuhlmann et al. (2014, p.1) stated that “engineering geodesy is an application-oriented science”. All the creativity of the surveying engineer is needed to design a monitoring system for a civil engineering structure. There are no specific rules because every case is unique. It depends on the type of the civil engineering structure which varies from high-rise buildings, tunnels in the underground, power plants, bridges, roads and much more. It depends on the environment which varies from desert, inner city, off-shore or high-alpine. There are various types of bridges (figure 2-13) so even for this specific type of engineering structure no general rules can be constituted. But there are many more things which must be taken to mind but cannot be numerated. They are not only technical nature, very often the engineer is confronted with unexpected practical problems. At a subway construction site in Delhi, India, monkeys were interrupting a continuous measurement process by stealing the prism targets. Furthermore, it must be taken into consideration that during the monitoring measurements the bridge could be under construction or in operation. Road traffic, trains and pedestrians are passing by. This has an effect on the monitoring and its measurements and on the other hand the operation of the bridge should not be affected by monitoring. Last but not least the monitoring itself has to be efficient in an economical way.



FIGURE 2-13 RADEZKY BRIDGE IN GRAZ

From these facts we can conclude that technical expertise and experience are two key elements to design and maintain an effective monitoring system which fulfills the requirements with high performance. The task of setting up a monitoring system is very interdisciplinary. The surveyor needs an understanding of the measurement object, its construction and operation as well as the outer and inner effects which could cause deformation. A major problem is the different technical language of the various engineering disciplines involved.

**For the design of a bridge monitoring system some basic information is needed:**

- aim of the monitoring system
- expected cause of the deformation

- dimensions of the prospected deformation
- size of the surveillance area
- prediction of the temporal development of the deformation process
- accessibility of the measurement object
- several factors which could influence the measurement process
- available budget

**The requirements for a bridge monitoring system are the following:**

- Definition of an appropriate coordinate reference system.
- Design of an effective geodetic monitoring network.
- Sensor selection: depending on the requirements suitable sensors have to be evaluated.
- Specification of the measurement accuracy.
- Quality: The performance of the monitoring systems has to be constantly observed.
- Redundancy: With time survey points could be destroyed. Hence a sufficient number of redundant survey points is needed. In case of a measurement object sensitive to safety it could be necessary to operate with different measurement methods to compensate a possible loss of a distinct measurement technique.
- Adaptability: As mentioned before, every monitoring system is confronted with a lot of unpredictable events. Therefore, the monitoring system should offer room for adaptations.
- Timetable: For the coordination of the measurements a timetable is needed. In some cases, only short time slots are available for measurements (e.g. tunneling).
- Alerting: If thresholds are exceeded the system must alert appropriate to an emergency plan.
- Documentation: Extent, content and form of the documentation must be specified.
- Economic: Budgetary constraints are always a topic.

As shown in the list above and mentioned before, a high level of knowhow is necessary to develop an effective monitoring system fulfilling these extensive requirements.

# 3 SIMULATING BRIDGE DEFORMATION

## 3.1 A BRIDGE MODEL FOR THE IGMS

Content of this master's thesis is the design and development of a small-scale bridge model for the IGMS to enable the evaluation of static and dynamic monitoring systems and various sensors. Without a bridge model with which measurements and sensor testing could be carried out under laboratory conditions such tasks could only be performed outdoor with real bridges or by usage of external laboratories. Laboratories offer a controlled environment ideal for sensor and equipment testing. The designed bridge model offers a much wider spectrum of different test arrangements and experiments. The bridge model could also be used within lectures and laboratory practical's. From this planned purpose the requirements for the model were derived.

The first step was an investigation about small scale bridge models for geodetic research purposes and the definition of the requirements and desired capabilities. Several other research institutions and universities are using bridge models. The swiss federal laboratories for material science and technology (EMPA) has built a model of a cable-stayed bridge for various research work. ISIS Canada Research Network built a pre-stressed concrete girder for examination of calculated and measured deflections (Mufti et al., 2014). The Civil and Materials department of the University of Illinois developed a model of a cable-stayed bridge. For the detection of cable damage, a Brillouin scattering measurement system was used for monitoring deck strain (Sabet et al., 2015).

### **Requirements for the IGMS model:**

- a.) Knowledge of the physical characteristics
- b.) Predefined dimensions
- c.) Modular design for a possible future expansion or adaption
- d.) Opportunity for testing of different sensors
- e.) Deformability
- f.) Mechanical production through the internal engineering service
- g.) Costs

#### **a.) Knowledge of the physical characteristics**

For the system identification the physical characteristics of the bridge model (transfer function) must be known. Especially the behavior of the bridge model under various static and dynamic load cases is of special interest for sensor and equipment testing. See chapter 2.2.3.

#### **b.) Predefined dimensions**

The size of the model is set by the dimensions of the IGMS measurement laboratory. Apart from this smaller model dimensions and weight are easier to handle and for example reduce the size of the bridge bearing.

**c.) Modular design for a possible future expansion**

The set-up of the model should enable expansion and technical adaptations for different configurations for future research work.

**d.) Opportunity for testing of different sensors**

The model was designed for tests of and measurements with total stations and prisms installed on the bridge deck as well as accelerometers. Additionally, a laser triangulation sensor was used for additional distance measurements. The installation of strain gauges, fiber optical sensors, temperature sensors and so on is possible without major adaptations to the model.

**e.) Deformability**

The model should be suitable for static and dynamic deformation and vibration testing. This means that it must be possible to deflect the bridge deck with appropriate force. This means that the needed force for the deflection should not be too high ( $< 20$  [kg]). Based on the measurement range of the planned sensors a deflection of up to  $20$  [mm] was considered as proper. The options for vibration stimulation are explained in chapter 3.5.

**f.) Mechanical production through the internal engineering service**

The production of the bridge model and its implementation in the IGMS laboratory through the internal engineering service must be feasible. Therefore, the opinion of the institute's technicians Mr. Denkmaier and Mr. Lummerstorfer were obtained into the design process.

**g.) Costs**

The costs for the needed materials were also taken into consideration. At the beginning no budget was determined. On the basis of the requirements no cost estimation was possible at the beginning of the work. The final layout of the bridge model required materials in the value of below  $500$  € (structural steel, several small items). A vibration testing system primarily consisting of a shaker (see chapter 3.5.1) is available at the TU Graz. Thankfully the system was provided free of charge by the institute for mechanics (IFM) under direction of Univ.-Prof. Dr.-Ing. habil. Katrin Ellermann. All other equipment (total station, accelerometer etc.) is available at the IGMS.

## 3.2 FUNDAMENTALS OF THE APPLIED MECHANICS

From the physical point of view the bridge model can be simplified to a clamped beam. Beam theory is covered by the applied mechanics. In the following a very short introduction is given.

### 3.2.1 VIBRATIONS

An oscillation is a process where a state variable of the oscillation  $x = x(t)$  is subject to more or less regular temporal variation. Typical examples are oscillations of bridges under traffic load or the movement of the piston in an engine. The term vibration designates mechanical oscillations. The short introduction to oscillations is based on Flesch (1993, p.5-8).

#### Classification of vibration

- Harmonic vibrations: At harmonic vibrations a parameter  $x$  changes cosine or sinusoidal.

$$x = A \cdot \sin(\omega t + \theta) \quad (3.1)$$

With  $x$ ...time-dependent amplitude of the harmonic vibration  
 $A$ ...Amplitude  
 $\omega$ ...angular frequency  
 $\theta$ ...phase angle

- Periodic vibrations: With many movements the progress of a certain parameter  $x$  repeats after a time  $T$  (period).

$$x = f(t) = f(t + n\tau) \quad (3.2)$$

With  $n$  being an integer,  $\tau$  the period and  $t$  the time.

- Random vibrations: The magnitude for a certain point in time is not predictable. Only statistical statements are possible about random vibrations.

The behavior of oscillatory systems is influenced by the following physical properties:

- Mass
- Stiffness
- Damping behavior

#### Equation of motion for a SDOF-system

Eigenfrequencies and eigenmodes are structural properties independent from stress (Wenzel et al., 2005, p.178). It makes sense to use them for the assessment of the structural health status of a building

(maintenance on condition, see chapter 1.1). The equation of motion of a forced damped vibration of a SDOF (single degree of freedom) system after Wenzel et al. (2005, p.179) reads as follows:

$$m \cdot \ddot{x} + r \cdot \dot{x} + c \cdot x = F(t) \quad (3.3)$$

The angular frequency is defined as

$$\omega = \sqrt{\frac{c}{m}} \quad (3.4)$$

the damping ratio according to Lehr (Ernst Lehr, 1896 – 1945)

$$D = \frac{r}{2\sqrt{m \cdot c}} \quad (3.5)$$

and the transformed equation of motion

$$\ddot{x} + 2 \cdot D \cdot \omega \cdot \dot{x} + \omega^2 \cdot x = \frac{F(t)}{m} \quad (3.6)$$

With **m** being the mass, **c** the stiffness of the spring and **r** the damping.

### 3.2.2 EXPERIMENTAL METHODS OF STRUCTURAL DYNAMICS

The goal of experimental methods of structural dynamics is to acquire knowledge about the mechanical properties of components, structures or buildings stimulated by dynamic loads. The following objectives were defined by Flesch (1993, p.99):

- Measurement of the response oscillation caused by dynamic loads
- Determination of the dynamic parameters of structures and buildings like eigenfrequencies, eigenmodes or damping coefficients
- Investigation of stability against oscillations

Through the progress of sensor technology (see chapter 1.4) and analysis methods in the last decades such methods have been applied more often and today they are state of the art in civil engineering. One distinguishes between field trials and laboratory experiments. For dynamic testing either a natural or artificial stimulation of the structure is needed. Natural stimulation means for example weather phenomena like wind or loads induced by traffic. The disadvantage of this stimulation is that the progression of the force is unknown which means that no transfer function can be determined. Potentially not all eigenmodes are stimulated. The options for artificial stimulation are described in chapter 3.5 in more detail.

### 3.3 FUNDAMENTALS OF THE FINITE ELEMENT METHOD

The **Finite Element Method** (short FEM) is a commonly used technique in engineering and mathematical fields. It is a numerical method for the solution of continuous problems. With FEM it is possible to calculate deformation, stress, strain, support reactions, influence lines et cetera. The benefits of using FEM-software are reductions in development time, lower costs, early recognition of weaknesses, fewer test series and selected optimization of the construction. The improvement of computer performance and the development of off the shelf FEM-software lead to a wide spread use. In the following a short introduction to FEM is given based on Heunecke et al. (2013) and Flesch (1993). The basic idea of FEM is to subdivide a complex body (e.g. a bridge) or structure (e.g. a part of the earth surface like a slope) into small parts, so called finite elements. These discrete finite elements are for example bars, beams, plates, shell elements, tetrahedrons or hexahedrons, depending on the task and the geometry desired to model. The single elements are connected through nodal points (figure 3-1). It is also possible to insert intermediate nodal points between two nodal points which form the corner of an element.

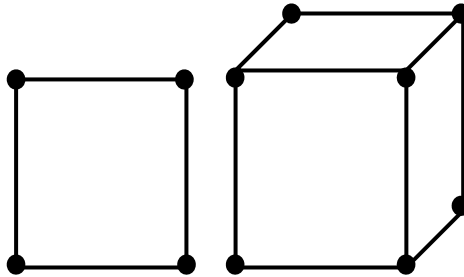


FIGURE 3-1 NODAL POINTS OF RECTANGULAR (LEFT) AND CUBIC (RIGHT) ELEMENTS

The fundamental equation of FEM which needs to be solved is the force-displacement relation.

$$K \cdot u = f \quad (3.7)$$

The deformation state is expressed by the product of the global stiffness matrix  $K$  and the displacement in the nodal points  $u$ ,  $f$  describes the forces which are effective at the nodal points. The equation states that there is equilibrium between the acting forces and the occurring displacements.

The displacement  $u$  of an element is represented in the following equation:

$$u = N_e u_e \quad (3.8)$$

The index  $e$  denotes to the regarded finite element.  $N$  is the so-called shape function. The relationship between strain and displacement is expressed with the following equation:

$$\varepsilon = Lu = LN_e u_e = B_e u_e \quad (3.9)$$

$B_e$  is the strain-displacement matrix. The relationship between strain and stress includes the elasticity matrix  $D$  which contains the two material parameters Young's modulus  $E$  and Poisson's ratio  $\mu$ :

$$\sigma = D(\varepsilon - \varepsilon_0) + \sigma_0 \quad (3.10)$$

$\sigma$  is stress,  $\sigma_0$  is the initial stress and  $\varepsilon_0$  is the initial strain.

There is an analogy between geodetic network analysis and finite element modelling. The stiffness matrix  $K$  corresponds to the normal equation system of an adjustment of a geodetic network and the force vector  $f$  to the vector  $n$  (Heunecke et al., 2013, p.124; Lienhart, 2006, p.77).

### 3.4 DEVELOPMENT OF THE MODEL

Based on the general requirements the deflection behavior and modal analysis were calculated for various beam geometries to identify the best design parameters for the model. This process was iterative. Basic estimates were calculated by hand, thereafter more complex models were developed and analyzed by using specialized software packages.

From the beginning it was decided to build the bridge model out of steel. The dimensions of the model were roughly deviated from the requirements explained in chapter 3.1. It was especially considered the possibility to bend the model with an appropriate force for the deformation measurement testing. From these initial random parameters an iterative design process started in finding the proper dimensions for the model.

The equation of the deflection curve  $\omega(x)$  due to a single point force is (figure 3-2):

$$\omega(x) = \frac{Fl^3}{48EI_y} \left[ 3\frac{x}{l} - 4\left(\frac{x}{l}\right)^3 \right] \quad (3.11)$$

Equation 3.12 applies to a beam with a locating bearing and a floating bearing. The maximum deflection  $\omega_{max}$  is:

$$\omega_{max} = \frac{Fl^3}{48EI_y} \quad (3.12)$$

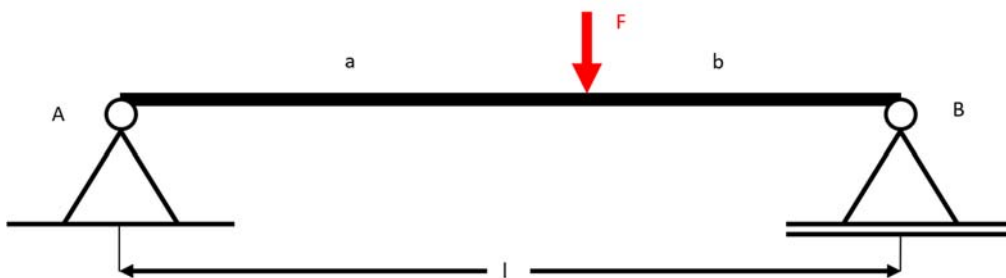


FIGURE 3-2 SINGLE POINT FORCE LOAD CASE OF A BEAM

After this first step two software packages, RuckZuck and AbaqusCAE, were used for more detailed calculations, also of eigenfrequencies and -modes.

#### RuckZuck

RuckZuck is a software for dimensioning and static calculation of 2D bar structures. It was developed by the *Mursoft Wörgötter, Kump OEG*, a software company residing in Graz, Austria. The software enables quick calculation of different load cases of static systems (figure 3-3). Individual structures can be designed, consisting of bars, pins, joints and supports. Various load cases can be designed by using concentrated, line or temperature loads. The software also offers the opportunity to calculate

Eigenfrequencies. RuckZuck 6.0 was used for quick calculation of beam deflection for various beam geometries.

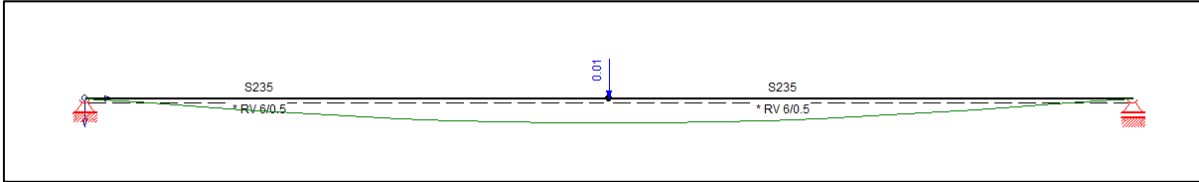


FIGURE 3-3 RUCKZUCK BEAM MODEL WITH STATIC LOAD AND DEFLECTION CURVE

**Abaqus/CAE**

This software is suitable for finite element analysis and computer-aided engineering and offers stress and deformation analysis, thermal and fluid flow analysis, electromagnetism, process simulation and a lot more. The software was first released in 1978 by *Abaqus Inc.* and is now a product of *Dassault Systems*. Abaqus/CAE or “Complete Abaqus Environment” interface integrates modeling, analysis and visualization of the results. The following describes the typical steps for creating and analyzing a numerical model. More detailed information can be found in the Abaqus User manual.

Abaqus has no built-in system of units. It is important to specify all input data in a consistent unit system. Through all the models the SI system was used. Abaqus is divided into modules where each module deals with a specific aspect of the modelling process such as defining the model geometry, setting interactions or generating a mesh.

The whole model is built by single components called parts. The geometry of a part has to be defined in the part module. All the materials and their parameters (e.g. Poisson’s ratio or Elasticity module) are specified in the property module and assigned to the individual parts. The individual parts are put together to a complete model in the assembly module. Thereafter a mesh through the whole model is calculated. Different static and dynamic load cases as well as the boundary conditions can be defined. The temporal order and type of calculation is scheduled with so called steps. After all this preliminary work the calculation is executed within the job module.

TABLE 3-1 MATERIAL PARAMETERS OF STRUCTURAL STEEL

Structural steel	
Mass density	7850 kg/m <sup>3</sup>
Young’s modulus	210 kN/mm <sup>2</sup>
Poisson’s ratio	0.3

The simple beam geometry was modeled by cubic parts (figure 3-4). The boundary conditions are realized by a floating bearing on the right side and a locating bearing on the left side (figure 3-2). Table 3-1 shows the used material parameters for structural steel. The 3D FE model consists of 4800 mesh elements and 15000 nodes.

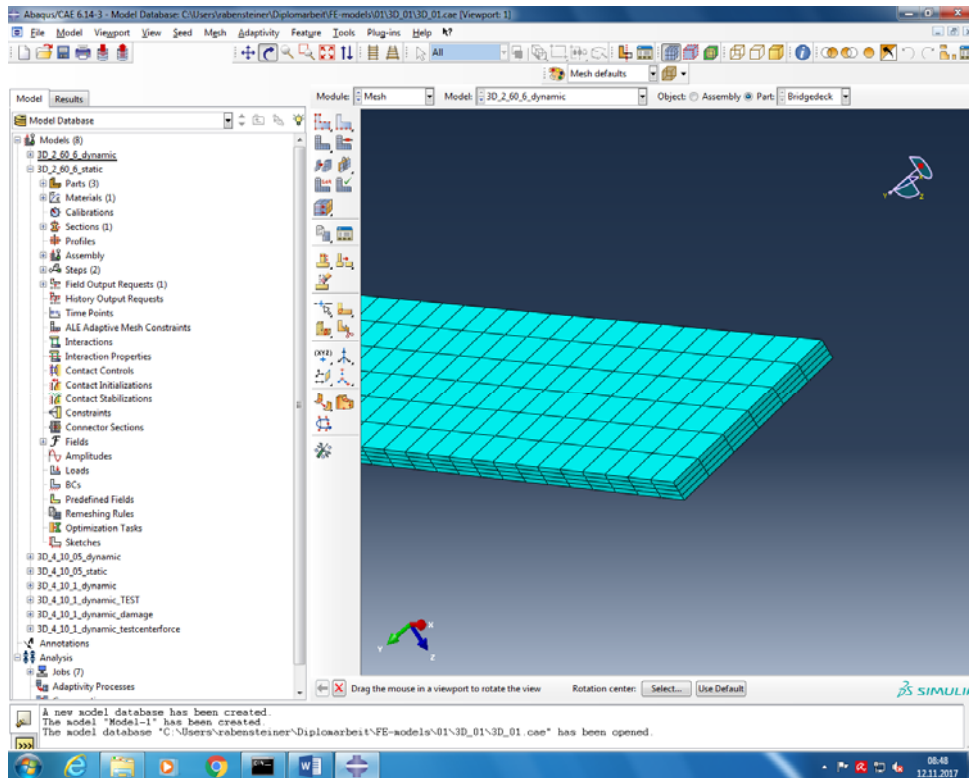


FIGURE 3-4 SCREENSHOT OF ABAQUS GUI WITH THE MESHED 3D BRIDGE DECK

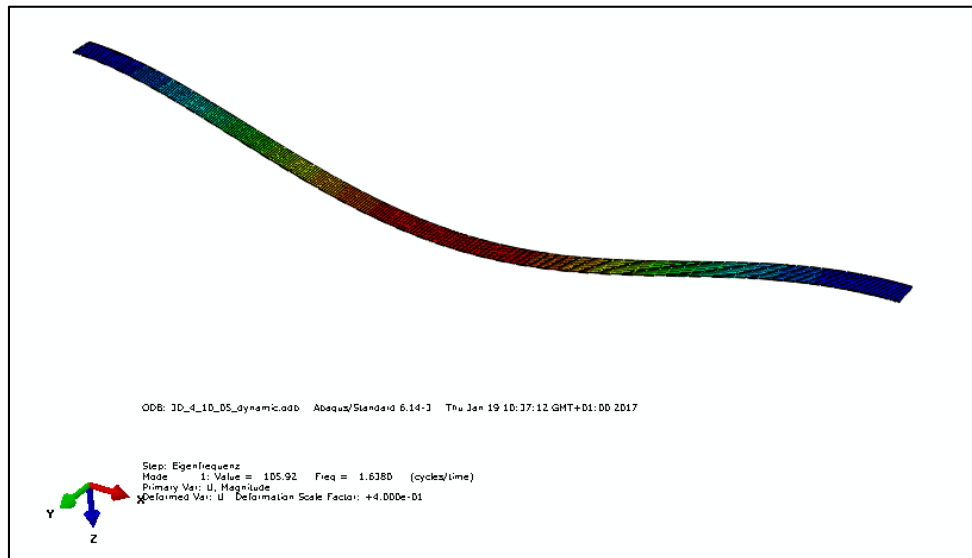


FIGURE 3-5 SCREENSHOT OF THE DEFORMATION OF THE 3D BRIDGE MODEL UNDER A STATIC LOAD

### Final dimensions of the bridge model

Static and dynamic load cases were calculated and evaluated (figure 3-5). Finally, the decision was made for a model made of structural steel with 2.0 m length, 60.0 mm width and 6 mm height. The beam has a dead weight of 5.652 kg. These parameters are the best tradeoff between the various requirements mentioned in the chapter before. A detailed comparison between the calculated theoretical values and the measured values of the real bridge model will be given in chapter 5. Eigenvalues and modes were calculated through modal analysis (figure 3-6) and are shown in table 3-2.

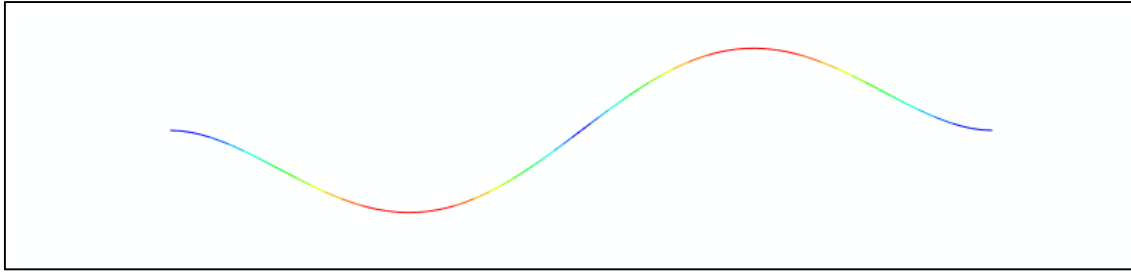


FIGURE 3-6 ANALYSIS OF EIGENMODES WITH ABAQUS

TABLE 3-2 EIGENVALUES OF THE BRIDGE MODEL CALCULATED WITH ABAQUS

mode number	eigenvalue	mode number	eigenvalue
1	5.4	11	304.5
2	17.8	12	360.1
3	37.2	13	374.6
4	54.1	14	393.4
5	63.7	15	451.9
6	97.3	16	536.6
7	138.2	17	609.1
8	174.1	18	628.7
9	186.4	19	646.8
10	241.8	20	728.0

Figure 3-7 shows the displacement of the center node of the beam due to a 24 N point force. Figure 3-8 shows the abating vibration due to a 5 N strong impulse impact (at the center of the beam).

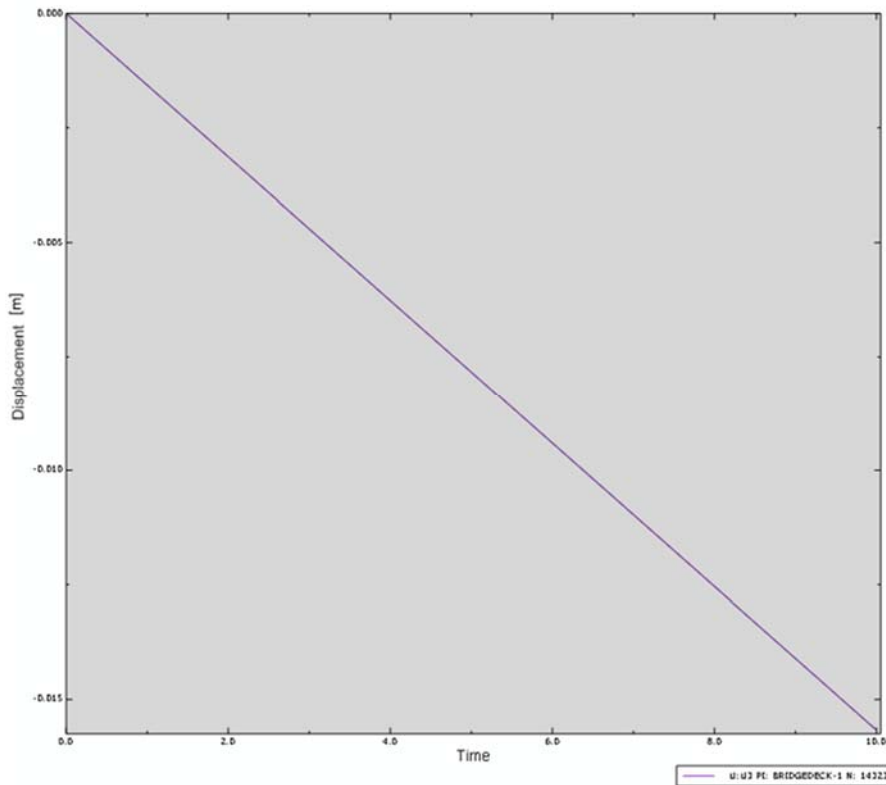


FIGURE 3-7 DISPLACEMENT DUE TO A STATIC FORCE OF 24 N

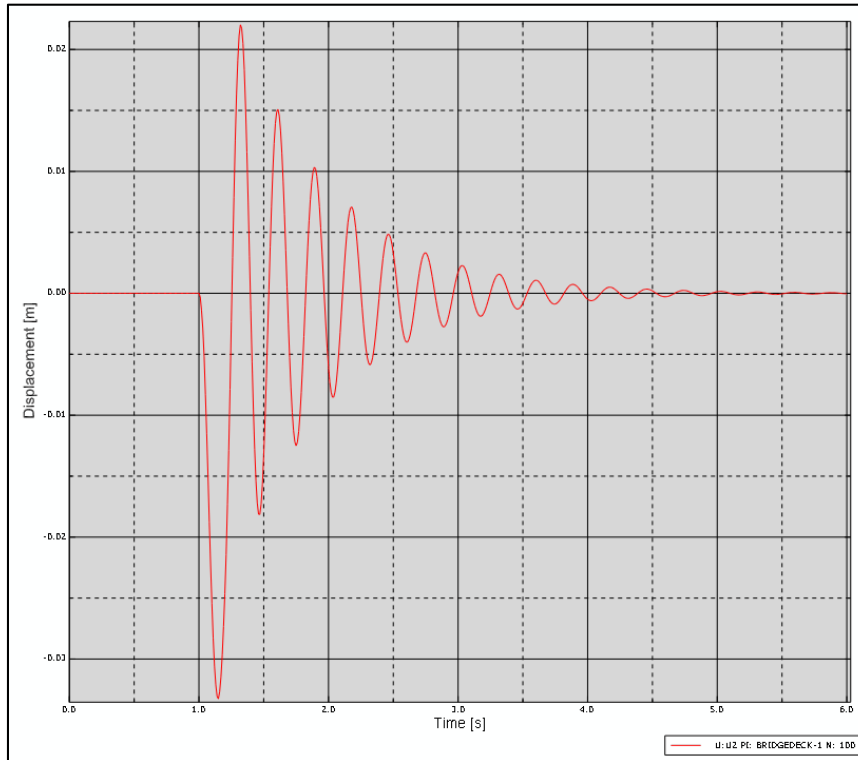


FIGURE 3-8 DEFLECTION OF THE BRIDGE DECK DUE TO A DYNAMIC IMPACT OF A 5 N FORCE

FEM is a numerical approximate solution. The interpretation of FEM results is demanding and errors within the modelling must be recognized as such. The calculated deformations  $\delta$  will generally differ from the measured values  $d$  (Chen, 1986).

$$\Delta = \delta - d \quad (3.13)$$

The reasons for these differences are listed below after Chen (1986):

- Errors within the material parameters
- Wrong modelling of the behavior of the material
- Errors in loading (causative) effects
- Measuring errors in  $d$
- Discretization errors (regarding the object geometry)

It's a matter of fact that every model is imperfect due to assumptions and uncertainties. In chapter 5 measured values from the built bridge model and calculated values from the FEM model are compared. With measured values an evaluation of the FEM model can be executed and it can be calibrated. The reader might be amazed that a sophisticated FEM software like Abaqus was used for the modelling of this simple model. On the one hand the software was simply available at IGMS and on the other hand a FEM model might be useful for further investigation. Possible future adaptations of the bridge model can be added to the FE-model. The usage of FEM models within advanced deformation analysis methods (integrated analysis) was mentioned in chapter 2.3.2.

## 3.5 VIBRATION STIMULATION

For scientific work it was important to know the input parameters generating oscillations of the beam. Various systems and techniques were identified. In order to avoid the purchase of a new system for this specific master thesis the loan from existing systems of other institutes of the TU Graz was favored.

For the testing of the sensors it was necessary to generate vibrations within the dynamic measurement range of the sensors. The sensor with the lowest dynamic measurement range is the total station with a maximum of 20 Hz (Leica MS60, see chapter 2.4).

### 3.5.1 VIBRATION STIMULATION SYSTEMS FOR LABORATORY EXPERIMENTS

**The following systems were reviewed:**

- a.) Shaker
- b.) Impact hammer
- c.) Hydraulic cylinders
- d.) Vibration table

#### **a.) Shaker:**

A so-called shaker is a transducer capable of producing a vector force. They are commonly used for vibration testing, to investigate the dynamic behavior of structures and components (modal analysis) or for fatigue and resonance testing. But they are also appropriate as velocity transducers or high-speed actuators.

In scope of this master's thesis an electrodynamic permanent magnet shaker V406 from Brüel&Kjaer (see appendix B) was used for the experiments (see also chapter 4.1). It covers a wide frequency band from 5 Hz to 9 kHz, is capable of producing a sine vector force of 196 N and a maximum displacement of 17.6 mm.

#### **b.) Impact hammer:**

An impact hammer is a common hammer instrumented with a force transducer in its head which enables it to deliver a measurable force. The oscillations are produced with a stroke on the test object. The vibrations induced by the impact respectively the response signal from the test object are measured with an accelerometer. It offers high flexibility due to its small dimensions. A disadvantage is the non-reproducibility of the impact force and position.

#### **c.) Hydraulic cylinders:**

For vibration testing of large and heavy objects like bogies of railway vehicles servo-hydraulic cylinders are used. Such systems are large, complex and expensive and therefore considered unsuitable for the experiments.

#### **d.) Vibration table:**

A so-called vibration table was taken into consideration as it was used by Neitzel (2007) for the testing of velocity and acceleration sensors. These vibration tables were rejected since they do not offer the whole spectrum needed for the experiments especially regarding the displacement capability.

### 3.5.2 VIBRATION STIMULATION SYSTEMS FOR REAL BRIDGES

The Austrian Institute of Technology (AIT) is using a mobile reaction mass exciter for vibration stimulation of infrastructure objects and buildings. The **Mobile Seismic Simulator (MoSeS)** is loaded on a truck (see figure 3-9), off loadable through a skip loader device (Austrian Institute of Technology, 2015). Vibrations are generated through a moving mass which is driven by a hydraulic cylinder (see figure 3-9). The maximum achievable exciter force is 15 kN (25 kN with anchor support). The achievable frequency range is 0 to 80 Hz with the possibility to use frequency sweeps. It is able to produce sine wave, random waveforms and time signal replication excitation (Austrian Institute of Technology, 2014).

It is used for field testing of the effect of vibration stimulation of existing infrastructure like bridges or buildings. The impact of vibration, for example as a result of construction work, to the environment can be examined as well as the health condition of buildings. Such experiments also enable the adaption and calibration of calculation models.



FIGURE 3-9 MOBILE SEISMIC SIMULATOR FROM AIT (PICTURE AIT)

# 4 DEVELOPMENT OF A MEASUREMENT SYSTEM

After the dimensions of the bridge model were defined (chapter 3) a measurement system as well as a system for dynamic stimulation were developed. This chapter provides an insight into both systems. In subchapter 4.3 the post processing and analysis of the acquired data is explained.

## 4.1 INSTRUMENTATION AND SENSORS

As stated in chapter 3.5.1 an electrodynamic permanent magnet shaker V406 from Brüel&Kjaer (figure 4-1) was used for the experiments. The shaker was positioned below the bridge deck. It can be linked to the beam (deck) via a bar. At the end of the bar a force transducer is installed for the measurement of the forces induced by the shaker. The force transducer can be glued to the beam with a two-component adhesive. In some cases, it is sufficient to place the beam loosely (without using adhesives or a mechanical connection) on the force transducer. The shaker is operated with a PC and LMS test.lab software from Siemens. LMS test.lab is an integrated software package for noise and vibration testing. For shaker control the spectral testing unit of LMS test.lab was used. The PC is connected to the LMS Scadas data acquisition system (figure 4-2). A force amplifier is interconnected between the shaker and the LMS Scadas.



FIGURE 4-1 SHAKER V406



FIGURE 4-2 PC FOR SHAKER CONTROL, LMS (UPPER LEFT) AND AMPLIFIER (LOWER LEFT)

The shaker V406 is capable of producing a maximum random force of up to 89 N and a maximum displacement of 17.6 mm. It has a useful frequency range from 5 Hz to 9 kHz (Brüel & Kjaer, 2012).

A Leica 360° mini prism (GRZ101) is mounted via a screwed joint on top of the beam for measurements with the total stations. In the beginning a Leica TS16 was used. Later on, a Leica MS60 was in use. On top of the deck three HBM B12/200 accelerometers are installed (figure 4-3), also via a screwed joint. The principle of the acceleration transducer is based on a seismic longitudinal vibration system. It has a fixed mass and relative damping between mass and body (HBM, 2000, p.13). The relative displacement of the mass to the body is proportional to the effective acceleration. It is transferred into an electrical signal for further processing (HBM, 2000).



FIGURE 4-3 ACCELEROMETERS AND 360° MINI PRISM MOUNTED ON THE TEST BED

For the verification of the measurements from the total station and the accelerometers a laser triangulation sensor (LTS) optoNCDT ILD1700-50 (figure 4-4) from  $\mu$ -Epsilon is installed above the prism. It has a measurement rate of up to 2500 kHz and a resolution of 3  $\mu$ m (Micro-Epsilon, 2008).



FIGURE 4-4 OPTONCDT ILD1700-50 MOUNTED ABOVE THE PRISM

In figure 4-5 the schematic composition of the measurement and data acquisition system with its sensors as well of the bridge model with its support and bearing is shown:

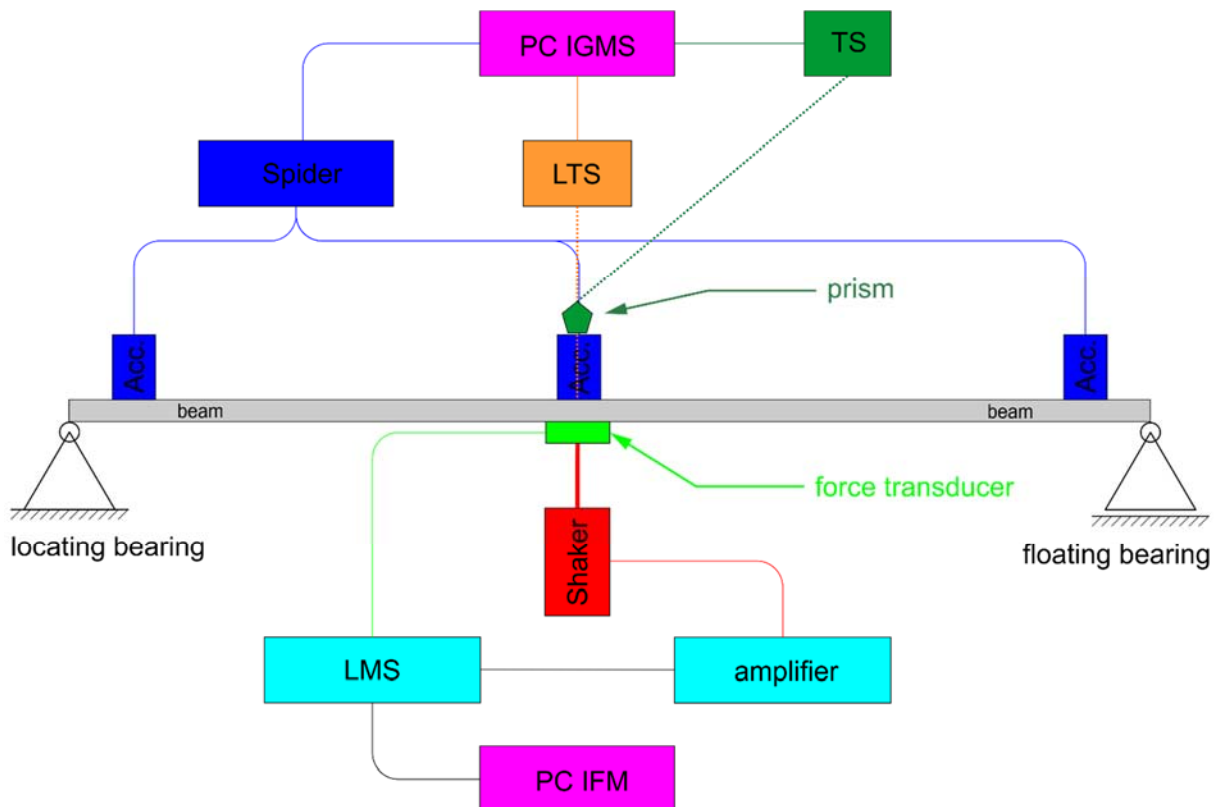


FIGURE 4-5 SCHEMATIC COMPOSITION OF THE MEASUREMENT SYSTEM

Spider ...Data recording unit (HBM)

LMS ...LMS SCADAS data acquisition system (Siemens)

## 4.2 TEST OF THE MEASUREMENT SYSTEM

For the verification of the functionality of the measurement system a small test bed was designed by the institute's technician Mr. Lummerstorfer before the manufacturing of the final bridge model. The second purpose of this sensor test system was to gain data of the different sensors to implement the data post-processing with Matlab software.

Basically, the test bed is a rigid beam with a floating bearing on one side and the shaker on the other side (figure 4-6 and 4-7). The prism, the accelerometers and the laser triangulation sensor are installed. Simulation of stress and strain is not possible, only rigid body movement can be simulated. Various experiments were conducted to check the functionality of all the sensors and to acquire data for the implementation of the analysis process with MATLAB software.

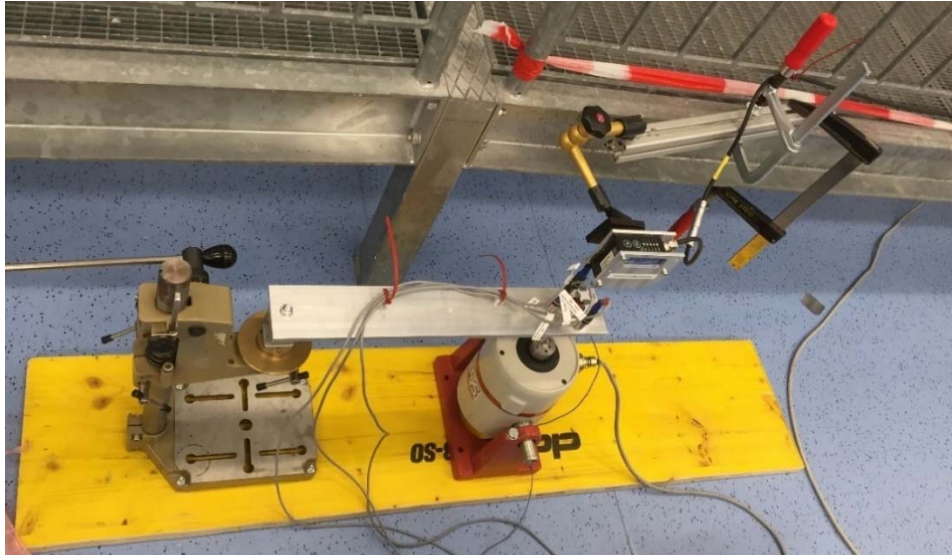


FIGURE 4-6 SENSOR TEST BED



FIGURE 4-7 SENSOR TEST BED

The accelerometers are operated via a PC which is connected to a HBM Spider data acquisition system via USB and operated via HBM Spider Beam software. The laser triangulation sensor is operated via the same PC and controlled via a software package from  $\mu$ -Epsilon.

Problems with the data acquisition were detected with the Leica TS16. Theoretically the TS16 has a measurement rate of up to 20 Hz with angular measurement only (Leica GeoCOM command 2003). The remote operation of the TS16 is realized with MATLAB and Leica GeoCOM (ASCII-based communication with the total station) via a PC with a RS232 serial port (with a baud rate of 115200). The basis GeoCOM scripts were provided by the IGMS and adapted by the author. The datafiles from the measurements with the TS16 showed various errors. Numerous characters were missing in the file. It is believed that these errors arise from a problem with the data transfer or writing of the data files. Lienhart et al. (2016) investigated the use of total stations for bridge vibration monitoring. Various approaches were presented to increase the measurement frequency as well as the resolution. It is critical to use the correct steering commands (Leica GeoCOM), a sufficient wait time and baud rate.

However, the error was not identified and also not investigated deeper. A modified MATLAB script, the use of a different PC and a Leica MS60 solved the problem.

Also, a faulty working accelerometer was identified. One of the three used HBM B12/200 accelerometers delivered twice as high acceleration data than the two other sensors (figure 4-8).

The error is reproducible. Errors with the sensor calibration can be eliminated. The sensor delivers before and after a calibration the same values. Plugs and connection of the sensor and the Spider data acquisition system were cross checked. The error source was not identified and not further investigated. In the following experiments measurement values of the presumably faulty accelerometer were not used as reference.

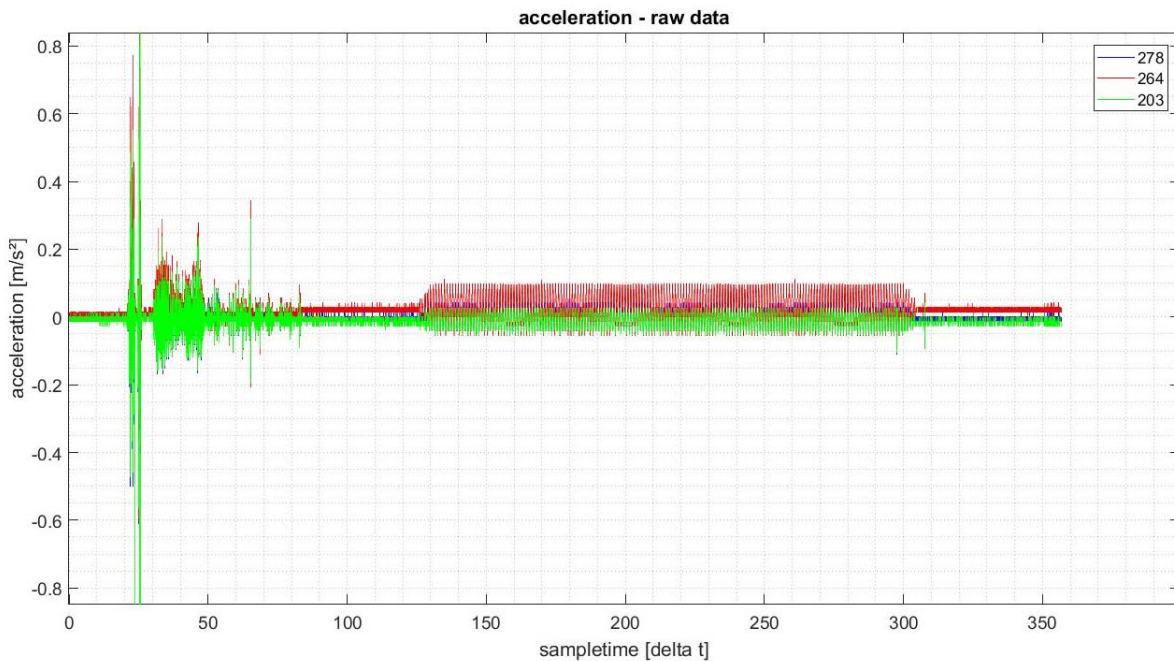


FIGURE 4-8 RAW ACCELERATION DATA FROM THE THREE USED HBM B12/200

### 4.3 DATA PROCESSING AND ANALYSIS

The collected data of the different sensors was post-processed and analyzed with the software package MATLAB (R2017a).

#### 4.3.1 POST-PROCESSING OF ACCELEROMETER MEASUREMENTS

The accelerometers measure acceleration (figure 4-9). To derive velocity and position data from accelerometer measurements the measured acceleration needs to be integrated. The relationship between position  $\mathbf{r}$ , velocity  $\mathbf{v}$  and acceleration  $\mathbf{a}$  is expressed with the following three equations:

$$\vec{r} = \int \vec{v} dt \tag{4.1}$$

$$\vec{v} = \frac{d\vec{r}}{dt} = \int \vec{a} dt \quad (4.2)$$

$$\vec{a} = \frac{d^2\vec{r}}{dt^2} = \frac{d\vec{v}}{dt} \quad (4.3)$$

Due to the vertical mounting of the accelerometers the sensor coordinate system coincides with the object coordinate system.

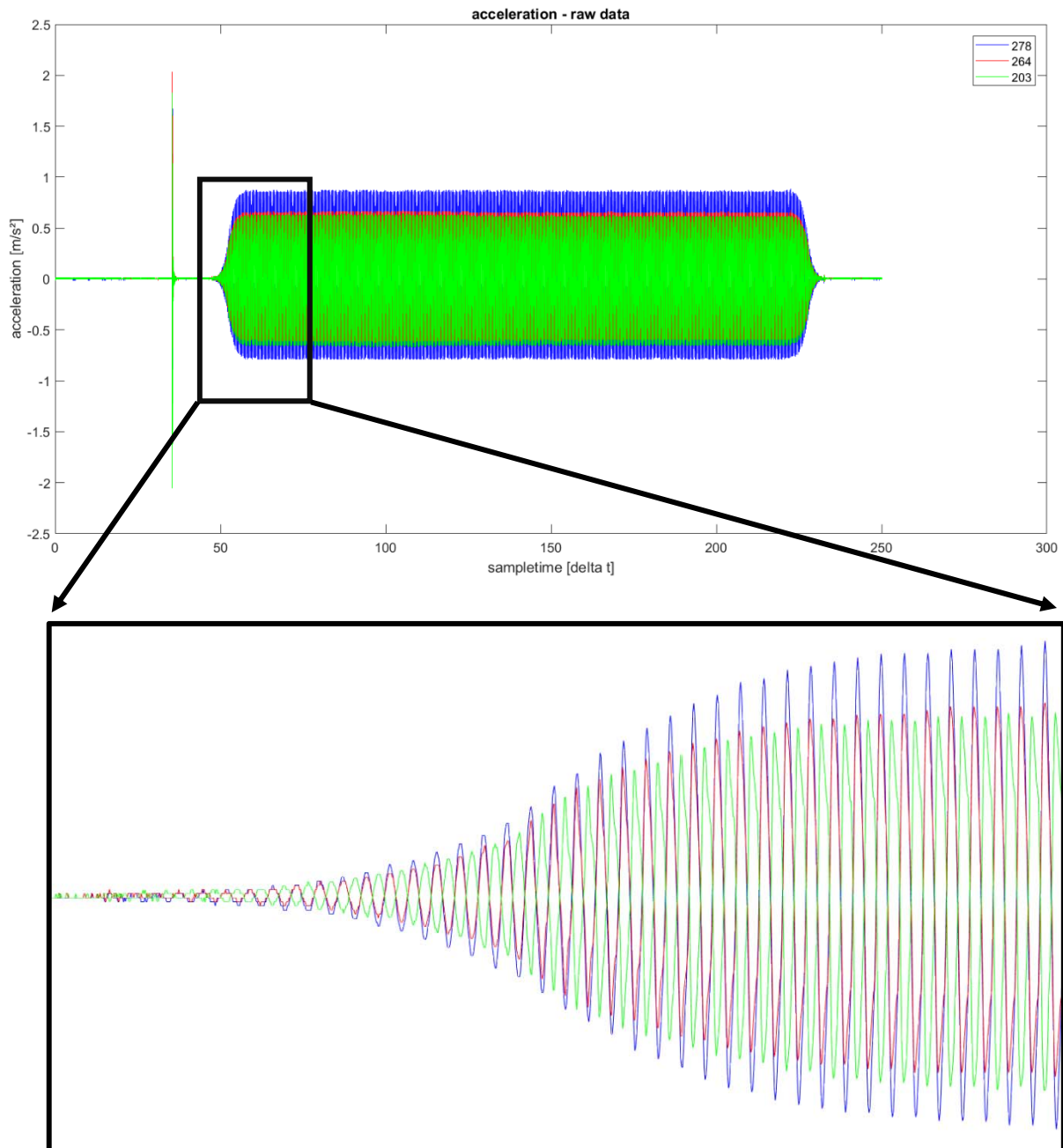


FIGURE 4-9 RAW DATA FROM THE THREE HBM B12 ACCELEROMETERS

In order to derive the correct position from acceleration, filters must be applied to the raw data. Initially the calculation of position was implemented after Neitzel (2007). To receive the position  $y_i$  from the measured acceleration values  $a_i$  ( $i = 1...n$ ) double integration is necessary. Numerical integration methods are applied because the measured values are available only at certain points with

the sampling rate  $\Delta t$  (time interval). A high sampling rate leads to a more accurate integration. Several numerical integration algorithms are available (e.g. Simpson formula, rectangle rule, trapezoidal rule). Dependent on the numerical integration method an integration error occurs which leads to a linear or higher degree path of the position. The author used the trapezoidal method proposed by Neitzel (2007). Additionally, the trapezoidal integration algorithm is already implemented within MATLAB.

$$y_{i+1} = \Delta t^2 \cdot a_i - y_i + 2y_i \tag{4.4}$$

The position is calculated from the two precursor position values, the measured acceleration and the time interval. Normally initial velocity and initial position must be known for appropriate integration. The position ( $y_0$  and  $y_1$ ) values (so called initial conditions) for the first integration step ( $i = 1$ ) are set zero which leads to an incorrect path. Known issues with accelerometers are offset- and drift errors which occur within the signal and manipulate the result (Slifka, 2004, p.13). Figure 4-10 shows the wrong distance proceeding as the result of the double integration of a sine wave vibration (like in figure 4-9). Figure 4-11 shows the wrong displacement progress in comparison to the laser triangulation data. It becomes clear how crucial the removal of drift errors is in order to get the correct position path. Neitzel first removes an adjustment parable. The high-frequency trend is removed through a moving average filter.

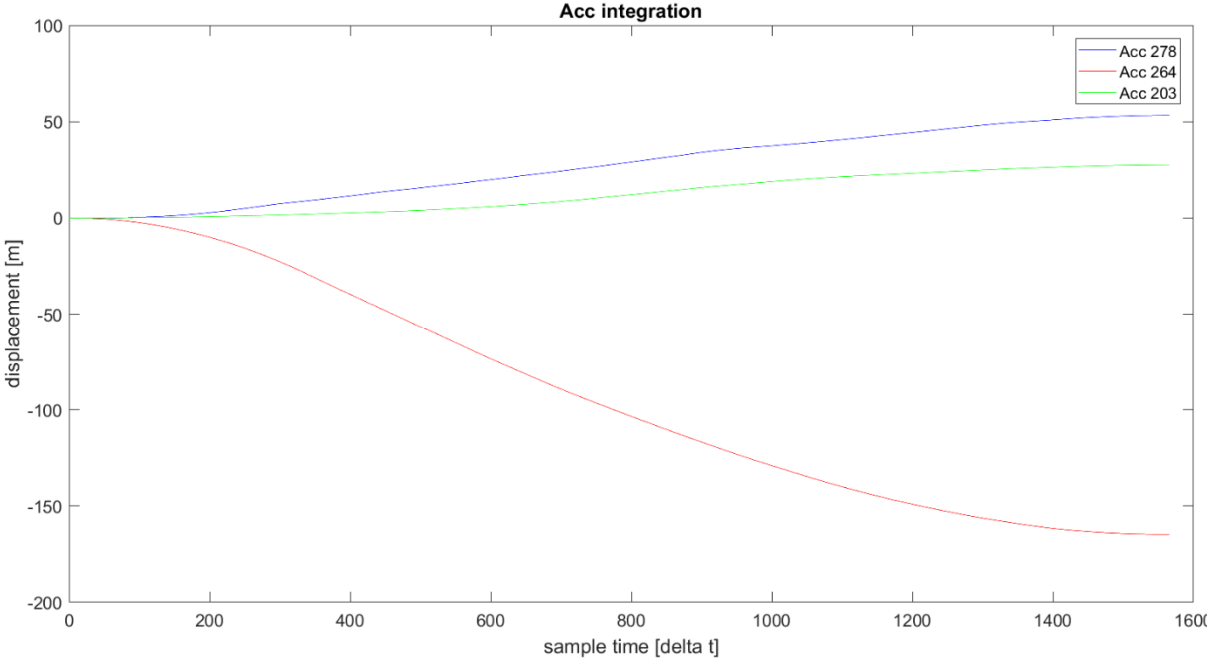


**FIGURE 4-10 INTEGRATION ERRORS**

The implementation of this solution was not successful and confirmed by the LTS displacement measurements. The author believes that the source for the disappointment can be found in the filtering of the accelerometer data. This process is highly fragile regarding the relief of disrupting influences from the raw accelerometer data.

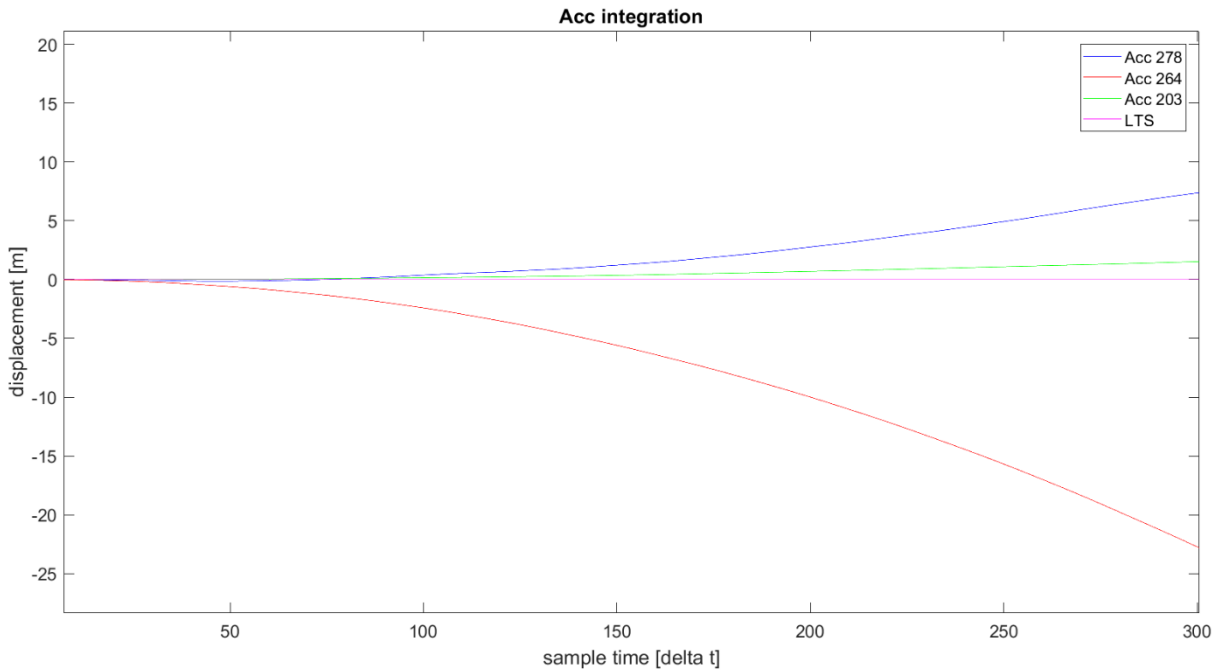


FIGURE 4-11 INTEGRATION ERROR IN COMPARISON TO THE LTS DATA

A second approach was tried out after Slifka (2004, p.13). He designed a two-step numerical trapezoidal integration procedure with a three-staged high pass filter system (figure 4-12) which does not require knowledge of the initial conditions (in comparison to the approach from Neitzel).

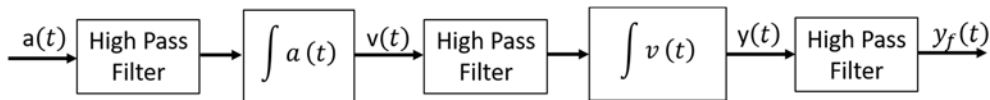
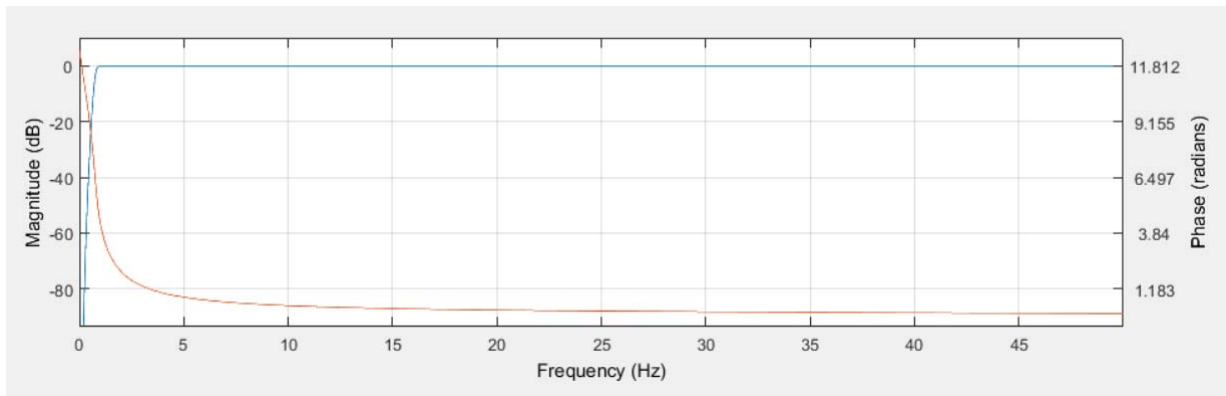


FIGURE 4-12 BLOCK DIAGRAM OF THE DOUBLE INTEGRATION AFTER SLIFKA

To eliminate the above-mentioned errors from the signal a high pass filter is applied before every integration step. An IIR (infinite impulse response) Butterworth filter was designed within MATLAB (see table 4-1 and figure 4-13).

TABLE 4-1 HIGHPASS FILTER PARAMETERS

Filter parameter	
response type	high pass
design method	infinite impulse response (IIR)
filter characteristic	Butterworth
filter order	minimum order
passband frequency	0.9 Hz
stopband frequency	0.5 Hz
passband ripple	0.5 dB
stopband ripple	30 dB



**FIGURE 4-13 MAGNITUDE RESPONSE OF THE USED HIGHPASS FILTER**

The calculated values (figure 4-14 and 4-15) were crosschecked with the position results from the total station and the laser triangulation sensor. To verify the whole process the laser triangulation position data was differentiated to acceleration values. The synchronized displacement data from the LTS and the accelerometer are shown in figure 4-16. In figure 4-17 the differentiated acceleration values from the LTS are compared to the measured values from the accelerometer.

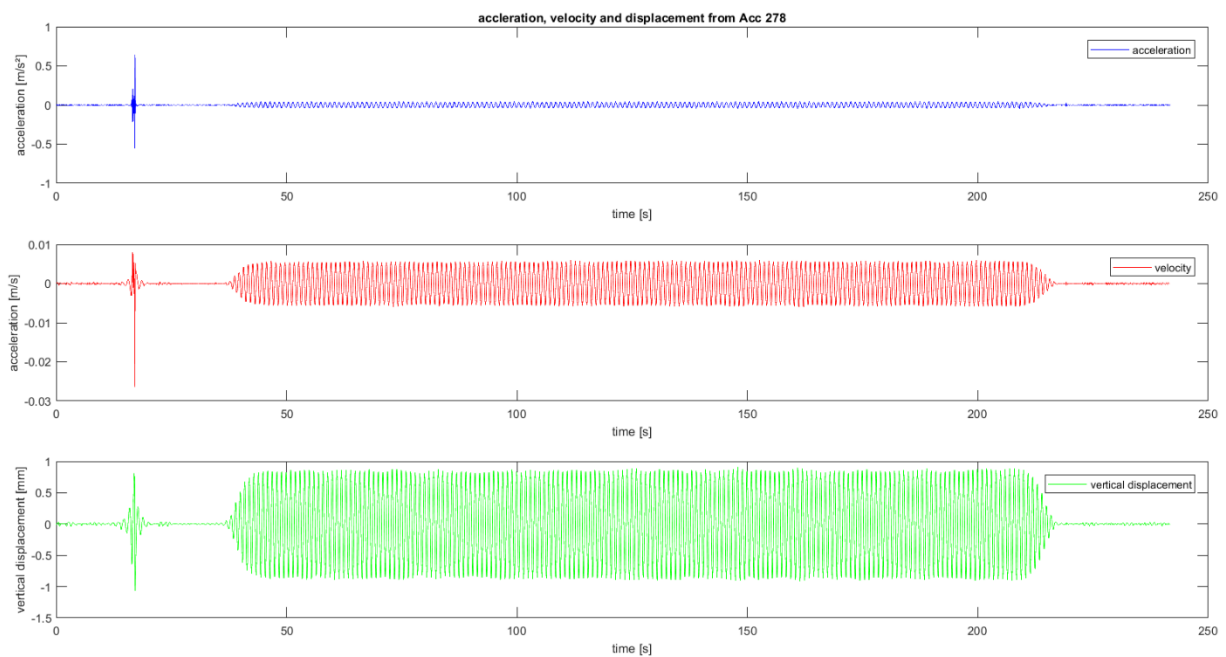


**FIGURE 4-14 ACCELERATION, VELOCITY AND POSITION FROM ACCELEROMETER 278**

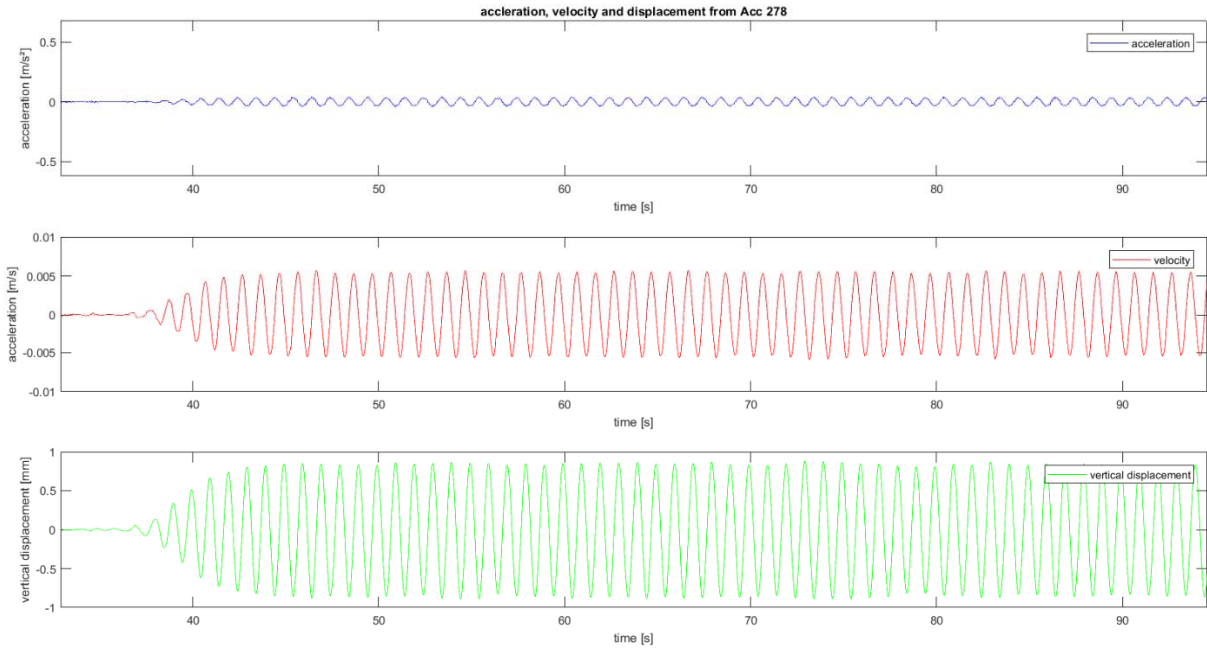


**FIGURE 4-15 ACCELERATION, VELOCITY AND POSITION FROM ACCELEROMETER 278, ZOOMED IN**

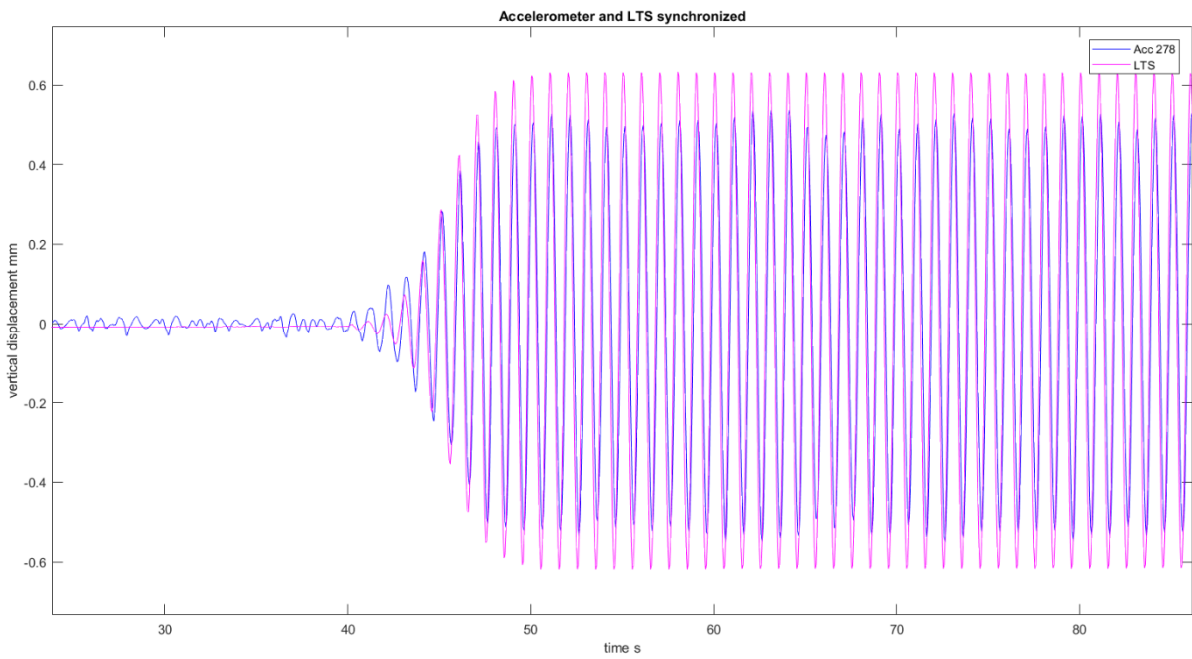


**FIGURE 4-16 ACCELEROMETER AND LTS POSITION DATA SYNCHRONIZED**

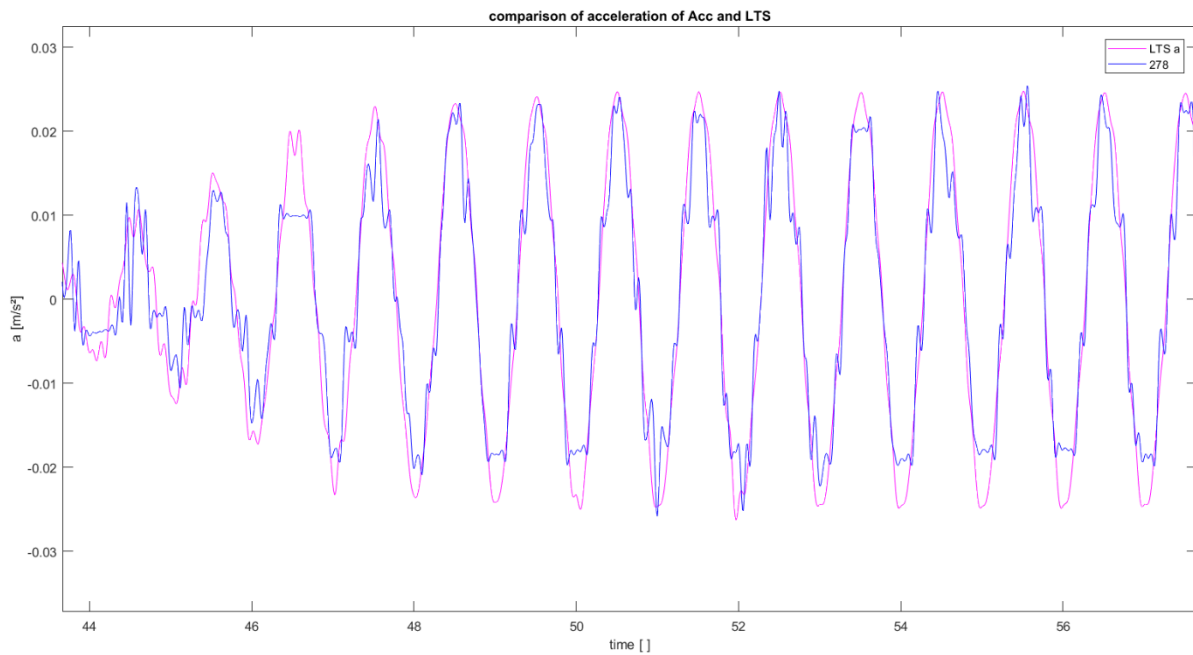


FIGURE 4-17 COMPARISON OF ACCELERATION BETWEEN ACCELEROMETER AND LTS VALUES

### 4.3.2 POST-PROCESSING OF TOTAL STATION MEASUREMENTS

The total station measures beside several other values the slope distance, the horizontal angle (Hz) and the vertical angle (V) to the target. The 3D polar coordinates (z-displacement) were calculated with the following equations:

$$\Delta z_i = s_i \cdot \cos \beta_i \quad (4.5)$$

$$z_i = z_s + \Delta z_i \quad (4.6)$$

$s$  donates the slope distance,  $\beta$  the vertical angle and  $z_s$  is the z-coordinate of the total station. Only relative displacement of the prism was measured in the vertical direction which means that the total station was not orientated within the reference system of the IGMS laboratory (figure 4-18). Figure 4-18A shows the Dirac impulse, figure 4-18B shows the buildup of the sine vibration. The ATR (Automated Target Recognition) as well as the compensator were calibrated before the measurements.

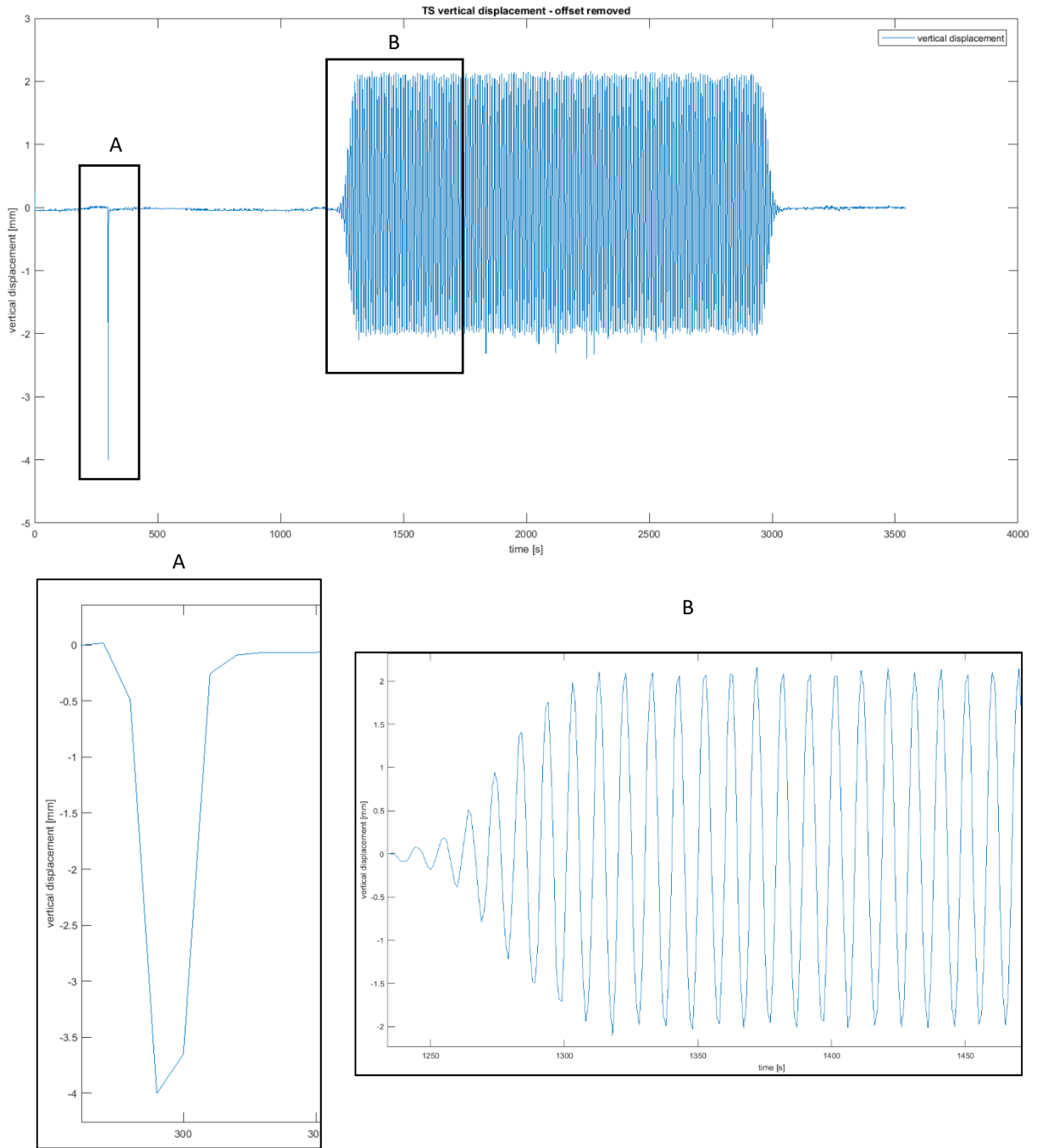


FIGURE 4-18 CALCULATED POSITION FROM TS AND ENLARGED AEREAS A AND B

### 4.3.3 POST PROCESSING OF LASER TRIANGULATION DATA

The optoNCDT 1700-50 is a so-called laser optical sensor. It uses a laser beam to determine the distance to an object by using the principal of optical triangulation, hence the designation laser triangulation sensor (LTS). The laser beam is monitored by a CCD-array. Every change of the distance between the sensor and the object leads to a change of the position of the laser point on the CCD-array. Via trigonometric functions the distance is calculated from this position change. The signal conditioning electronics and the processing is integrated within the sensor. To remove the offset the

mean value was subtracted. No further post-processing was applied to the data (figure 4-19). Figure 4-19A shows the Dirac impulse, figure 4-19B shows the buildup of the sine vibration.

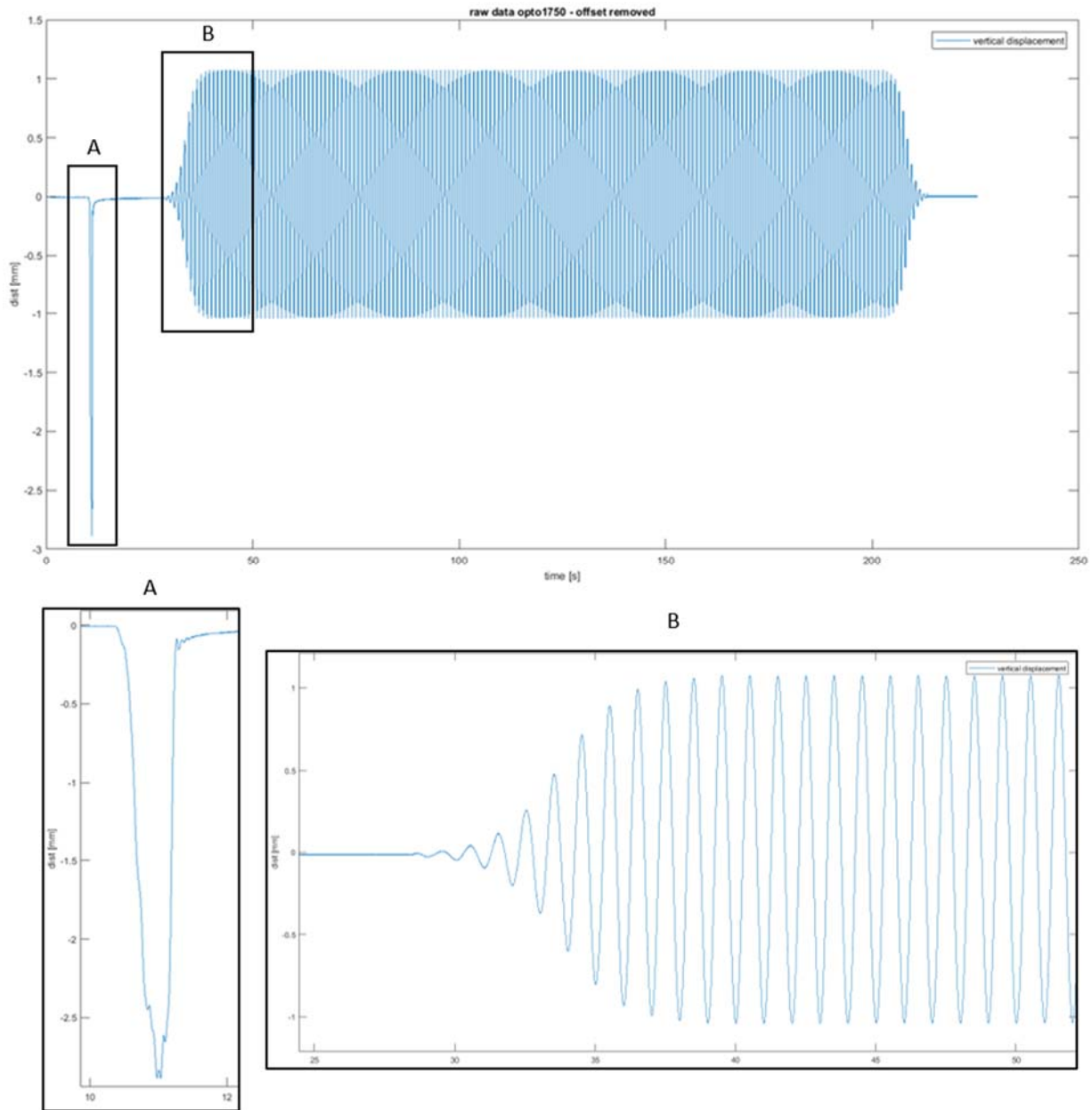


FIGURE 4-19 LTS RAW DATA WITH OFFSET REMOVED AND ENLARGED AREAS A AND B

#### 4.3.4 DATA SYNCHRONISATION

Crucial for every monitoring using multiple sensors is the time synchronization. One of the most commonly used methods is the time delay estimation (TDE) through correlation. By the cross-correlation function (CCF) it is possible to compare two time series  $x(t)$  and  $y(t)$ . These two timeseries represent a realization of random processes  $\xi(t)$  and  $\eta(t)$  which are assumed to be stationary Gaussian processes. The cross-covariance function expresses the affinity of the two timeseries.

$$\gamma_{xy}(t_1, t_2) = Cov(X(t_1), Y(t_2)) = E[X(t_1) - \mu_x(t_1)](Y(t_2) - \mu_y(t_2))] \quad (4.7)$$

The cross-correlation function is defined as follows:

$$\rho_{xy}(t_1, t_2) = \frac{\gamma_{xy}(t_1, t_2)}{\sqrt{\sigma_x^2(t_1)\sigma_y^2(t_2)}} \tag{4.8}$$

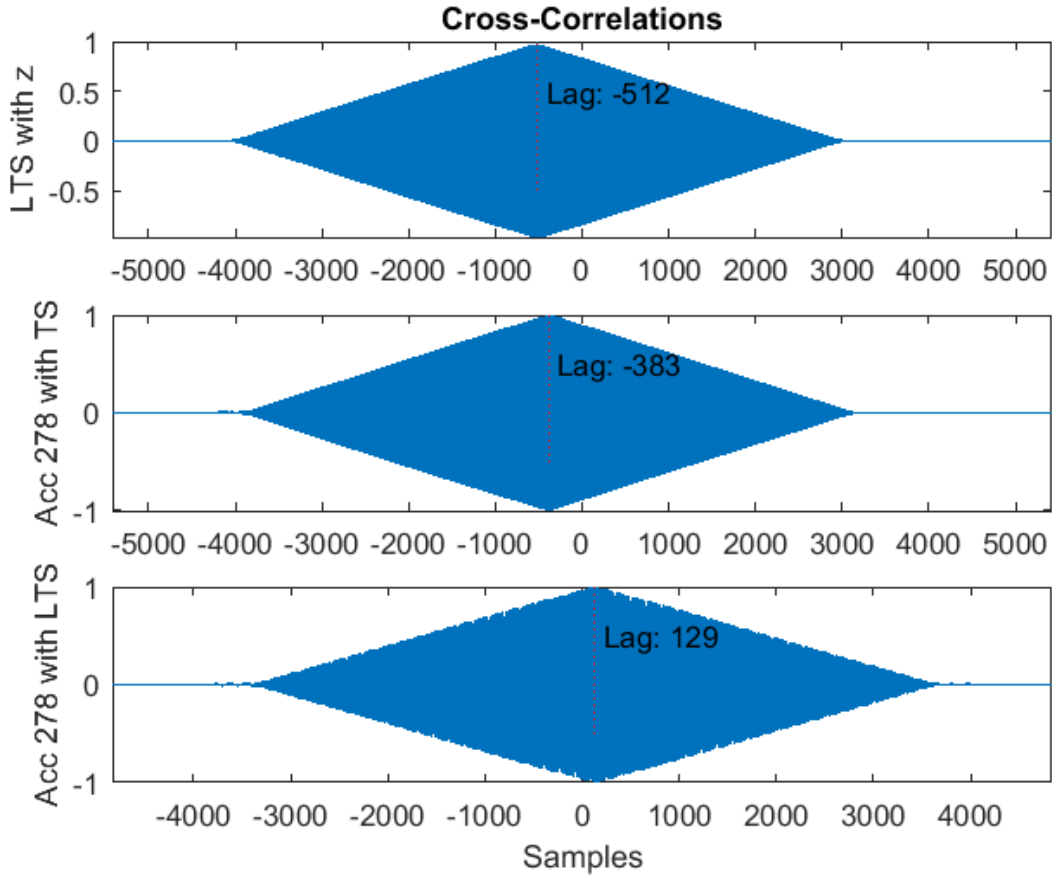


FIGURE 4-20 TIME LAGS BEWTWEEN ACCELEROMETER, LTS AND TS

Given two time series of finite length (in practice every time series is of finite length) the CCF has one maximum which denotes the time lag between the two timeseries (figure 4-20). Sine waves appear often at vibration monitoring (e.g. vibration of a bridge induced by road traffic) and also the used shaker V406 for vibration stimulation induces sine waves into the bridge model. To achieve better cross correlation results an artificial peak (approximation of the Dirac impulse) was induced before every measurement run. These peaks are visible at the beginning of the time series in figure 4-14, 4-18 and 4-19. Figure 4-21 shows the CCF result without an abrupt movement. The flat maximum as a result of bad correlation properties of the two time-shifted sine waves is clearly visible. Before every single test series, the beam with the prism and the accelerometers was moved abruptly upwards. This technique to improve correlation properties was mentioned by Gojicic (2016, p.16).

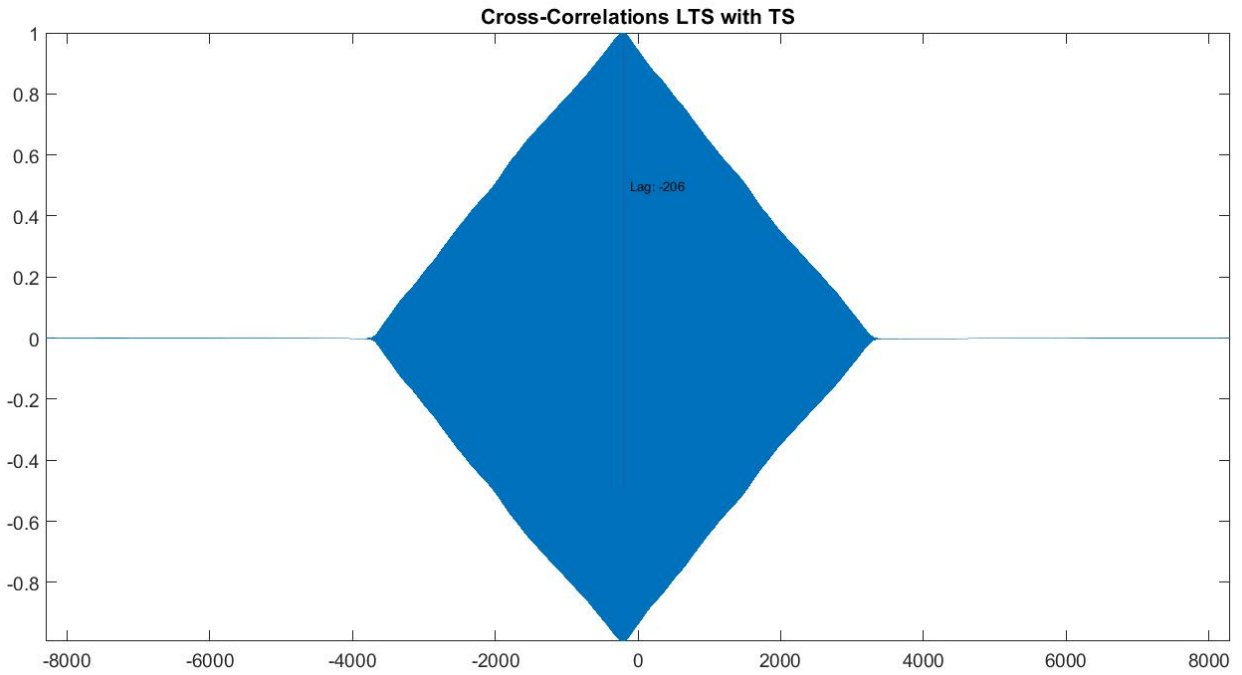


FIGURE 4-21 CROSS-CORRELATION BETWEEN LTS AND TS WITHOUT IMPULSE

The calculated lag correlates to the delay of the timeseries. Figures 4-22 and 4-23 show the synchronized time series from the total station, the laser triangulation sensor and the accelerometer. In both figures the mentioned Dirac impulse with a high amplitude is clearly visible at the beginning of each time series.

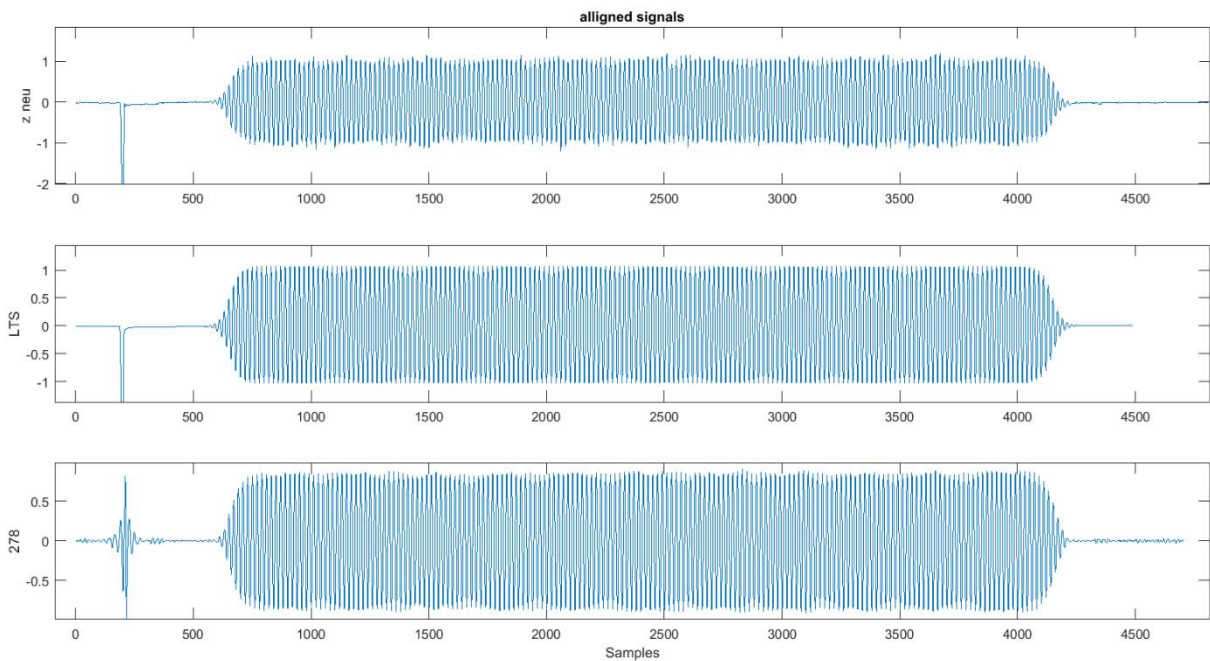


FIGURE 4-22 SYNCHRONIZATION OF ACCELEROMETER, TS AND LTS TIME SERIES

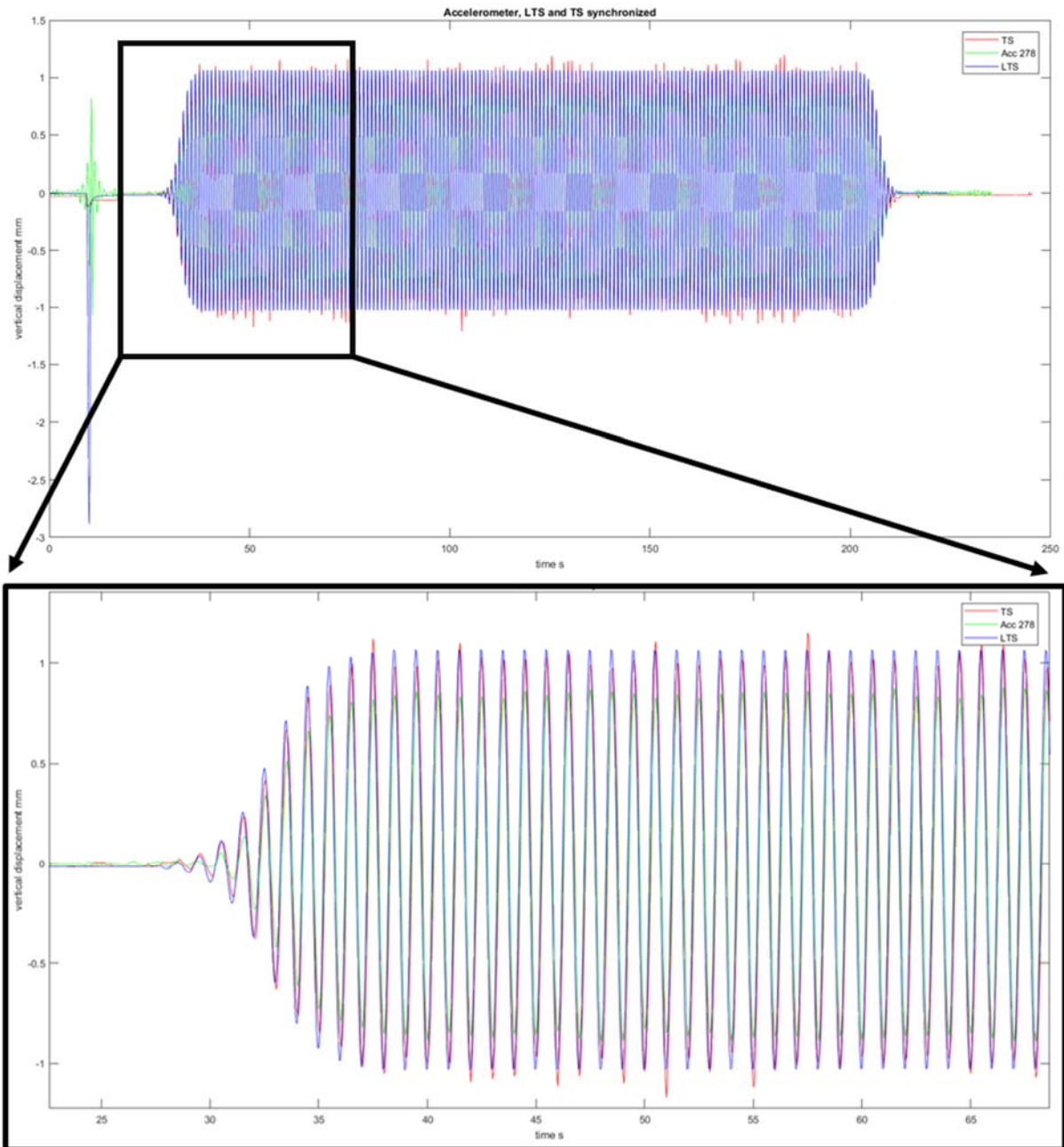


FIGURE 4-23 SYNCHRONIZATION OF TS, LTS AND ACCELEROMETER DATA

As can be seen in figure 4-23 the synchronization of the three timeseries through CCF was successful. The individual timeseries were aligned by shifting them according to the calculated lag. The results of the certain experiments are analyzed in detail within the following chapter.

## 4.4 CONCLUSION

A dynamic monitoring system consisting primarily of a total station, three accelerometers and a laser triangulation sensor was developed. A system for vibration stimulation by using a shaker was installed. Acceptance trials with a small test bed identified an unreliable accelerometer and a problem with the total stations' data acquisition system. An analysis process was implemented with MATLAB software. The data from the sensors is post-processed and synchronized via usage of the cross-correlation function. From observed acceleration displacement was derived. For the review displacement data was differentiated to acceleration. The implementation of this monitoring system to the realized bridge model is given in the next chapter.

# 5 APPLICATION TO THE BRIDGE MODEL

Chapter five explains the realization of the bridge model as well as the implementation of the measurement system (see also chapter 4.1) in detail. The results of various experiments conducted with the bridge model are shown. A comparison between measured values from the bridge model and calculated values from the FE-model is also given.

## 5.1 THE IGMS BRIDGE MODEL

The model is implemented on the horizontal comparator of the IGMS laboratory. This calibration facility is made of reinforced concrete and is 30 m long. It is equipped with a motor-driven trolley able to carry prisms and other items. The position of the trolley is measured with a laser interferometer. The comparator bench is primarily used for calibration and investigation of EDM and geodetic prisms. The solid design of the comparator bench made it possible to mount the bridge model on it. The mass of the bench is much greater than the mass of the bridge model so basically, we are not worried to influence the bench or in the worst case even to damage it. To verify this assumption an additional accelerometer was installed directly on the comparator bench in the immediate vicinity of the floating bearing.

The manufacturing of the designed bridge model was the task of Ing. Dietmar Denkmaier from the IGMS. The IGMS is equipped with a mechanical workshop thereby no external services were needed for the construction of the model.

### 5.1.1 MECHANICAL CONFIGURATION OF THE MODEL

The suspension for the bridge bearings is mounted on the steel-reinforced grooves of the comparator support. The suspension is made of a modular construction system called "Item" (building kit system). These aluminum profiles offer light weight and at the same time sufficient stiffness and stability. The locating bearing consists of two triangle shaped Item-profiles, the beam is clamped in-between them (see figure 5-1). The floating bearing is realized by two non-moving aluminum cylinders which are clamped in two Item-profiles (see figure 5-2). Figure 5-3 shows the bridge model mounted on the comparator bench. To strut the construction a longitudinal Item girder was placed between the two bearings (see figure 5-4).



FIGURE 5-1 LOCATING BEARING

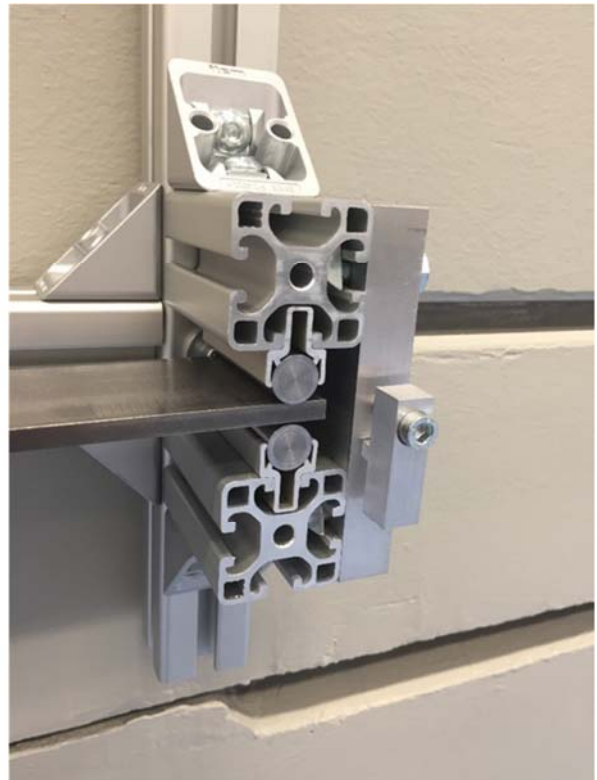
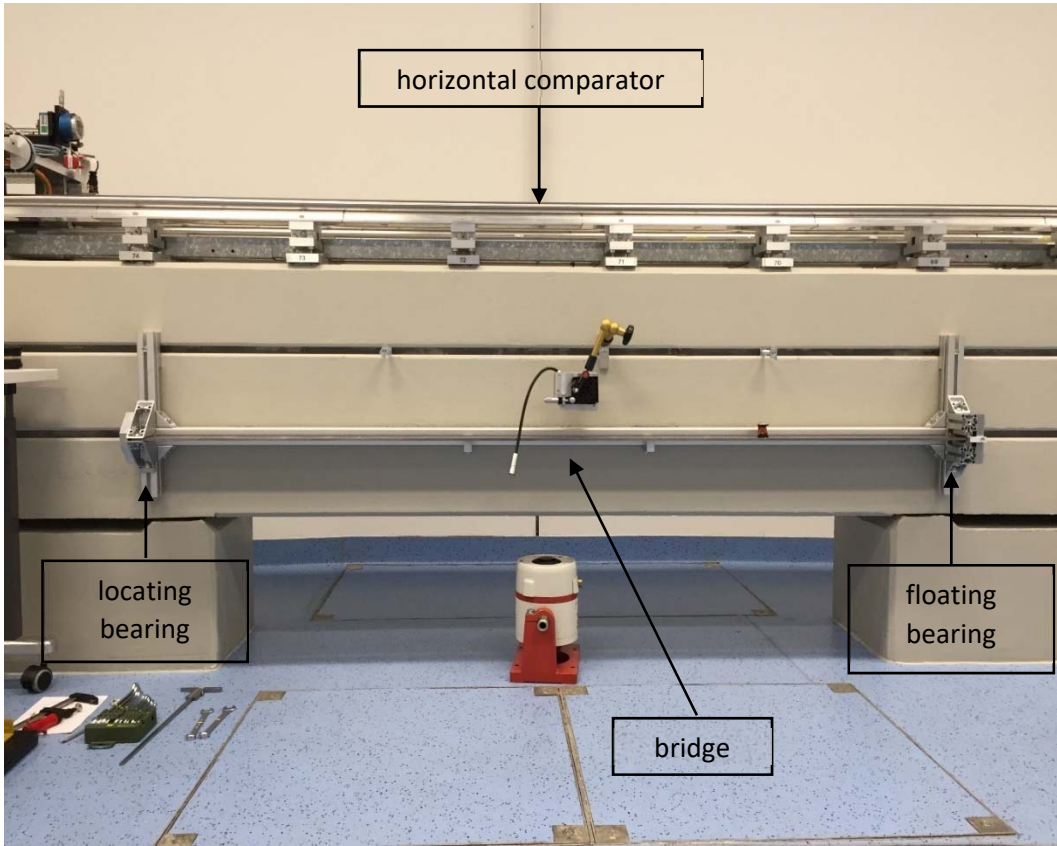
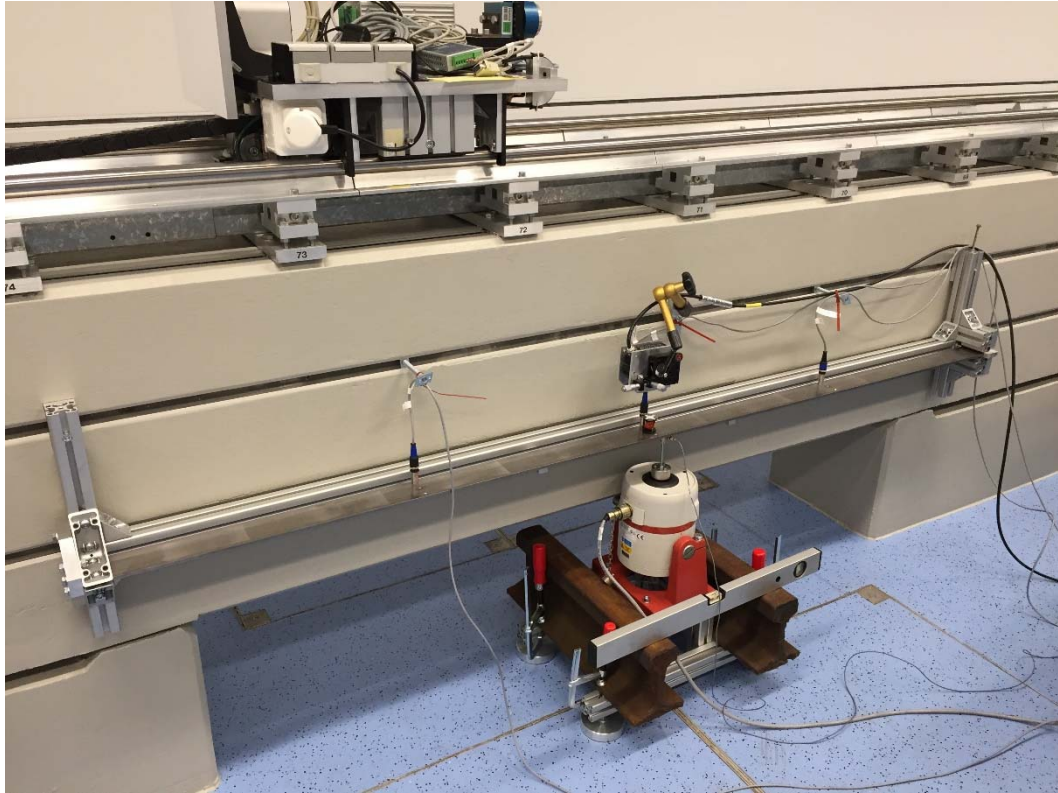


FIGURE 5-2 FLOATING BEARING



**FIGURE 5-3 BRIDGE MODEL MOUNTED ON THE COMPARATOR BENCH**



**FIGURE 5-4 BRIDGE MODEL**

### 5.1.2 OPERATING LIMITS OF THE BRIDGE MODEL

Operating limits of the bridge model regarding the input force (regulated in V) and the vibration frequency were defined together with Mr. Denkmaier (see Appendix A). The operating limits of the current design and configuration of the model are not the mechanical load limits of the construction. Rather they were defined for protecting the shaker and its subsystems from damage. And on the other hand, the propagation of the vibrations into the comparator bench as well as the influence of the bridge construction itself is unknown. The realization of the bridge model and especially its bearings can only be assumed as an approximation of the physical model (clamped beam). For safe and reasonable experiments above the defined operating limits a comprehensive investigation of the dynamic behavior of the bridge model is recommended.

### 5.1.3 INSTRUMENTATION OF THE MODEL

The instrumentation of the bridge model was already explained in chapter 4.1. The surface of the beam was burnished and cleaned. Bolt holes for the installation of the prism and the accelerometers (HBM B12) were placed on three cross sections with one-meter separation (see figure 5-5). Sensors can be mounted from above as well as from the downside of the beam. The LTS was again installed directly above the prism by a jointed arm mounted on the comparator bench. Additional accelerometers (PCB M353B15) can be installed on the deck with adhesive.



FIGURE 5-5 PRISM AND ACCELEROMETER

The shaker was placed on a platform made of an Item-structure which was additionally loaded with steel rails. The shaker was only operated in the vertical axis. During all experiments no movement of the shaker was observed visually. The platform is moveable to any desired position along the bridge model. The shaker induces the force via a specially designed bar into the bridge deck. The original bar from the IFM was considered as too small and additionally it was crooked. The newly designed bar is vertically adjustable. On the end of the bar the force transducer is installed (see figure 5-6). The connection between the force transducer and the bridge deck can be realized via an adhesive. For experiments in the low frequency ( $< 2$  Hz) range no direct connection is needed due to the gravity and the dead weight of the beam. Color marks were applied on the bar to detect deflections and torsions

of the interconnection. The total station was mounted on a pillar in a distance of approximately five meters to the bridge model.

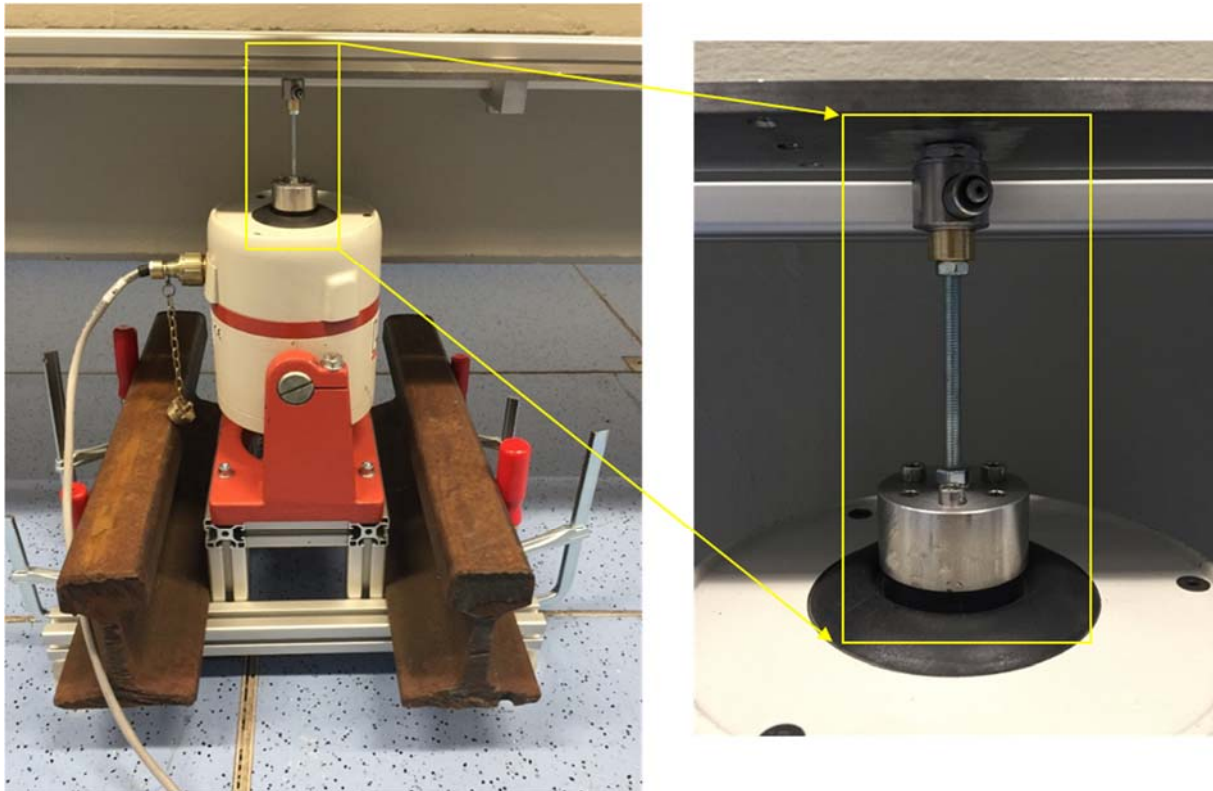


FIGURE 5-6 CONNECTION OF THE SHAKER WITH THE BRIDGE DECK

## 5.2 EXPERIMENTS WITH THE BRIDGE MODEL

Static as well as dynamic deformation experiments were carried out. The analysis of these measurements is given in the following sub-chapters.

### 5.2.1 STATIC EXPERIMENTES

#### Refinement of the FE-model

The whole FE-model was revised after results from the real bridge model were available. As shown in chapter 5.2.2 the results of the modal analysis of the FE-model fit well to the measured values from the real model. An error within the FE-model computed with the Abaqus software was identified because the initial calculated deformations did not match the measured values from the static experiment shown in the following.

#### Static loading

For the investigation of static deformation, a load was placed on the bridge deck. Figure 5-7 shows the static deformation due to a load of 0.8 kg which was placed in the middle of the bridge deck. The TS and the LTS measured a vertical displacement of 2.45 mm. The result of the FEM calculation is 2.58 mm. Accelerometers cannot detect static deformation but they can detect the moment of loading and de-loading. It was also possible to align the accelerometer signal with the TS and the LTS through CCF.

The moment of loading (5-7A) and the moment of de-loading (5-7B) is zoomed in. Of course, the FEM result shows a linear movement at these moments. The upward swing of the bridge deck due to the off-loading is captured by the LTS and the TS, the TS shows a much higher peak. There is a suspicion that these effects are associated with the orientation of the prism. Lienhart & Lackner (2016b) investigated the impact of the prism orientation on automated total station measurements. They discovered single deviations of several millimeters at specific prism positions. Lienhart & Lackner stated that the reason for this may be that at specific prism orientations the automated target recognition system (ATR) detects two adjacent prism facets which leads to an incorrect calculation of the prism center.

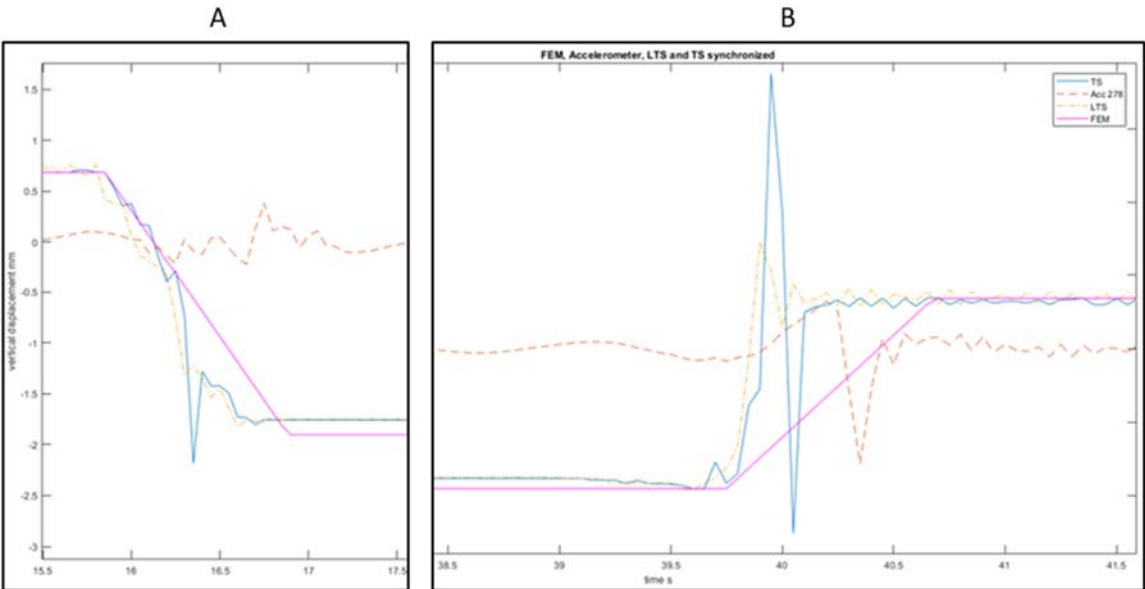
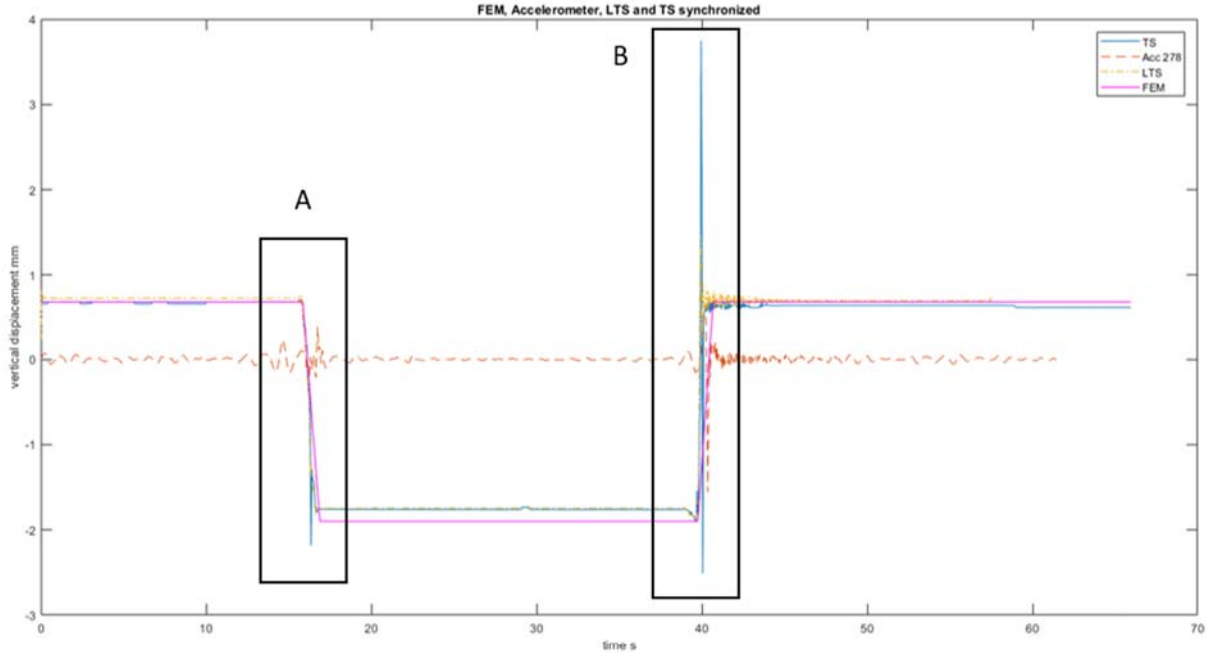


FIGURE 5-7 FIGUR STATIC DEFORMATION EXPERIMENT WITH ENLARGED AREAS A AND B

Figure 5-8 shows the residuals (difference) between LTS and TS measurements during static loading. The moment of loading and de-loading is clearly marked by the two peaks. A low noise and a constant offset of 0.04 mm is recognizable.

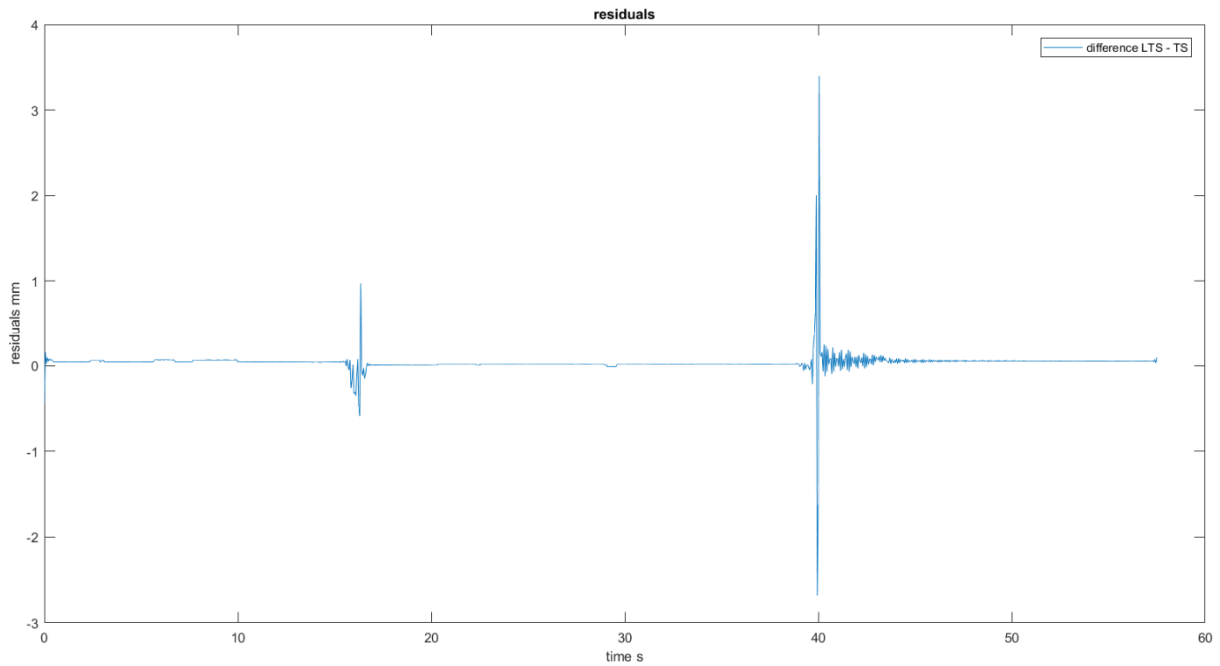


FIGURE 5-8 PLOT OF THE RESIDUALS

## 5.2.2 DYNAMIC EXPERIMENTES

### Modal analysis

An experimental modal analysis was carried out to compare the spectrum of the measured acceleration to the computed values from the FE-model (see chapter 3.4). A vibration was excited by hand (comparable to a Dirac impulse). The positions of the hand strokes on the bridge deck were varied as well as the position of the accelerometers. The position of the accelerometers and the prism for the following data shown in detail is presented in figure 5-9. The spectrum of the accelerometers of one of the experiments is shown in figure 5-10. The first three eigenvalues can be clearly identified. In table 5-1 the calculated and the corresponding measured eigenvalues are compared. The values show a good match.

TABLE 5-1 COMPARISON BETWEEN MEASURED AND CALCULATED EIGENVALUES FROM ACCELEROMETER

calculated values		measured values	
mode number	eigenvalue	mode number	eigenvalue
1	5.4	1	5.5
2	17.8	2	17.8
3	37.2	3	36.5

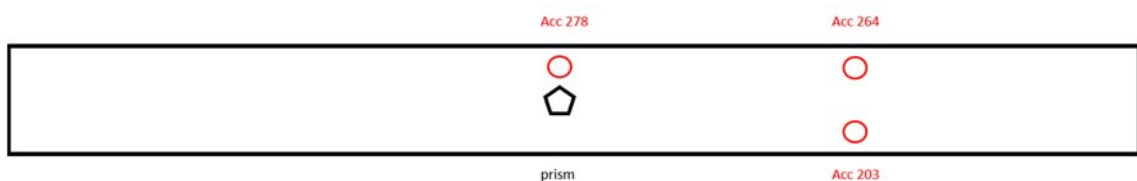


FIGURE 5-9 POSITION OF THE PRISM AND THE ACCELEROMETERS

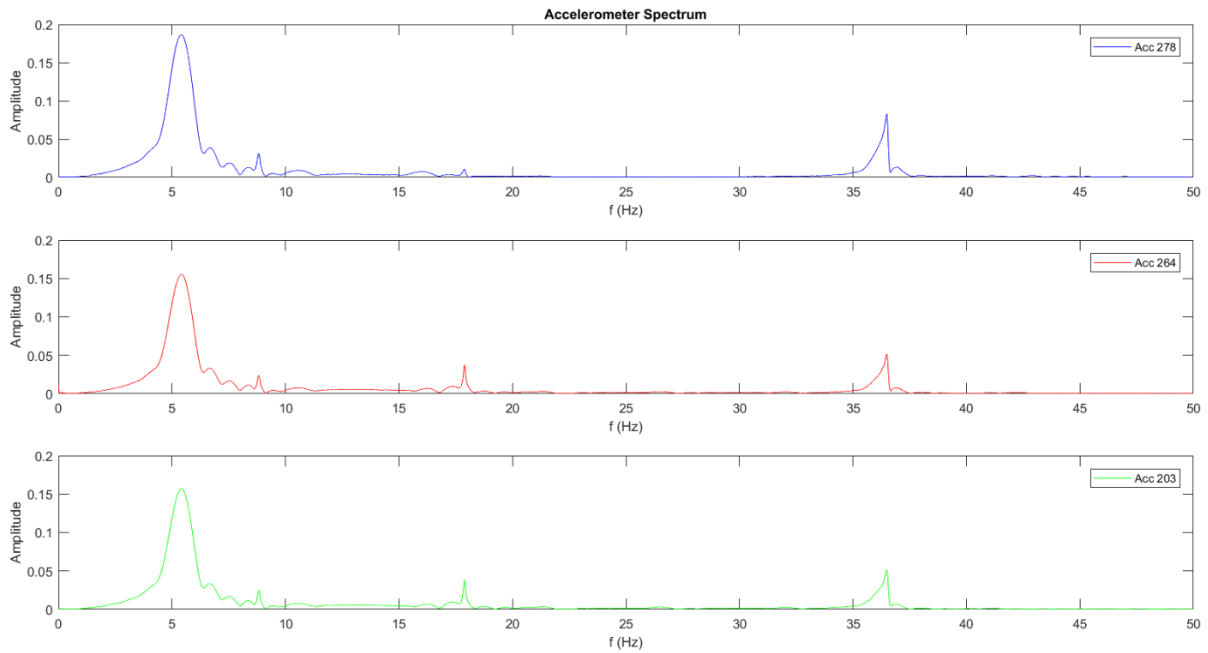


FIGURE 5-10 ACCELEROMETER SPECTRUM

Figure 5-11 shows the spectrum of the LTS distance measurements. Due to the sampling rate of 2500 Hz higher numbers of eigenvalues are recognizable. Within the measurement run shown in figure 5-11 the first eight eigenvalues can be identified. The values are compared in table 5-2.

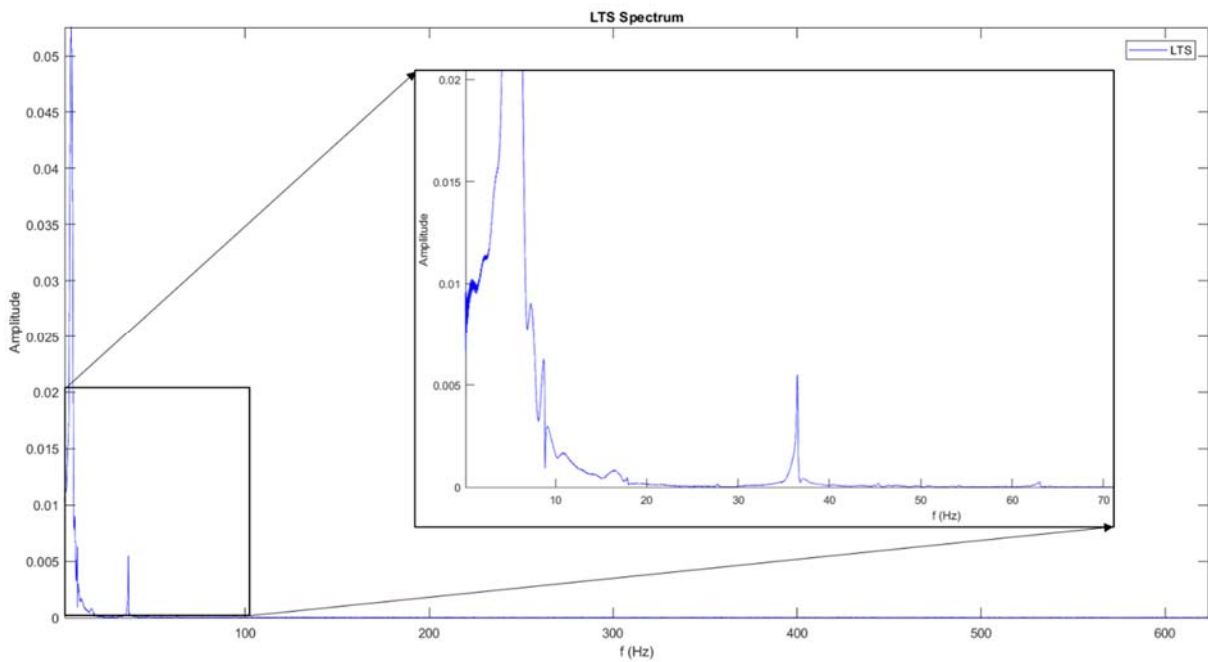


FIGURE 5-11 LTS SPECTRUM

TABLE 5-2 COMPARISON BETWEEN MEASURED AND CALCULATED EIGENVALUES FROM LTS

calculated values		measured values LTS	
mode number	eigenvalue	mode number	eigenvalue
1	5.4	1	5.4
2	17.8	2	16.5
3	37.2	3	36.5
4	54.1	4	45.4
5	63.7	5	63.0
6	97.4	6	94.3
7	138.26	7	133.8
8	174.1	8	179.4

Due to an insufficient measurement rate in this case the total stations (Leica TS15 and MS60) are able to capture only the first eigenvalue. Figure 5-12 shows the frequency spectrum of the acceleration compared to the particular spectrum of deformation from the three used sensors. All data was resampled to 100 Hz although the TS data above 20 Hz must be ignored. In the deformation spectrum of the TS noise is visible between 1 and 3 Hz. This noise may be the result of the used prism and the measurement rate as mentioned before. Some noise in the same frequency area is also visible in the LTS displacement spectrum. The displacement amplitudes from the LTS and the accelerometer are twice as high as the one from the TS. The higher eigenvalues within the LTS results are not visible due to the amplitude intensity.

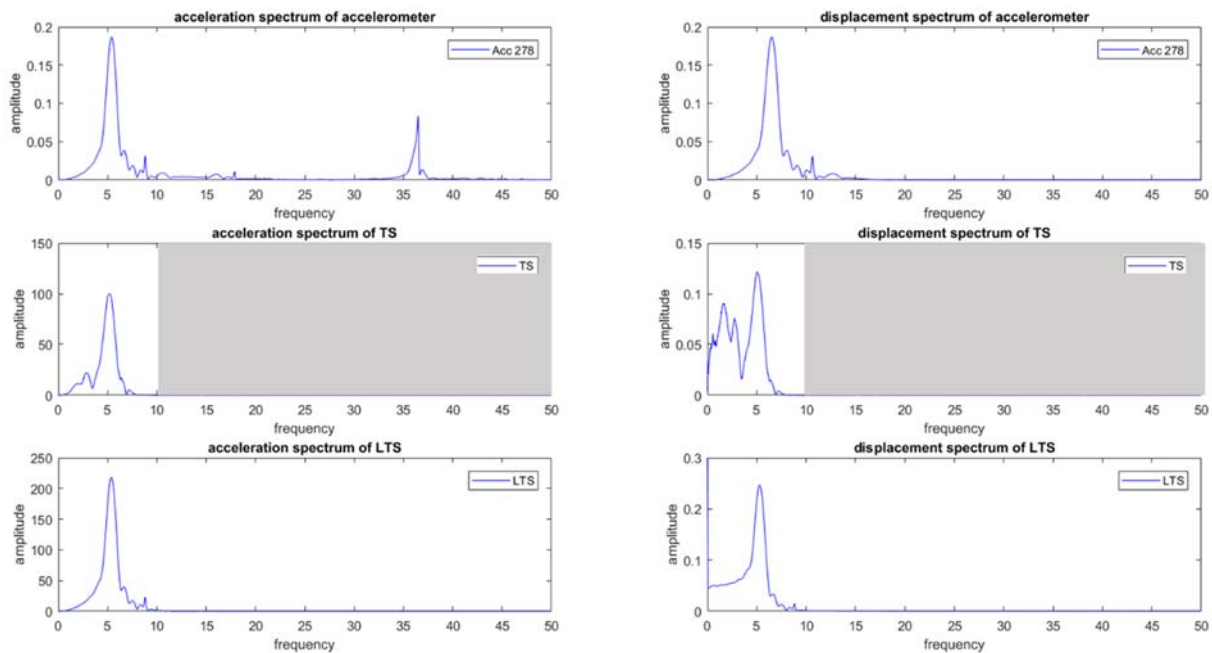
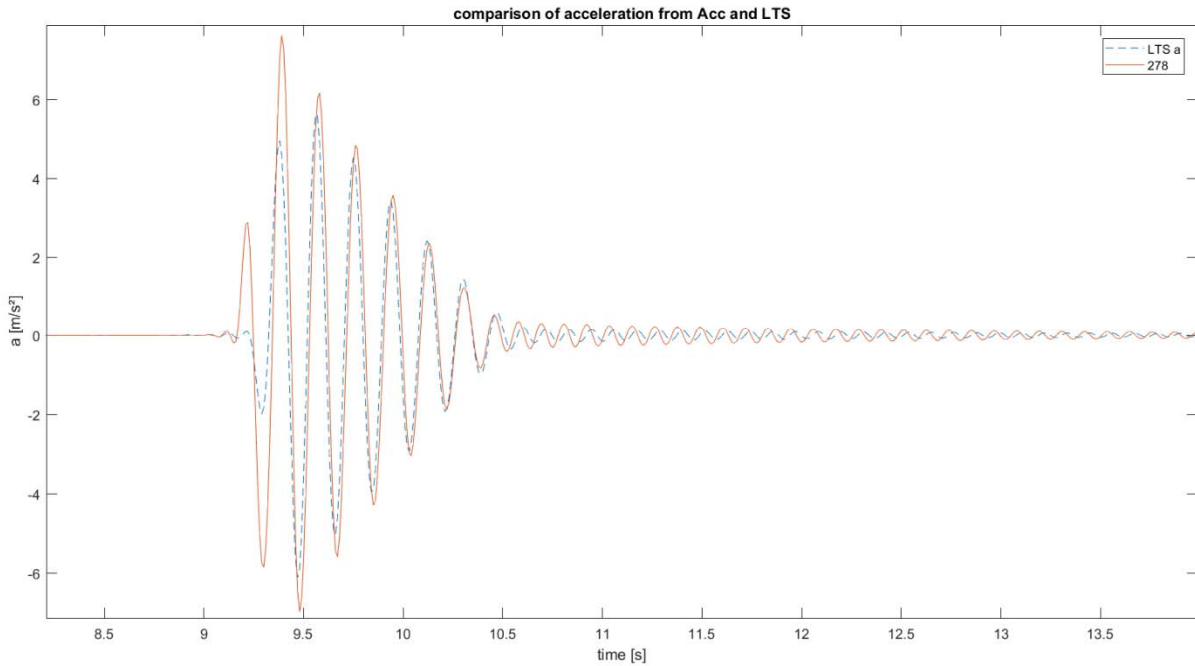


FIGURE 5-12 FREQUENCY SPECTRUM OF ACCELERATION AND DEFORMATION FROM THE THREE USED SENSORS



**FIGURE 5-13 COMPARISON OF MEASURED ACCELERATION FROM THE ACCELEROMETER AND CALCULATED ACCELERATION VIA DIFFERENTIATION OF THE LTS DATA**

Figure 5-13 compares the measured acceleration from one of the accelerometers and calculated acceleration from measured distance (LTS) through differentiation. The measured eigenvalues shown in table 5-3 are the results of certain measurements and not of a complete and comprehensive modal analysis. The scope of this thesis is sensor testing and not a detailed modal analysis of the bridge model.

**TABLE 5-3 CALCULATED AND MEASURED EIGENVALUES**

mode number	eigenvalue			
	FEM	LTS	Acc.	TS
1	5.4	5.4	5.5	5.3
2	17.8	16.5	17.8	/
3	37.2	36.5	36.5	/
4	54.1	45.5	/	/
5	63.7	63.0	/	/
6	97.4	94.3	/	/
7	138.26	133.8	/	/
8	174.1	179.4	/	/

### Sine wave monitoring

Due to the limitations of the used force amplifier (LDS PA100) for the shaker control the maximum displacement achieved are roughly four millimeters, depending on the input parameters. With this certain force amplifier (limitation to gain value of 1) it is not possible to operate the shaker up to its maximum performance (see Appendix A). Additionally, a cooling fan and a suspension kit for the shaker would be necessary.

In figure 5-14 the displacement can be seen of a run with a 1 Hz sine wave and 10 V input force.

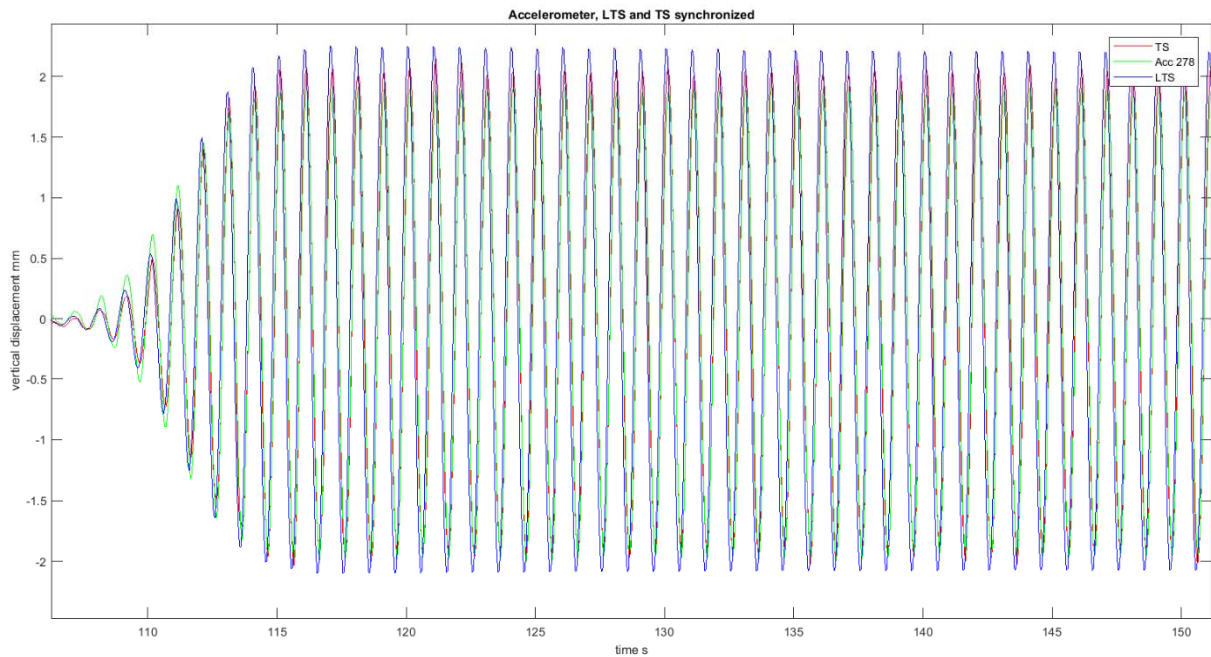


FIGURE 5-14 DISPLACEMENT DUE TO A SINE WAVE STIMULATION

Figure 5-15 shows the displacement of the synchronized times series of the TS, the LTS and the Accelerometer (No. 278). The accelerometers, the LTS and the prism were positioned at the same measurement section (middle of the bridge deck).

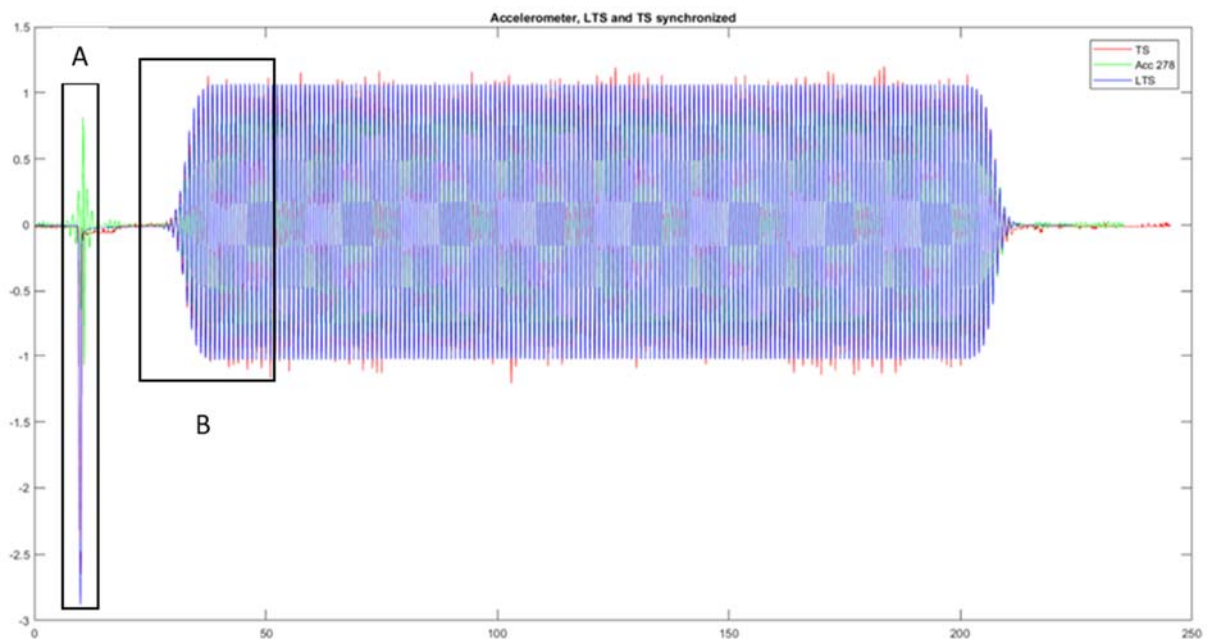


FIGURE 5-15 SYNCHRONIZED TIMESERIES

Figure 5-16 shows the Dirac impulse (A) at the beginning of the measurement run used for the synchronization via cross-correlation. It shows a faster response of the accelerometer in comparison to the TS and the LTS. The peak of the LTS is higher compared to the TS. The reason for this can be found in the higher sampling rate (2500 Hz compared to 20 Hz of the TS) and the slower reaction of the TS due to the ATR modus. Figure 5-17 shows the beginning of the sine wave vibration (1 Hz) induced by the shaker. The start-up phase of the vibration was set to 20 seconds (from zero to maximum

displacement). In comparison to the fast Dirac impulse the three sensors show a similar reaction with no time delay. The accelerometer shows a smaller displacement than the other sensors.

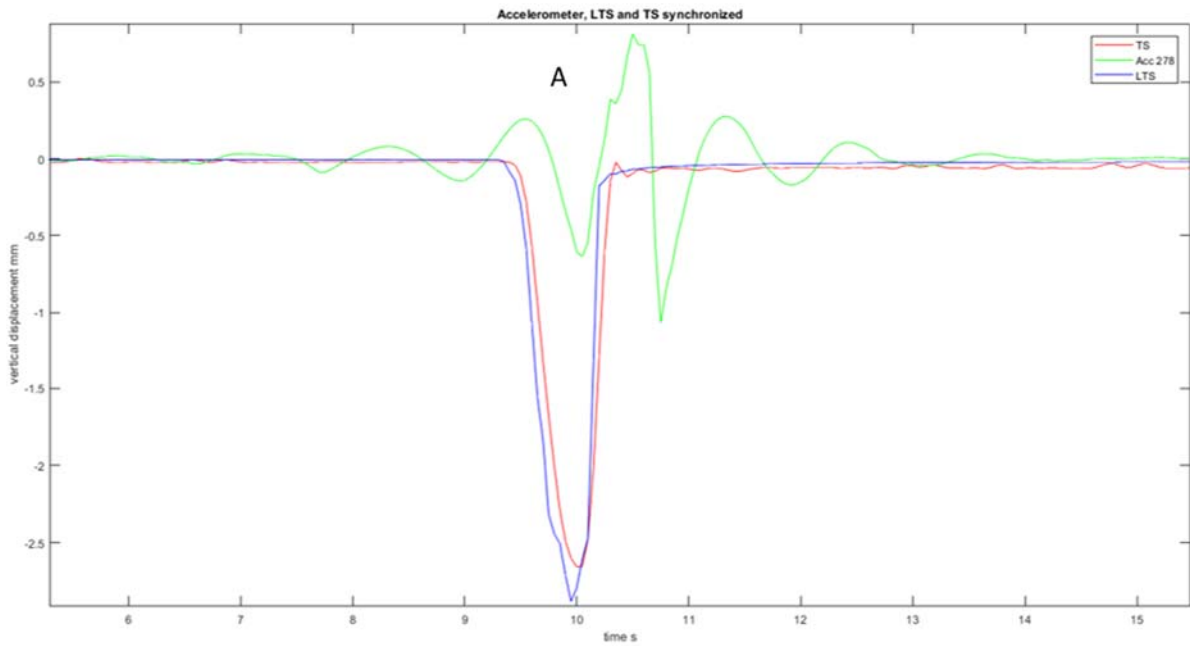


FIGURE 5-16 DIRAC IMPULSE (A)

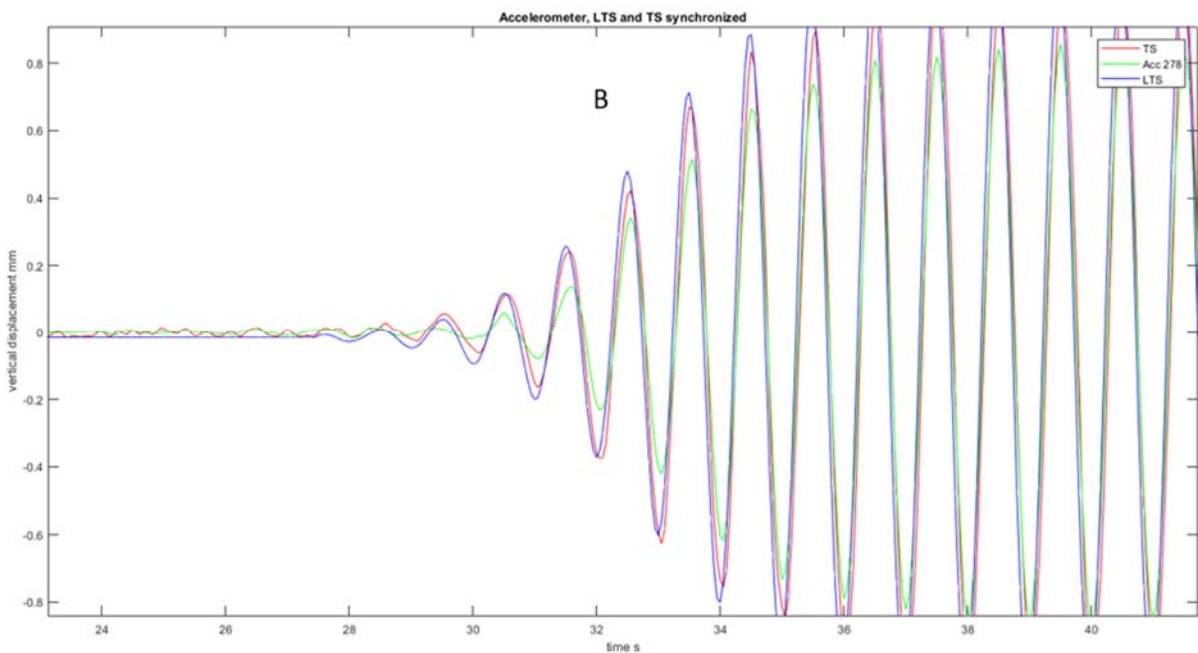


FIGURE 5-17 START OF THE VIBRATION (B)

Figure 5-18 shows the peaks of the sine wave (the single measurement values are labeled through markers). For time synchronization both data sets are resampled to a similar rate. The data of this certain experiment was resampled to its original rate (20 Hz for the TS and 2500 Hz for the LTS) to highlight the poorer resolution of the TS (figure 5-19).

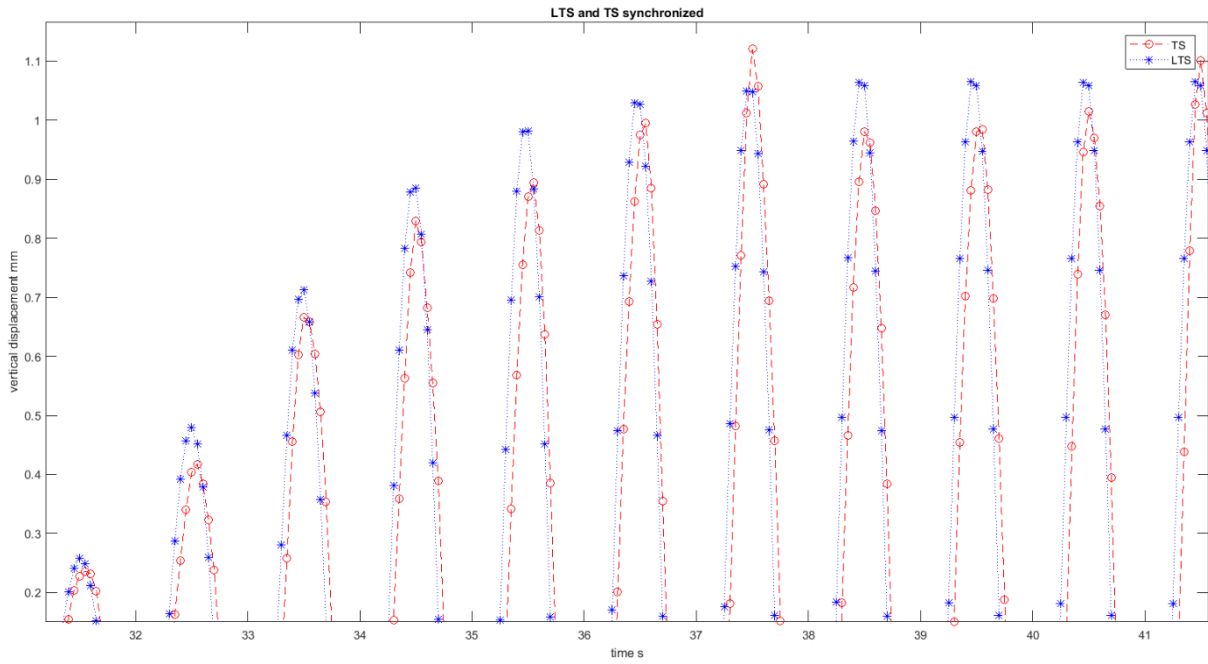


FIGURE 5-18 DISPLACEMENT PEAKS

As it was mentioned by Lienhart et al. (2016) the resolution of the dynamic ATR measurements of 0.3 mgon of the TS must be taken into consideration. At the given slope distance of 4.95 m this angular resolution corresponds to a spatial resolution of 0.023 mm. The effect of the limited spatial resolution of the angle measurements can also be seen in the data where a discretization of 0.022 mm is identifiable (figure 5-20).

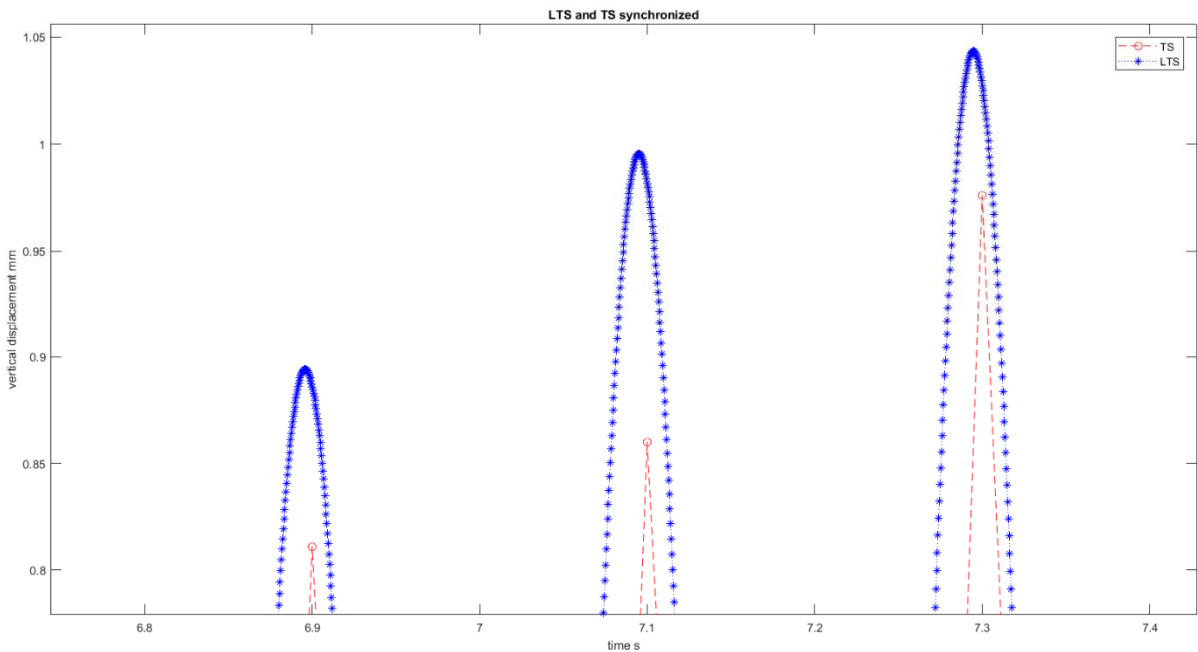


FIGURE 5-19 TS AND LTS DATA WITH ORIGINAL SAMPLING RATES

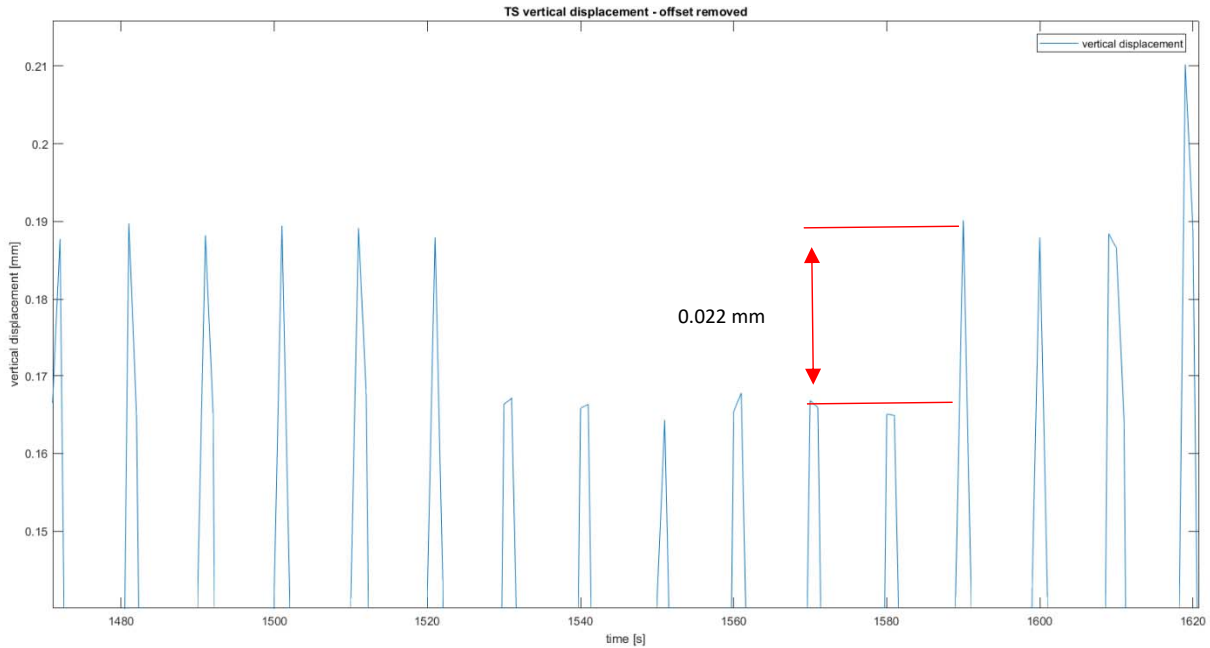


FIGURE 5-20 ANGLE RESOLUTION OF THE TS

State of the art IATS like the Leica MS60 offer video stream recording with 20 Hz (or even higher). The advantage is that the angular resolution of the on-axis camera is five times higher than the ATR resolution in dynamic mode. Lienhart et al. (2016) successfully performed vibration monitoring of a bridge with a MS50 and its on-axis camera. A second advantage by using the on-axis camera is the possibility of using natural targets and hence a fully contact-free vibration measurement system.

### Monitoring of the comparator bench abutment

An additional accelerometer (PCB M353B15) was mounted on the steel grooves on the abutment of the comparator bench (see figure 5-21). Figure 5-22 shows the measured acceleration in comparison to one of the HBM B12 accelerometers mounted on the bridge deck during a measurement run with a 6 Hz sine wave vibration.



FIGURE 5-21 ACCELEROMETER MOUNTED ON THE COMPARATOR BENCH

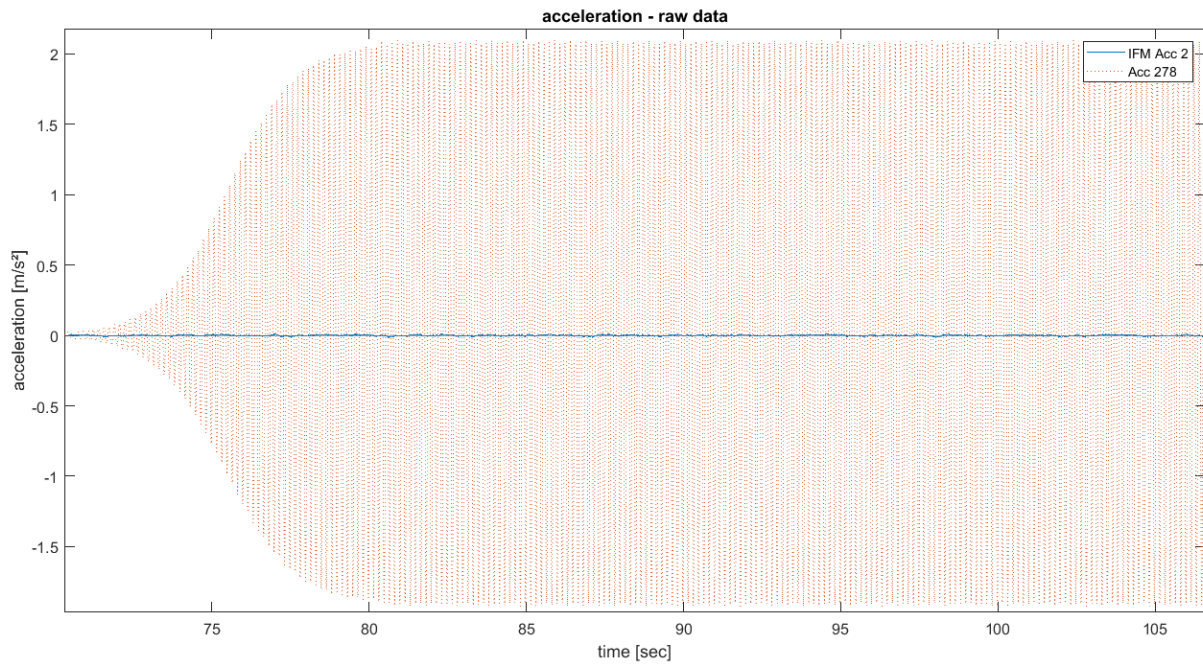


**FIGURE 5-22 ACCELERATIONS MEASURED ON THE BRIDGE DECK AND ON THE COMPARATOR BENCH**

It can be concluded that the operation of the bridge model with the shaker within the defined limits (see appendix A) does no damage to the comparator bench. But there is the possibility that the shaker operation does influence experiments on the comparator bench. Therefore, it is recommended not to operate the shaker during experiments with the comparator bench or any other testing activities within its vicinity.

## 6 CONCLUSION AND OUTLOOK

In this thesis, a bridge model for the evaluation of static and dynamic vibration monitoring systems was developed. Through the investigation of state of the art monitoring systems and sensor technology as well as the desired needs of the IGMS for future experiments first parameters for the requirement of such a model were derived. The design of the bridge model and especially its geometric dimensions were analyzed with a FEM software. It had to be guaranteed that the model is able to deliver deformations, vibrations and eigenfrequencies within the range of the sensors. Several other requirements regarding the feasibility, production and operation of the model had to be considered. In a first stage the model is equipped with geodetic prisms for measurements with total stations, with a laser triangulation sensor for distance measurements and accelerometers. This basic monitoring system was reviewed before installation. An analysis routine was implemented with MATLAB software. The synchronization of the three different sensor types and the derivation of displacement from measured acceleration can be considered the biggest challenge.

The bridge deck is made of steel, the bearings and suspensions are made of aluminum profiles. The whole model is mounted on the comparator bench in the IGMS laboratory. It is equipped with a locating and a floating bearing. Artificial vibrations of the bridge deck can be excited by a so-called shaker system. With it a maximum displacement of 4 mm and sine vibration of up to 50 Hz can be excited. The model is modifiable so other types of sensors can be installed and tested as well.

The mechanical behavior of the bridge model regarding the influence of the support structure to vibration excitation should be investigated deeper. Maybe the set limitations for shaker operations can be increased. This topic should be examined by a mechanical engineer because advanced knowledge within the field of structural analysis as well as experimental modal analysis is needed.

For the use of total stations for high frequent monitoring tasks various aspects must be taken into consideration. Correct measurement modes as well as software commands (e.g. Leica GeoCOM) for remote operations must be set. For correct data transfer between PC and total station a sufficient baud rate and serial or USB port must be used. As shown in the chapter before the prism type can also have an influence on the data quality. It might be interesting to investigate the suitability of the various prism types for dynamic monitoring applications.

There are several research topics regarding sensor technology. For ambient vibration monitoring of structures, a sufficient sampling rate is necessary. In recent years, the performance of total stations has improved. Distance and angle measurements with a rate of up to 20 Hz are possible. Image assisted total stations have an integrated on-axis camera. The pictures are captured with a CMOS array with 10 Hz sampling rate or higher. The advantage is that no artificial target like a geodetic prism is needed to be installed on the measurement object. Instead natural targets can be used. Fiber optical sensors get in focus especially for the use within structural health monitoring systems. Such sensors can be installed on the model for static and dynamic monitoring testing. They can also be used as accelerometers. The feasibility of such sensors for vibration monitoring may be of interest. MEMS sensors for the measuring of motion are emerging within the geodetic field of applications. The suitability of terrestrial laser scanners for vibration monitoring might be another interesting field of investigation.

# SOURCE DIRECTORY

## ABAQUS (2014)

Abaqus 6.14 Documentation, <http://abaqus.software.polimi.it/v6.14/index.html>, last accessed on 25.02.2018. Simulia.

## AUSTRIAN INSTITUTE OF TECHNOLOGY (2014)

**Mobile Seismic Simulator.** Poster. Austrian Institute of Technology GmbH, Mobility Department, Vienna.

## AUSTRIAN INSTITUTE OF TECHNOLOGY (2015)

**Mobile Seismic Simulator.** Austrian Institute of Technology GmbH, Mobility Department, Vienna.

## CHEN Y. Q. & CHRZANOWSKI A. (1986)

An overview of the physical interpretation of deformation measurements. Deformation measurement workshop, MIT.

## BECKER M., RÖDELSPERGER S., LÄUFER G. & SCHNEIDER J. (2012)

Erfassung von hochfrequenten und langfristigen Deformationsprozessen mit terrestrischer Mikrowelleninterferometrie. Vermessung und Geoinformation, 1/2012, pp. 29-35.

## BRÜEL & KJAER (2012)

LDS V 406 and V 408 Shakers product data. Brüel & Kjaer AS, Denmark.

## DUNNICLIFF J. (1993)

Geotechnical instrumentation for monitoring field performance. John Wiley & Sons Inc., New York. ISBN 0-471-00546-0.

## FLESCH R. (1993)

Baudynamik praxisgerecht – Band 1 Berechnungsgrundlagen. Bauverlag Wiesbaden GmbH, Wiesbaden/Berlin. ISBN 3-7625-3010-6.

## GASSNER G., PETER F. & RULAND R. (2009)

HLS and WPS at SLAC. Department of Metrology, Stanford University.

## GeoDATA (2008a)

Shotcrete Strain Meter SSM-1, Datasheet Hardware. GeoDATA ZT GmbH, Austria.

## GeoDATA (2008b)

Rod Extensometer, Datasheet Hardware. GeoDATA ZT GmbH, Austria.

## GeoDATA (2008c)

Shotcrete Strainmeter SSM-1, Datasheet Hardware. GeoDATA ZT GmbH, Austria.

## GOJCIC Z. (2016)

Synchronization routine for real-time synchronization of modern total stations. M.Sc. thesis, TU Graz.

## GOLSER J. (2018)

Instrumentation and Monitoring. Unpublicized lecture script, Montanuniversität Leoben.

- GROSS D., HAUGER W., SCHRÖDER J. & WALL W. (2013)  
Technische Mechanik 1 - Statik. Springer Verlag, Berlin/Heidelberg. ISBN 978-3-642-36267-5
- GROSS D., HAUGER W., SCHRÖDER J. & WALL W. (2014)  
Technische Mechanik 2 - Elastostatik. Springer Verlag, Berlin/Heidelberg. ISBN 978-3-642-40965-3.
- GROSS D., HAUGER W., SCHRÖDER J. & WALL W. (2012)  
Technische Mechanik 3 -. Springer Verlag, Berlin/Heidelberg. ISBN 978-3-642-40965-3.
- HBM (2000)  
Montageanleitung Beschleunigungsaufnehmer B12. HBM Mess- und Systemtechnik GmbH, Germany.
- HBM (2018)  
FS65 Accelerometer. HBM Mess- und Systemtechnik GmbH, Germany.
- HEUNECKE O., KUHLMANN H., WELSCH W., EICHHORN A. & NEUNER H. (2013)  
Auswertung geodätischer Überwachungsmessungen. Wichmann Verlag, Berlin/Offenbach. ISBN 978-3-87907-467-9.
- KUHLMANN H., SCHWIEGER V., NIEMEIER W. & WIESER A. (2014)  
Engineering Geodesy – Definition and Core Competencies. FIG Congress 2014.
- LEICA (2009)  
Real Time GNSS Bridge Monitoring, Reporter 61. Leica Geosystems AG, Switzerland.
- LEICA (2015a)  
Leica Nova MS60 data sheet. Leica Geosystems AG, Switzerland.
- LEICA (2015b)  
Leica LS Digitalnivelliere, Datenblatt. Leica Geosystems AG, Switzerland.
- LEICA (2016a)  
Leica ScanStation P30/P40. Leica Geosystems AG, Switzerland.
- LEICA (2016b)  
Leica Viva GS14 data sheet. Leica Geosystems AG, Switzerland.
- LIENHART W. (2006)  
Analysis of Inhomogenous Structural Monitoring Data. Ph.d. thesis, Technische Universität Graz.
- LIENHART W. (2013)  
Fibre Optic Sensors. Unpublicized lecture script, TU Graz.
- LIENHART W. & ERHART M. (2015)  
State of the Art of Geodetic Bridge Monitoring. International Workshop of Structural Health Monitoring 2015.
- LIENHART W., ERHART M. & GRICK M. (2016a)  
High Frequent Total Station Measurements for the Monitoring of Bridge Vibrations. Joint International Symposium on Deformation Monitoring 2016, Vienna.

- LIENHART W. & LACKNER S. (2016b)  
Impact of Prism Type and Orientation on the Accuracy of Automated Total Station Measurements. Joint International Symposium on Deformation Monitoring 2016, Vienna.
- Metasensing (2018)  
<https://www.geomatics.metasensing.com/fastgbsar-r> , last accessed on 26.01.2018
- MICRO-EPSILON (2008)  
Betriebsanleitung optoNCDT 1700. Micro-Epsilon Messtechnik GmbH, Germany.
- MUFTI A., KLOWAK C., JAEGER L., BAKHT B. & TADROS G. (2007)  
Calculating deflections from observed strains. Vancouver. The 3<sup>rd</sup> International Conference on Structural Health Monitoring of Intelligent Infrastructure.
- MÖSER M., MÜLLER G., SCHLEMMER H. & WERNER H. (2008)  
Handbuch Ingenieurgeodäsie – Ingenieurbau. Wichmann Verlag, Berlin. ISBN 978-3-87907-296-5.
- NEITZEL F. (2007)  
Zur Genauigkeit von Schwingwegmessungen mit Hilfe von Beschleunigungs- und Geschwindigkeitssensoren. AVN, 6/2007, pp. 202-211.
- NIEMEIR W. (2008)  
Ausgleichsrechnung – Statistische Auswertemethoden. De Gruyter, Berlin, New York. ISBN 978-3-11-019055-7
- ROBERTS G., BROWN C. & OGUNDIPE O. (2010)  
Monitoring bridges by GNSS. FIG Congress 2010.
- RST Instruments (2018a)  
Portable Tiltmeter Brochure. RST Instruments, Canada.
- RST Instruments (2018b)  
Digital Inclinometer Systems Brochure. RST Instruments, Canada.
- SABET F., NAZARIAN E., INDART A. Z. & ANSARI F. (2015)  
Distributed Monitoring of Deck Strains for detection of Cable Damage in Cable-Stayed Bridges. SHMU, Torino.
- SANTA U. (2004)  
Bauwerksinspektion und –Überwachung. Ph.d. thesis, Universität für Bodenkultur Wien.
- SLIFKA L. D. (2004)  
An Accelerometer-based Approach to Measuring Displacement of a Vehicle Body. M.Sc. thesis, University of Michigan.
- TRIMBLE (2017)  
Trimble SX10 data sheet. Trimble Inc., USA.
- WENZEL H. & PICHLER D. (2005)  
Ambient Vibration Monitoring. John Wiley & Sons, Ltd., Chichester, West Sussex. ISBN 978-0-470-02430-0.

WELSCH W. & HEUNECKE O. (2001)

Models and terminology for the analysis of geodetic monitoring observations. 10<sup>th</sup> Int. Symposium on Deformation Measurements, pp. 390-409.

## LIST OF FIGURES

Figure 2-1 RIGID BODY MOVEMENT AND DEFORMATION (Heunecke et al., 2013, p.92-93).....	5
Figure 2-2 SYSTEM INPUT/OUTPUT RELATION AFTER LIENHART (2006) .....	6
Figure 2-3 ZERO ORDER SYSTEM after Lienhart (2006).....	7
Figure 2-4 first order system after Lienhart (2006).....	7
Figure 2-5 SECOND ORDER SYSTEM after Lienhart (2006).....	8
Figure 2-6 SYSTEM IDENTIFICATION (Welsch & Heunecke, 2001, p.399).....	8
Figure 2-7 STEPS OF DEFORMATION CAPTURE after Heunecke et al (2013, p.16).....	10
Figure 2-8 HIERARCHY OF DEFORMATION MODELS BY welsch and HEUNECKE (1999) .....	12
Figure 2-9 INTEGRATED ANALYSIS MODEL BY LIENHART (2006, p.7) .....	13
Figure 2-10 FastGBSAR-R (Metasensing, 2018).....	16
Figure 2-11 SCHEMATIC ASSEMBLY OF AN EXTENSOMETER (GEODATA ZT GMBH, 2008a).....	18
Figure 2-12 SHOTCRETE STRAINGAUGE (GEODATA ZT GMBH, 2008b) .....	18
Figure 2-13 RADETZKY BRIDGE IN GRAZ.....	20
Figure 3-1 NODAL POINTS OF RECTANGULAR (LEFT) AND CUBIC (RIGHT) ELEMENTS .....	26
Figure 3-2 SINGLE POINT FORCE LOAD CASE OF A BEAM .....	27
Figure 4-1 SHAKER V406.....	34
Figure 4-2 PC FOR SHAKER CONTROL, LMS (UPPER LEFT) AND AMPLIFIER (LOWER LEFT) .....	34
Figure 4-3 ACCELEROMETERS AND 360° MINI PRISM MOUNTED ON THE test bed.....	35
Figure 4-4 OPTONCDT ILD1700-50 MOUNTED ABOVE THE PRISM.....	35
Figure 4-5 SCHEMATIC COMPOSITION OF THE MEASUREMENT SYSTEM .....	36
Figure 4-6 SENSOR TEST BED.....	37
Figure 4-7 SENSOR TEST BED.....	37
Figure 4-8 raw ACCELERATION DATA FROM THE THREE USED HBM B12/200 .....	38
Figure 4-9 raw data from the three HBM b12 accelerometers.....	39
Figure 4-10 integration errors .....	40
Figure 4-11 integration error in comparison to the Its data .....	41
Figure 4-12 BLOCK DIAGRAM OF THE DOUBLE INTEGRation after slifka.....	41
Figure 4-13 magnitude response of the used highpass filter.....	42
Figure 4-14 acceleration, velocity and position from accelerometer 278 .....	42
Figure 4-15 ACCELERATION, VELOCITY AND POSITION FROM ACCELEROMETER 278, zoomed in.....	43
Figure 4-16 accelerometer and Its position data synchronized .....	43
Figure 4-17 comparison of acceleration between accelerometer and Its values .....	44
Figure 4-18 calculated position from ts and enlarged aereas A and b.....	45
Figure 4-19 LTS raw data with offset removed and enlarged aereas A and b .....	46
Figure 4-20 time lags bewtween Accelerometer, LTS and TS .....	47
Figure 4-21 cross-correlation between Its and ts without impulse .....	48
Figure 4-22 synchronization of accelerometer, TS and Its time series .....	48
Figure 4-23 synchronization of TS, Its and accelerometer data .....	49
Figure 5-1 LOCATING BEARING .....	52
Figure 5-2 floating bearing .....	52
Figure 5-3 bridge model mounted on the comparator bench .....	53
Figure 5-4 bridge model .....	53
Figure 5-5 prism and accelerometer .....	54
Figure 5-6 CONNECTION OF THE SHAKER WITH THE BRIDGE DECK.....	55

Figure 5-7 FIGUR STATIC DEFORMATION EXPERIMENT WITH ENLARGED AREAS A AND B .....	56
Figure 5-8 PLOT OF THE RESIDUALS .....	57
Figure 5-9 POSITION OF THE PRISM AND THE ACCELEROMETERS .....	57
Figure 5-10 accelerometer spectrum .....	58
Figure 5-11 LTS SPECTRUM .....	58
Figure 5-12 FREQUENCY SPECTRUM OF ACCELERATION AND DEFORMATION FROM THE THREE USED SENSORS .....	59
Figure 5-13 comparison of measured acceleration from the accelerometer and calculated acceleration via differentiation of the lts data.....	60
Figure 5-14 displacement due to a sine wave stimulation.....	61
Figure 5-15 synchronized timeseries.....	61
Figure 5-16 DIRAC IMPULSE (A).....	62
Figure 5-17 START OF THE VIBRATION (B) .....	62
Figure 5-18 DISPLACEMENT PEAKS .....	63
Figure 5-19 TS and lts data with original sampling rates .....	63
Figure 5-20 ANGLE RESOLUTION OF THE TS .....	64
Figure 5-21 ACCELEROMETER MOUNTED ON THE COMPARATOR BENCH.....	64
Figure 5-22 ACCELERATIONS MEASURED ON THE BRIDGE DECK AND ON THE COMPARATOR BENCH	65

## LIST OF TABLES

Table 2-1 GEOMETRICAL DISCRETIZATION.....	10
Table 2-2 CLASSIFICATION OF DEFORMATION MODELS after welsch .....	13
Table 2-3 LIST OF SENSORS .....	19
Table 3-1 MATERIAL PARAMETERS OF STRUCTURAL STEEL .....	28
Table 3-2 EIGENVALUES OF THE BRIDGE MODEL CALCULATED WITH ABAQUS.....	30
Table 4-1 highpass filter parameters.....	41
Table 5-1 comparison between measured and calculated eigenvalues from accelerometer .....	57
Table 5-2 comparison between measured and calculated eigenvalues from LTS .....	59
Table 5-3 calculated and measured eigenvalues .....	60

## APPENDIX A SPECIFICATIONS FOR THE BRIDGE MODEL

Operational limitations:

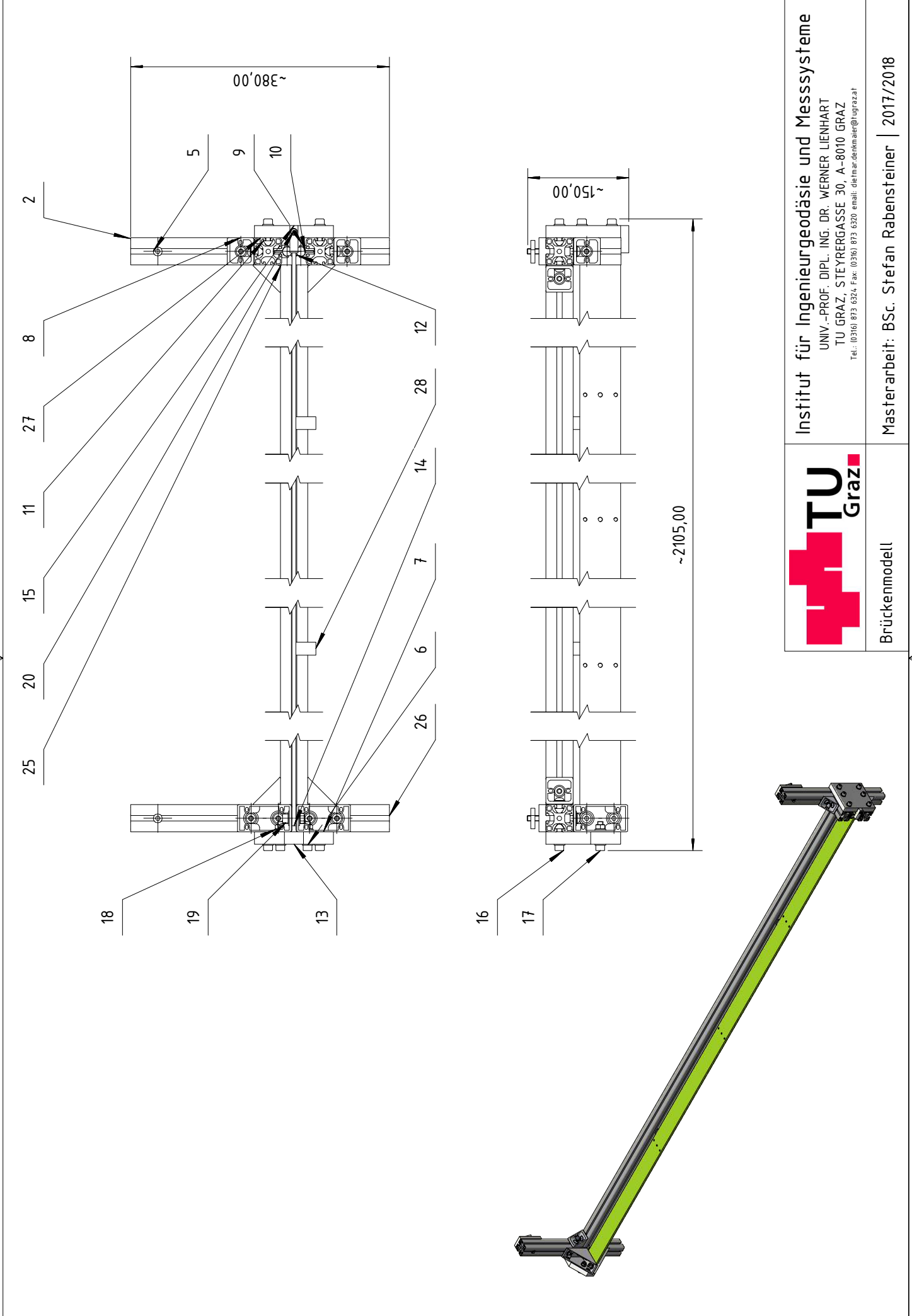
gain value	force V	frequency Hz
1	10	7
1	5	10
1	1	50

Part list bridge model:

OBJEKT	ANZAHL	BAUTEILNUMMER
1	1	Komparator-Auszug
2	1	ITEM 0002633 Profil 8 40x40 leicht L=185
3	4	Komparator-Distanzplatte
4	4	Halfenstein
5	3	ISO 4762 - M8 x 55
6	13	DIN 125 - A 8,4
7	2	0041132 Winkelsatz 8 80x80
8	6	ITEM 0041115 Winkelsatz 8 40x40
9	2	ITEM 0029434 Wellenklemmprofil 8 D14 L=60
10	2	ITEM 0047230 Welle D14 L=60
11	10	ITEM 0002618 Nutenstein 8 St M8
12	1	ISO 4762 - M8 x 65
13	2	Abschlussplatte-Loslager
14	1	Stahlband-Brücke
15	1	Loslager-Fixierung-Außen
16	10	ISO 4762 - M8 x 30
17	2	ISO 4762 - M8 x 35
18	4	ISO 4032 - M8
19	2	ISO 4762 - M8 x 25
20	1	ISO 4762 - M5 x 16
21	1	Shakerstütze
22	1	Shaker-Kraftaufnehmer
23	1	Shaker Grundgestell
24	1	Shaker
25	1	ITEM 0002633 Profil 8 40x40 leicht L=1970
26	1	ITEM 0002633 Profil 8 40x40 leicht L=380
27	2	ITEM 0002633 Profil 8 40x40 leicht L=70
28	2	Brückenstütze

Part list shaker support

OBJEKT	ANZAHL	BAUTEILNUMMER
1	4	ITEM 0002633 Profil 8 40x40 leicht L=120
2	4	ITEM 0041115 Winkelsatz 8 40x40
3	4	Justierplatte
4	4	ISO 4762 - M8 x 45
5	4	DIN 934 - M8
7	2	ITEM 0002633 Profil 8 40x40 leicht L=225
8	2	ITEM 0002633 Profil 8 40x40 leicht L=100
9	2	ITEM 0002633 Profil 8 40x40 leicht L=500
10	4	ITEM 0002618 Nutenstein 8 St M8
11	8	ISO 4762 - M8 x 40

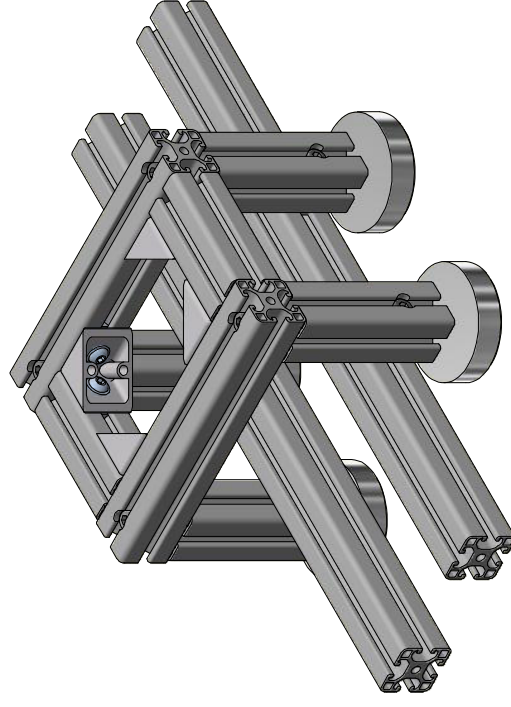
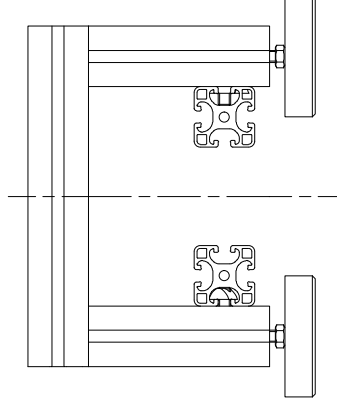
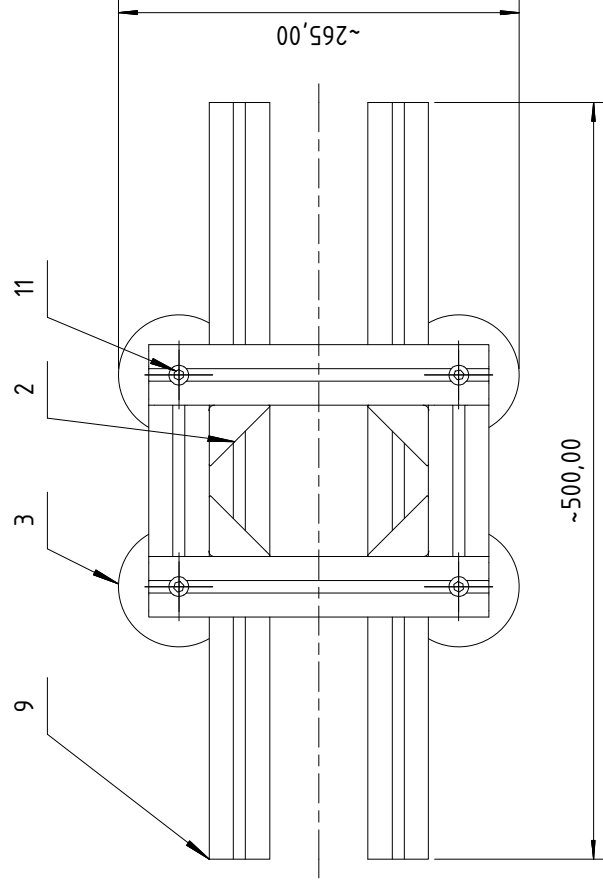
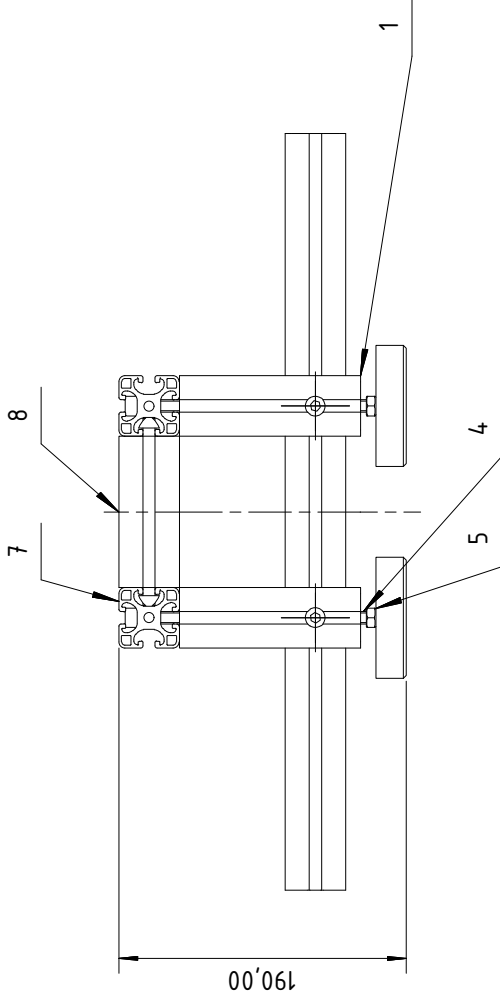


**TU Graz**

Institut für Ingenieurgeodäsie und Messsysteme  
 UNIV.-PROF. DIPL.-ING. DR. WERNER LIENHART  
 TU GRAZ, STEYRERGASSE 30, A-8010 GRAZ  
 Tel.: (0316) 873 6324, Fax: (0316) 873 6320, email: die.tmar.denkmaier@tugraz.at

Brückenmodell

Masterarbeit: BSc. Stefan Rabensteiner | 2017/2018



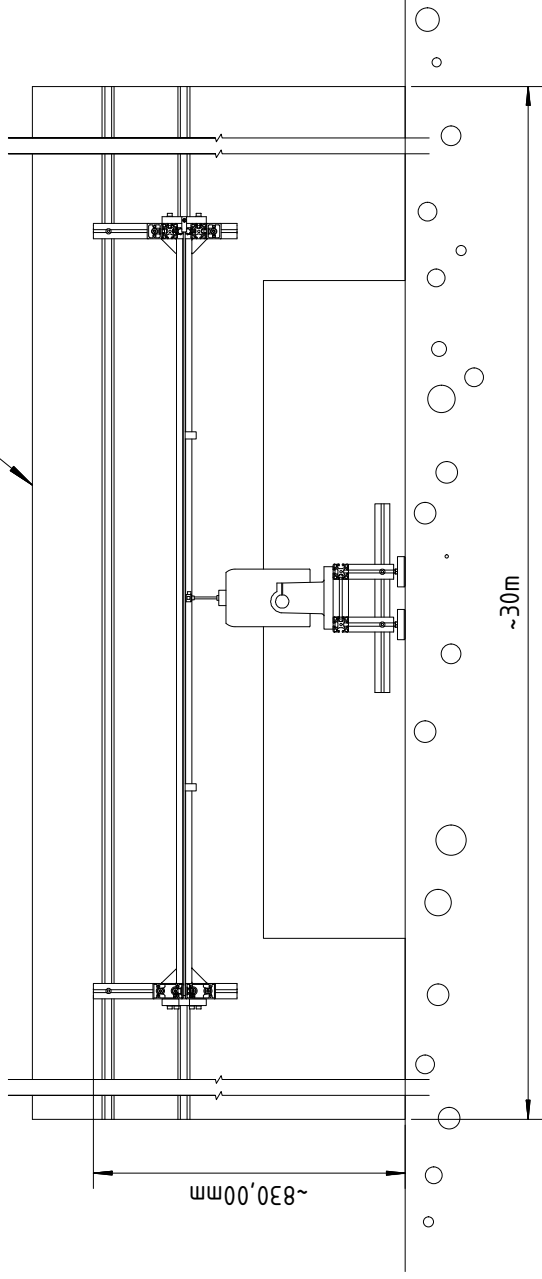
Institut für Ingenieurgeodäsie und Messsysteme  
 UNIV.-PROF. DIPL. ING. DR. WERNER LIENHART  
 TU GRAZ, STEYRERGASSE 30, A-8010 GRAZ  
 Tel.: (0316) 873 6324 Fax: (0316) 873 6320 email: dieimar.denkmaier@tugraz.at

Shakerstütze

Masterarbeit: BSc. Stefan Rabensteiner | 2017/2018

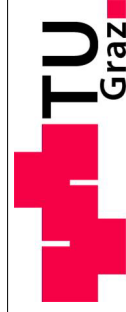
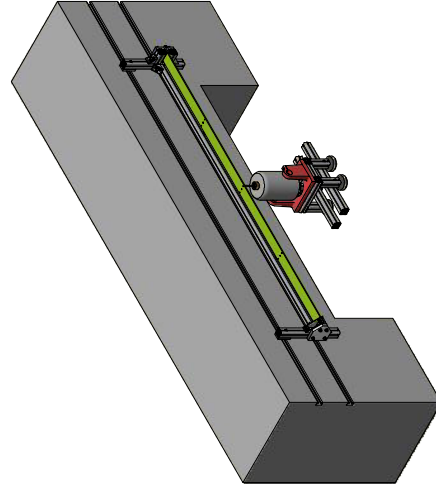
1

~225,00



~30m

~830,00mm



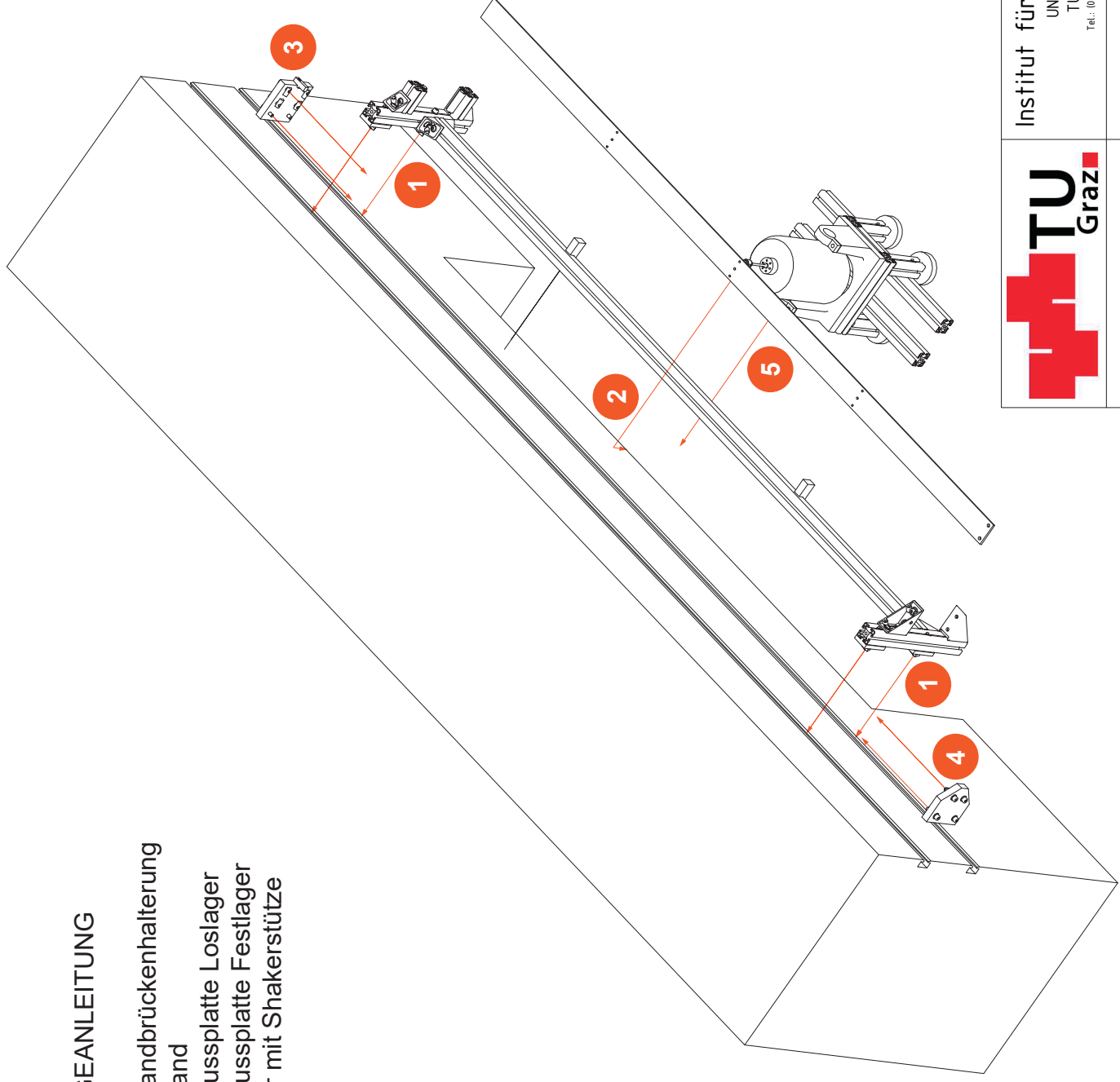
Institut für Ingenieurgeodäsie und Messsysteme  
UNIV.-PROF. DIPL.-ING. DR. WERNER LIENHART  
TU GRAZ, STEYRERGASSE 30, A-8010 GRAZ  
Tel.: (0316) 873 6324, Fax: (0316) 873 6320, email: die.mar.denkhaer@tugraz.at

Zusammenstellung  
mit Komparatorbank

Masterarbeit: BSc. Stefan Rabensteiner | 2017/2018

## MONTAGEANLEITUNG

- 1) Stahlbandbrückenhalterung
- 2) Stahlband
- 3) Abschlussplatte Loslager
- 4) Abschlussplatte Festlager
- 5) Shaker mit Shakerstütze



Institut für Ingenieurgeodäsie und Messsysteme  
UNIV.-PROF. DIPL.-ING. DR. WERNER LIENHART  
TU GRAZ, STEYRERGASSE 30, A-8010 GRAZ  
Tel.: (0316) 873 6324 Fax: (0316) 873 6320 email: [dieimar.denkhafer@tugraz.at](mailto:dieimar.denkhafer@tugraz.at)

Masterarbeit: BSc. Stefan Rabensteiner | 2017/2018

APPENDIX B SHAKER DATA SHEET

# PRODUCT DATA

## LDS V406 and V408 Shakers Metric

### Performance Parameters and Characteristics\*

Shaker	V406	V408
Standard LDS Amplifier	PA500L	
Sine Force (peak) – forced air cooled	196 N	196 N
Armature Resonance ( $f_r$ )	9 kHz	9 kHz
Useful Frequency Range	5 Hz – 9 kHz	5 Hz – 9 kHz
Effective Mass of Moving Element	0.200 kg	0.200 kg
Velocity (sine peak)	1.78 m/s	1.78 m/s
Maximum Acceleration (sine peak) – naturally cooled	50 g	50 g
Maximum Acceleration (sine peak) – forced air cooled	100 g	100 g
Max. Random Force (rms)	89 N	89 N
Displacement (pk-pk) – continuous	17.6 mm	17.6 mm
Suspension Axial Stiffness	12.3 N/mm	12.3 N/mm
Aux. Suspension Axial Stiffness	35.1 N/mm	35.1 N/mm
Shaker Body Mass – base mounted	14.1 kg	14.1 kg
Shaker Body Mass – trunnion mounted	22.7 kg	22.7 kg
Impedance at 500 Hz	2.5 $\Omega$	2.5 $\Omega$
Cooling Air Flow	0.014 m <sup>3</sup> /s	0.014 m <sup>3</sup> /s
Armature Diameter	38 mm	38 mm
Armature Insert Pattern:		
Centre Insert	1	1
2.54 mm PCD†	6	6
Insert Threads	M4	10/32 UNF

\* Shaker ratings are those which can be achieved with a larger amplifier than that supplied as standard.

† PCD inserts equi-spaced

This range of permanent magnetic shakers is ideal for vibration testing of components, small assemblies or modal and structural analysis. The shakers' efficient armature design enables them to deliver impressive peak forces and accelerations over a wide frequency range.

The V400 series are wide frequency band electro-dynamic transducers capable of producing a sine vector force up to 196 N. They are also suitable as non-seismic pick-ups and are widely used in educational and research establishments to investigate the dynamic behaviour of structures and materials.

### Features

- Wide frequency band combined with high peak forces
- Low mass, high performance armature construction
- Base or trunnion mounted
- Powered by compact, quiet and energy efficient amplifiers
- Robust, lightweight suspension system provides excellent torsional and traverse stiffness with minimal impact on system acceleration

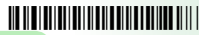
### Industry Applications

- Modal and structural analysis
- Electronic assembly testing
- Laboratory experiments and various medical purposes
- Fatigue and resonance testing
- Use as velocity transducer or high speed actuator



110070

Some of the features listed are available as standard, others as options. Please contact Brüel & Kjær for advice on the optimum specification to meet your system needs



### System Characteristics

V 406/8 Shaker + LDS Amplifier	PA 100E	PA 500L
System Sine Force (peak) – naturally cooled	98 N	98 N
System Sine Force (peak) – forced air cooled	98 N	196 N
System Velocity (sine peak)	1.52 m/s	1.78 m/s
System Displacement (pk-pk) – continuous	14.0 mm	17.6 mm
System Maximum ½-sine Shock Force*	90 N	200 N
System Random Force (rms) – ISO5344	38 N	89 N
Acoustic Noise at 1 m Distance:†		
Shaker‡ – naturally cooled	82 dBA	82 dBA
Shaker‡ – forced air cooled	105 dBA	105 dBA
Amplifier	silent	47 dBA
Total Heat Dissipation:		
Shaker	340 W	340 W
Amplifier	0.15 kW	0.8 kW
Shaker Cooler Fan	–	0.46 kW
Max. Working Ambient Temperature:		
Shaker	30° C	30° C
Amplifier	35° C	40° C
Electrical Requirement:		
Amplifier	1.3 kVA	1.3 kVA
Cooling Fan	0.2 kVA	0.25 kVA
Amplifier Rating	0.147 kVA	0.7 kVA
Maximum Shaker Weight		22.7 kg
Maximum Dimensions (H x W x D)		273.8 x 165 x 259 mm

\* ½-sine shock force is calculated with the standard payload, 2 ms pulse width, 10% pre/post pulse  
 † Measured at a height of 1.60m above floor level in enclosed cell  
 ‡ Maximum noise when running at full level

### Health and Safety

Designed in accordance with:

- EN 61010 – 1:2001

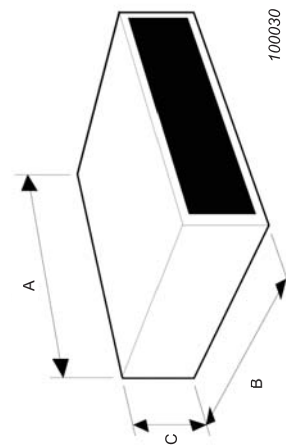
Complies with the following EU directives:

- EMC: 2004/108/EC
- Machinery: 2006/42/EC
- Low Voltage: 2006/95/EC

© Brüel & Kjær. All rights reserved.

### Amplifier Data

	PA 100E	PA 500L
A:	340 mm	340 mm
B:	290 mm	290 mm
C:	270 mm	270 mm
Wgt:	25 kg	25 kg



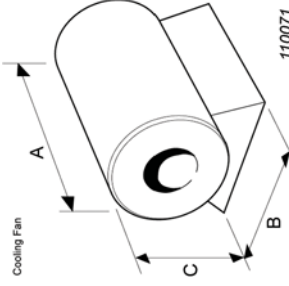
### Characteristics:

Rated Sinusoidal Power Output – matched resistive load	147 W (2R9)	500 W
Signal-to-noise Ratio	>75 dB	>75 dB
Total Harmonic Distortion – at rated output	Typically 0.5%	Typically 0.1%
Input Sensitivity for Maximum Output (400 Hz)	1.0 V rms	1.0 V rms
Amplifier Efficiency	58%	59%
Voltage Regulation	3%	2%
Maximum Continuous Sinusoidal VA Output (0.5 pf)	147 VA	700 VA
Frequency Range – at rated power	10 Hz–10 kHz	20 Hz–14 kHz
Output Current – at rated VA	7 A rms	18 A rms
Random Output Current	14 A pk	54 A pk
Maximum Output Current	7 A rms	18 A rms
Maximum Output Voltage	20 V rms	40 V rms
Maximum No Load Voltage	32 V rms	45 V rms
Overcurrent Trip Level	10 A rms	19 A rms
Protection	Fast acting current limit	Output device protection

### Shaker Options

<b>Insert Selection:</b>	
M4	◆
10/32" UNF	◆
<b>Mounting Selection:</b>	
Base Mounting	◆
Support Trunnion	●
<b>Other Options:</b>	
Cooling Fan	◆
Auxiliary Suspension	●
<b>Key:</b>	
◆ Standard – Available on shortest delivery	
● Option – Stocked item, available on short delivery	

### Cooling Fan



<b>Dim. A:</b>	389 mm
<b>Dim. B:</b>	241 mm
<b>Dim. C:</b>	249 mm
<b>Weight:</b>	17 kg

### Make Our Experience Your Advantage

From application engineering, installation and training through to maintenance, spares and repairs, Brüel & Kjær offers a total service approach to keep your system operating efficiently and reliably. All LDS systems (standards and specials) are designed and manufactured to ISO 9001. Brüel & Kjær offers a comprehensive range of vibration, measurement and analysis equipment. Please consult our website for details.